3D SEISMIC ANALYSIS OF HYDRAULIC STRUCTURES

A DISSERTATION

submitted in partial fulfilment of the
requirements for the award of the degree
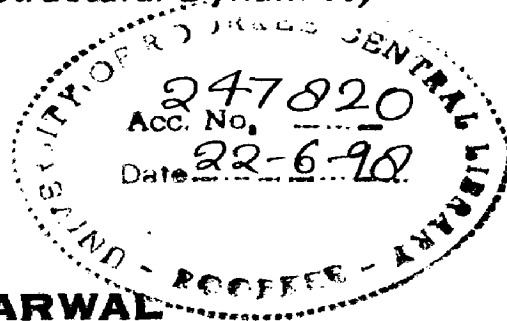*of*

MASTER OF ENGINEERING

in

EARTHQUAKE ENGINEERING

(With Specialization in Structural Dynamics)

By

ATUL AGARWAL

DEPARTMENT OF EARTHQUAKE ENGINEERING
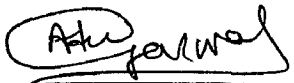UNIVERSITY OF ROORKEE
ROORKEE – 247 667 (INDIA)

JANUARY, 1997

CANDIDATE'S DECLARATION

hereby certify that the work presented in this dissertation titled "3D SEISMIC ANALYSIS OF HYDRAULIC STRUCTURES", in partial fulfillment of the requirements for the award of the degree of **MASTER OF ENGINEERING** in Earthquake Engineering with specialisation in **Structural Dynamics**, submitted to the Department of Earthquake Engineering, University of Roorkee, Roorkee, is an authentic record of my own work carried out for a period of seven months i.e. from July 1996 to January 1997 under the supervision of **Dr. D.K. Paul**, Professor, Earthquake Engineering Department, University of Roorkee, Roorkee and **Sh. R.N. Dubey**, Lecturer, Earthquake Engineering Department, University of Roorkee, Roorkee.
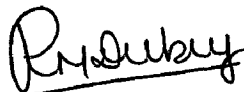
The matter embodied in this dissertation has not been submitted for the award of any other degree.

Place : Roorkee

Date ; 31 Jan. 1997

(Atul Agarwal)

This is to certify that the above statement made by the candidate is correct to the best of my knowledge.

R.N. Dubey

Lecturer,

Deptt. of Earthquake Engineering,

University of Roorkee,

Roorkee.

Dr. D.K. Paul

Professor,

Deptt. of Earthquake Engineering,
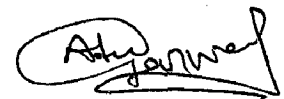
University of Roorkee,

Roorkee.

i

ACKNOWLEDGEMENTS

ABSTRACT

The earthquake behaviour of the major hydraulic structures is an extremely important problem since many important structures such as concrete gravity dam etc. are being built in the regions of high seismicity. In order to study the behaviour of such structures in general, a popular finite element package "COSMOS" has been used. The capabilities and the limitations of the package in analysing such structures have been studied.

Linear static and dynamic analyses have been carried out and free vibration characteristics have been evaluated to understand the behaviour and the effect of modellings on the response. A few problems related with hydraulic structures such as Wye section of a penstock, overflow and non-overflow section of dams and pier section of dams have been chosen to study their behaviour.

Although very limited capabilities of the software have been explored, the study has indicated that the preprocessor, solver and postprocessor are very powerful but there are still some limitations. Limitations are very obvious when modelling structures with curved surfaces. A comparison of 2D and 3D responses has been carried out and important conclusions are drawn. As a whole the package is quite robust and capable of handling the hydraulic structures. However, the package is limited to handle the hydrodynamic pressure and therefore it has to be calculated separately as virtual mass and mass are to be lumped at the virtual nodes.

CONTENTS

4.0 Conclusions

5.0 References

Appendix

LIST OF FIGURES

LIST OF TABLES

INTRODUCTION

1.1   General

Any structure to be located in an active seismic region must be designed to withstand safely the expected earthquake motion for that region. The frequent occurrence of destructive earthquakes during the past few decades have caused great damage to life and property, therefore, it is extremely important to ensure the safety of structures in future possible earthquakes. Further, the failure of a hydraulic structure such as dam is far more disastrous to a community than other structures, the element of risk one can take, while designing these structures are to be examined carefully. Mainly, the concrete gravity dams, piers of overflow sections and Wye section of a penstock considered as a part of various hydraulic structures.

Dams form an important element of multipurpose projects like hydroelectric, irrigation and flood control. The earthquake behaviour of major hydraulic structures is an extremely important problem since many important structures are being built in the regions of high seismicity. It is extremely important to design such structures to safely withstand earthquakes since a failure could be quite catastrophic. Along with the critical stresses due to static loads, the dynamic stresses due to earthquake excitation constitute quite a significant part in the overall displacement and stress pattern of a hydraulic structure like a dam.

Stability analysis of dams considering earthquake force as an equivalent static force has been used widely. The pseudostatic approximation for the seismic forces is based on seismic coefficients, which in turn are assessed on the basis of the seismicity of a site. The characteristics of a structure to be analyzed are not reflected in these coefficients. The advent of spectral response method and the feasibility of carrying out complex calculations, using computer have made it possible a rational dynamic analysis for earthquake loads.

With the advancement in computer technology and due to lot of saving in time and order of accuracy to be achieved, a large number of packages have been developed all over the world. Development of finite element packages have resulted in some of very powerful softwares like COSMOS, NASTRAN, ANSYS, SAP, STAAD ,

NISA, ABAQUS etc. Most of the designs and analyses are being carried out using either of the above softwares in various design and analysis organisations. In the present dissertation a very powerful software "COSMOS" has been studied for its potential to solve static and dynamic problems related with hydraulic structures. Few hydraulic structures mainly concrete gravity dams subjected to static and earthquake motion have been solved using COSMOS finite element software.

1.2 Objectives of the study

The main objectives of the study are as follows :

(1) To find out the capabilities of pre-processor of the finite element package "COSMOS" for its potential to model following hydraulic structures :

- o 2D/ 3D modelling of non overflow section of dams
- o 2D/ 3D modelling of overflow sections
- o 3D modelling of piers of overflow sections
- o Wye section of a penstock

(2) To explore the capabilities of the above package for the following analyses for some of the above hydraulic structures :

- o Static analysis
- o Natural Frequency Analysis
- o Earthquake Response Analysis.

(3) To study the 3D response of dam and pier sections.

(4) To compare the results of 2D and 3D analysis of various hydraulic structures.

(5) Based on the above study important conclusions are drawn with respect to the pre-processor, solver and the post-processor capabilities. The modelling issues are also summarized.

1.3 Scope of the study

The scope of the study is first to identify the various hydraulic structures such as concrete gravity dams (overflow and non-overflow section of concrete gravity dams),

2

piers and a Wye section of a penstock for modelling and solution with the COSMOS package.

The capabilities of the preprocessor of the COSMOS software will be assessed with respect to modelling of the above problems. Various issues, problems and advantages in modelling will be studied problem wise.

Out of the above problems, some will be identified for the solution of its natural frequencies and mode shapes. The same problems will then be solved for static and earthquake excitations to study the capability of the solver of the software.

These problems will then be studied for its free vibration characteristics, static and earthquake response. For some of the problems, the accuracy of results of 2D modelling with respect to 3D modelling will be studied.

Finally important conclusions will be drawn from the above exhaustive study about the capability of the package. A comparison of 2D/ 3D analysis of structures will also be made.

1.4 Layout of the Thesis

Chapter 2 presents the various features of the software COSMOS. The features available in COSMOS for linear static and dynamic analysis are presented in detail in this chapter. Also, light has been thrown on the capabilities of the COSMOS for handling non linear analysis.

Chapter 3 describes the various problems solved using the COSMOS. Some of the problems were selected for modelling only while analysis of some problems has been presented.

Chapter 4 includes the conclusions of the present work.

COSMOS SOFTWARE

2.1 General

COSMOS is a complete, modular, self-oriented finite element system developed by Structural Research and Analysis Corporation (SRAC), California, for personal computers and workstations. The software used is a COSMOS-M 1.71 Explorer version. The program includes modules to solve linear and nonlinear static and dynamic structural problems, in addition to solving problems in the fields of heat transfer, fluid mechanics, electromagnetics and structural optimization. Modules for special analysis options like fatigue are also available. (Ref. 5)

2.2 Structure of COSMOS

The COSMOS system consists of a preprocessor and a postprocessor, various analysis modules, interfaces, translators and utilities. The program is completely modular allowing the user to acquire the required modules

In COSMOS program, the user interacts only with the interface named GEOSTAR. GEOSTAR program, however, may be referred as a preprocessing, analysis and postprocessing tool. Using GEOSTAR, initial calls and transfers of control from one module to another modules of analysis are automated to give user a one screen solution.

The details of GEOSTAR program as shown in Fig. 2.1, controls the execution of the various modules of the COSMOS package and provides an interaction environment among them. These modules are :

STAR	for Linear Static Analysis
DSTAR	for Buckling , Frequency and Mode Shape Analysis
ASTAR	for Advanced Dynamic Linear Analysis

FSTAR	for Fatigue Analysis
OPTSTAR	for Shape and Sizing Optimization
NSTAR	for Nonlinear Static and Dynamic Analysis
HSTAR	for Heat Transfer Analysis
FLOWSTAR	for Fluid Flow Analysis
FLOWPLUS	for 2D and 3D Turbulent Fluid Analysis, and
ESTAR	for Electromagnetic Analysis

Various other programs, as shown in Fig. 2.1, can also be supported through one-way or two-way translators. (Ref. 5)

2.2.1 Features of GEOSTAR

GEOSTAR has a diverse set of geometric modeling capabilities combined with flexible meshing of complex models with ease. Loading, boundary, and initial conditions can conveniently be applied in association with geometric entities and in any defined coordinate system. GEOSTAR has many powerful capabilities and features that work in a user friendly environment. User can build the model, specify all the data required for analysis, execute the suitable analysis and evaluate the results, all from within GEOSTAR.

COSMOS package can be studied by dividing it in two parts :
- Basic System Modules
- Advanced Modules

2.3 BASIC SYSTEM MODULES

In COSMOS software, modules used for model creation, linear static analysis, frequency analysis and buckling analysis are referred in a one group named Basic System. This chapter focuses on presenting some of the salient features which user can apply using the Basic System. The Basic System is composed of three modules :

- GEOSTAR for model creation and results display,
- STAR for linear static analysis, and
- DSTAR for Buckling and modal analysis.
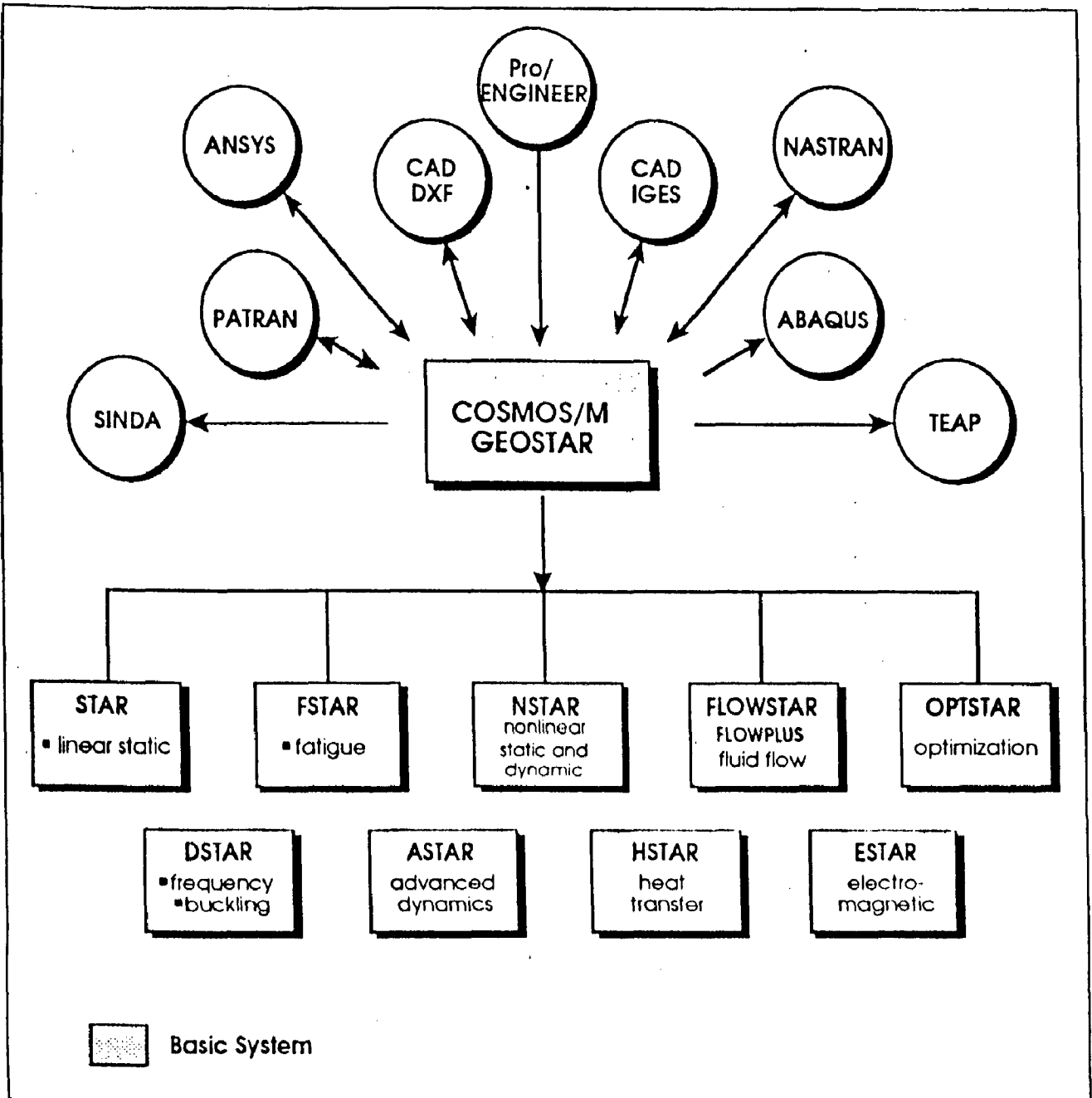
Fig. 2.1 COSMOS Modules and Translators

The integrated system facilitates, the user in modeling, analyzing and evaluating user's own design within one graphical environment. (Ref.3)

2.3.1 Modules in Basic System

The basic system consists of two main modules STAR and DSTAR and a submodule, STRESS, which performs stress calculations. These modules interact with each other as shown in the Fig 2.2
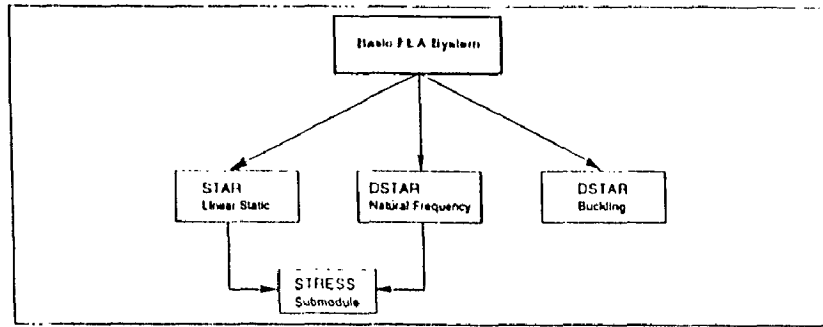
Fig. 2.2 Basic System Modules

The linear static analysis module (STAR) uses the linear theory of structures, based on the assumption of small displacements, to calculate deformations. For many structures (for example, frames) the computation of stresses is performed in a separate submodule STRESS.

The module STAR calls the STRESS submodule to calculate the element and nodal stresses for most elements.

The DSTAR module evaluates natural frequencies and the corresponding mode shapes of a system. The module can also calculate the buckling loads and the associated mode shapes. For modal analysis, the STRESS submodule also calculates the element and nodal virtual stresses for most elements based on the results from DSTAR. (Ref.3)

2.3.2 Linear Static Analysis Module (STAR)

STAR uses the linear theory of structures, based on the assumption of small displacements, to calculate structural deformations. As mentioned earlier, STAR calls

7

the stress submodule to calculate element and nodal stresses for most elements based on the results from STAR or DSTAR (modal analysis only). Stresses for multiple load cases are obtained in a single run and the combination of load cases is possible in the post-processing stage. Stresses can be obtained in any defined coordinate systems. The STRESS module supports all of STAR features.

In a typical linear static stress analysis, user will determine the stresses, displacements, strains and reactions in the finite element model. The analysis is linear if the nonlinearities due to various sources can be either linearized or completely ignored. Results from a linear analysis include nodal displacements, nodal and element stresses, forces, reactions etc. These results can be graphically viewed on the screen or inspected in the output file.

The following are some important features of the linear static stress analysis module STAR : (Ref.3)

- Extensive element library
- Isotropic, orthotropoic, anisotropic and composite material properties.
- Temperature- dependent material properties
- Failure criteria for composite elements
- Prescribed displacements, with or without other loadings.
- Coupled degrees of freedom and constraint equations
- Thermal, gravitational and centrifugal loads
- Beam loading
- In-plane effects in the stiffness evaluation
- Multiple load cases in a single run
- Soft spring option to prevent instabilities
- Substructuring capability (for large problems) to build and analyze the chosen superelements through condensation and recovery process
- Fluid Solid interaction
- Gap-friction problems
- Grid force balance and reaction force calculation
- Asymmetric loading of axisymmetric models
- Strain energy and error calculations
- Combining static and dynamic analysis results

2.3.3 Frequency and Buckling Analysis Module (DSTAR)

The DSTAR module evaluates natural frequencies and the corresponding mode shapes of a system (modal analysis). The module can also calculate the buckling loads and the associated mode shapes of eigenvalue buckling problems.

In a typical buckling analysis, the quantities to be computed include the critical loads at which the structure becomes unstable, and the corresponding buckling mode shapes. For eigenvalue buckling, the first few modes are of practical importance. The buckling modes can be plotted or animated during post processing.

Modal Analysis which determines the natural frequencies and mode shapes is an important phase in the design of many structural components. Similar to buckling, modal analysis involves the computation of eigenvalues, and DSTAR provides many type of eigenvalue erection techniques. The vibration modes can be plotted or animated on the screen .(Ref.3)

The following are some important features of the DSTAR module :

- A variety of eigen value extraction procedures :
  - Subspace iteration,
  - Lanczos,
  - Jacobi,
- Calculation of complex eigenvalues
- Frequency shift to calculate eigenvalues in a specified range or to treat models with rigid body modes.
- Sturm sequence to check for missed modes
- Lumped and consistent mass matrices for representing structural mass
- In plane effects on stiffness
- Soft spring option to treat models with rigid body modes
- Non Axisymmetric mode extraction for axisymmetric models

2.3.4   Basic system limits

The pre- and postprocessing module GEOSTAR and the analysis modules STAR and DSTAR which constitute the Basic system, have the size limits given in Table A.1 & Table A.2.

Table A.1 shows Modeling size limits in GEOSTAR. Table A.2 shows Analysis limits in the Basic system.

2.3.5   Modeling and Analysis Cycle in the Basic System

The basic steps involved in a finite element analysis are :

- Create the problem geometry.
- Mesh the defined geometry with appropriate type of element(s).
- Apply constraints on the finite element model.
- Define the loads on the model.
- Define the material and sectional properties.
- Submit the complete finite element model for analysis.
- Interpret and analyze the results.

These steps can be schematically represented as shown in following flow chart :
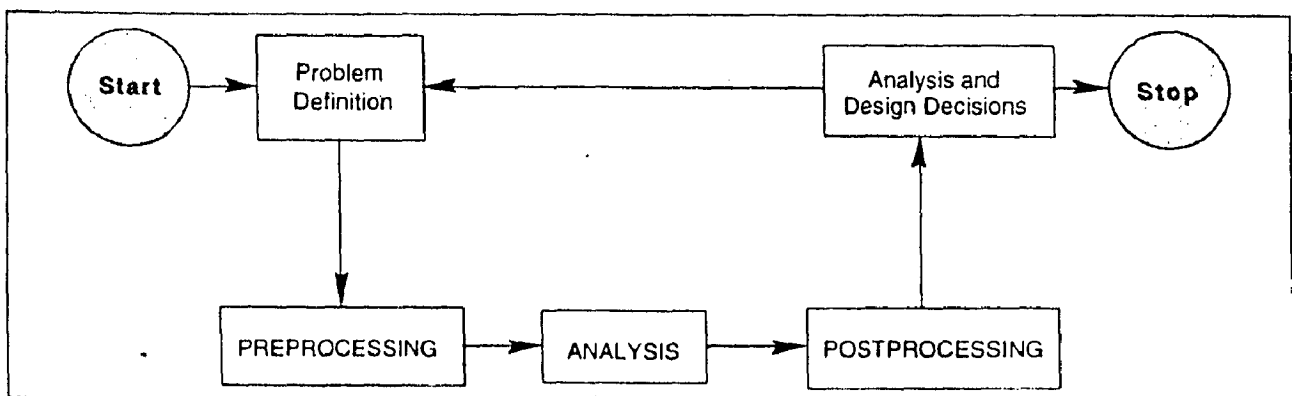
Fig. 2.3 Finite Element Modeling And Analysis Steps

Preprocessing refers to the operations such as defining the model geometry, mesh generation, applying loads and boundary conditions, and other operations that

10

are required prior to submitting the model for analysis. The term analysis refers to the phase of specifying the analysis options and executing the actual analysis. Postprocessing refers to the manipulation of the analysis results for easy understanding and interpretation in a graphical environment. (Ref.3)

2.3.6 Flow Charts and Commands for analysis in the Basic System

Figures 2.4-2.6 show the flow charts for linear static analysis, buckling analysis and modal analysis respectively.

In Tables A.3-A.5 various commands used in linear static analysis, buckling analysis, & modal analysis respectively are given in tabular form with brief description of the function to be performed. (Ref.3).

2.3.7 Element Library for Basic System

The basic system features an extensive element library to suit finite element modeling and analysis requirements for all types of practical problems. These elements model behaviour of 1-D, 2-D and 3-D problems in linear static, buckling and natural frequency and mode shape computations.

A brief description of the available elements available in Basic System is given in Table. A.6. Summary of properties which can be applied to elements in the basic FEA system is given in Table A.7. (Ref.3)

Linear Static Analysis
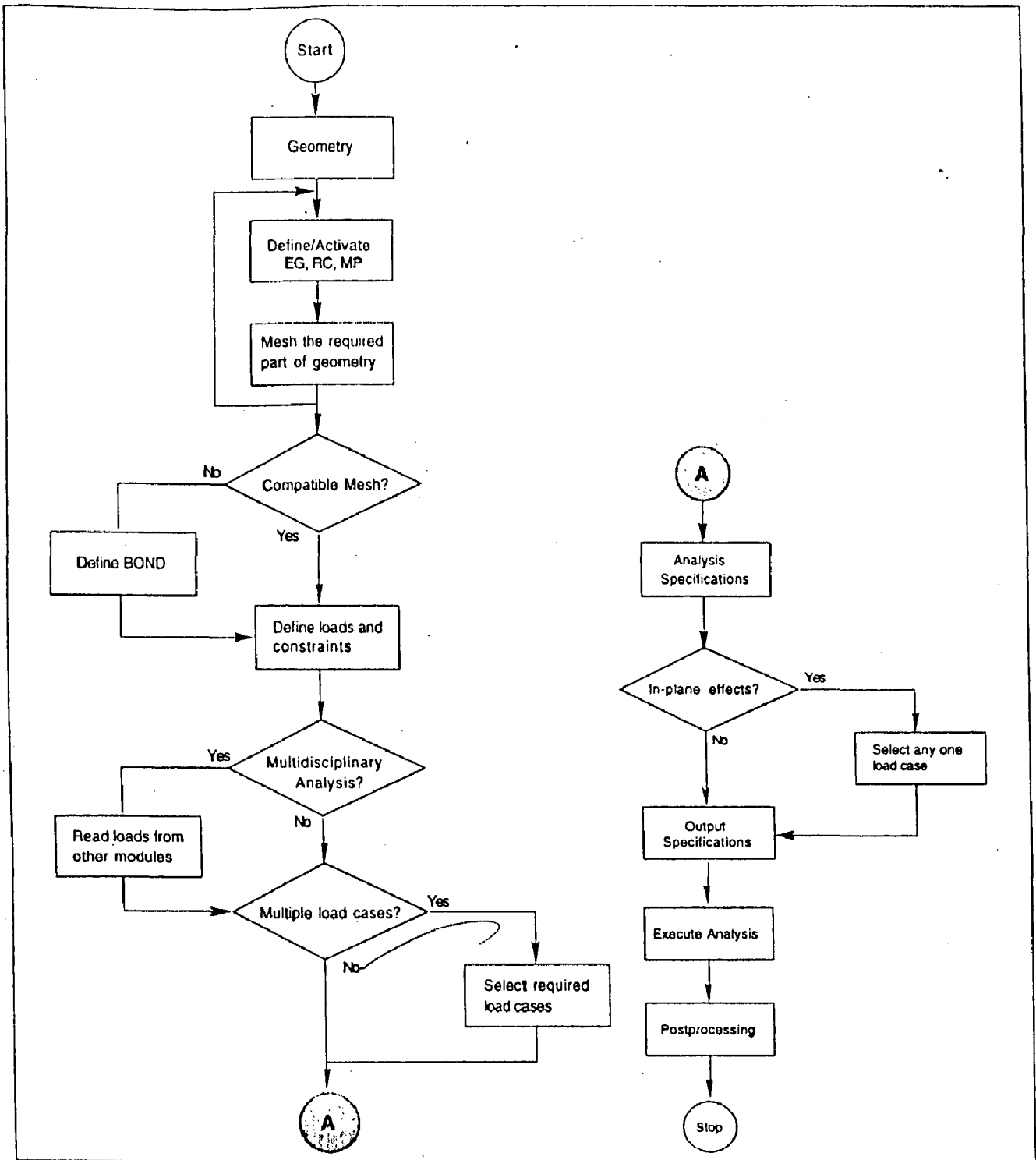
Fig. 2.4 Flow Chart for Linear Static Analysis in Basic System
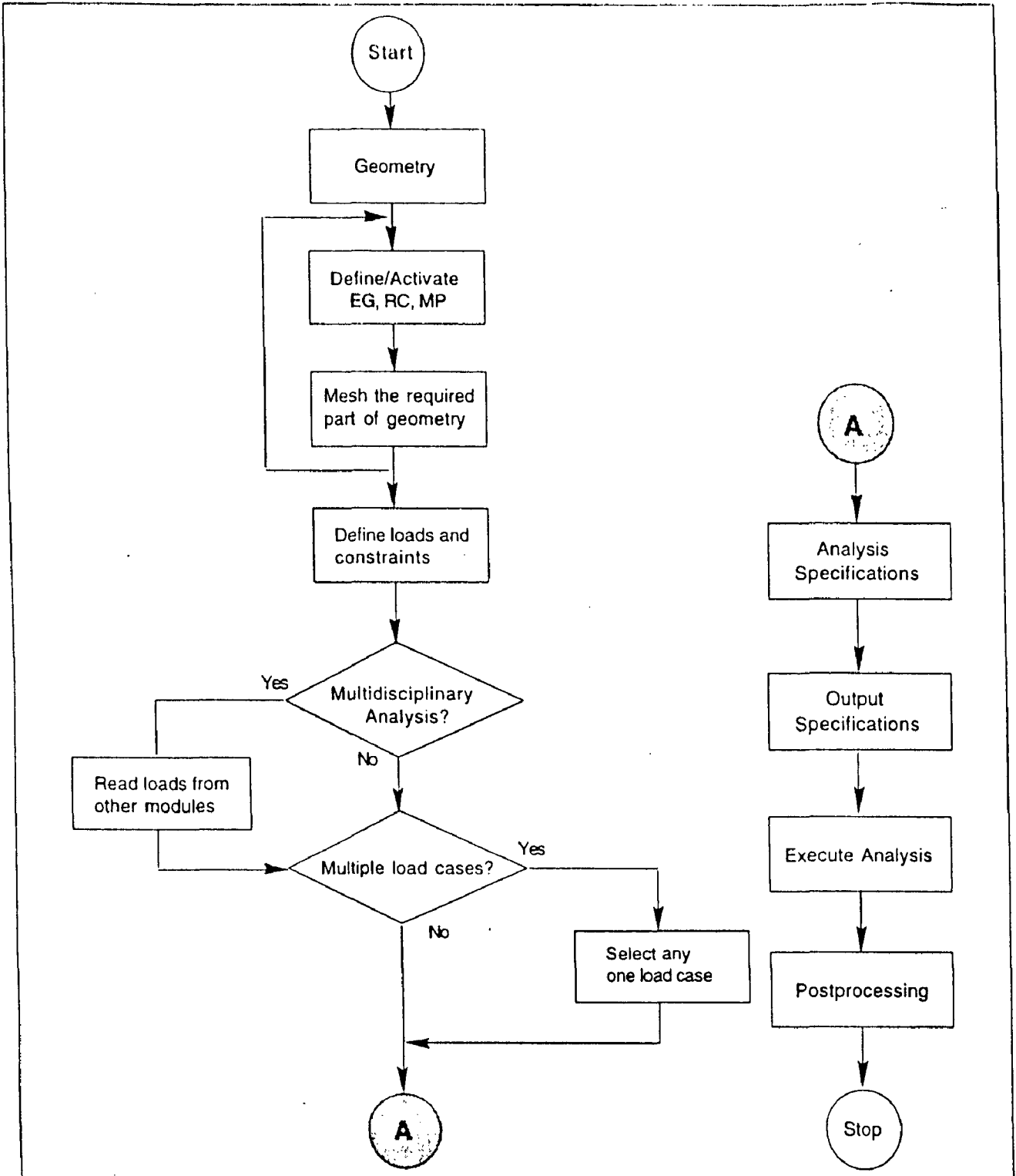
Fig. 2.5 Flow Chart for Buckling Analysis in the Basic System

Modal Analysis
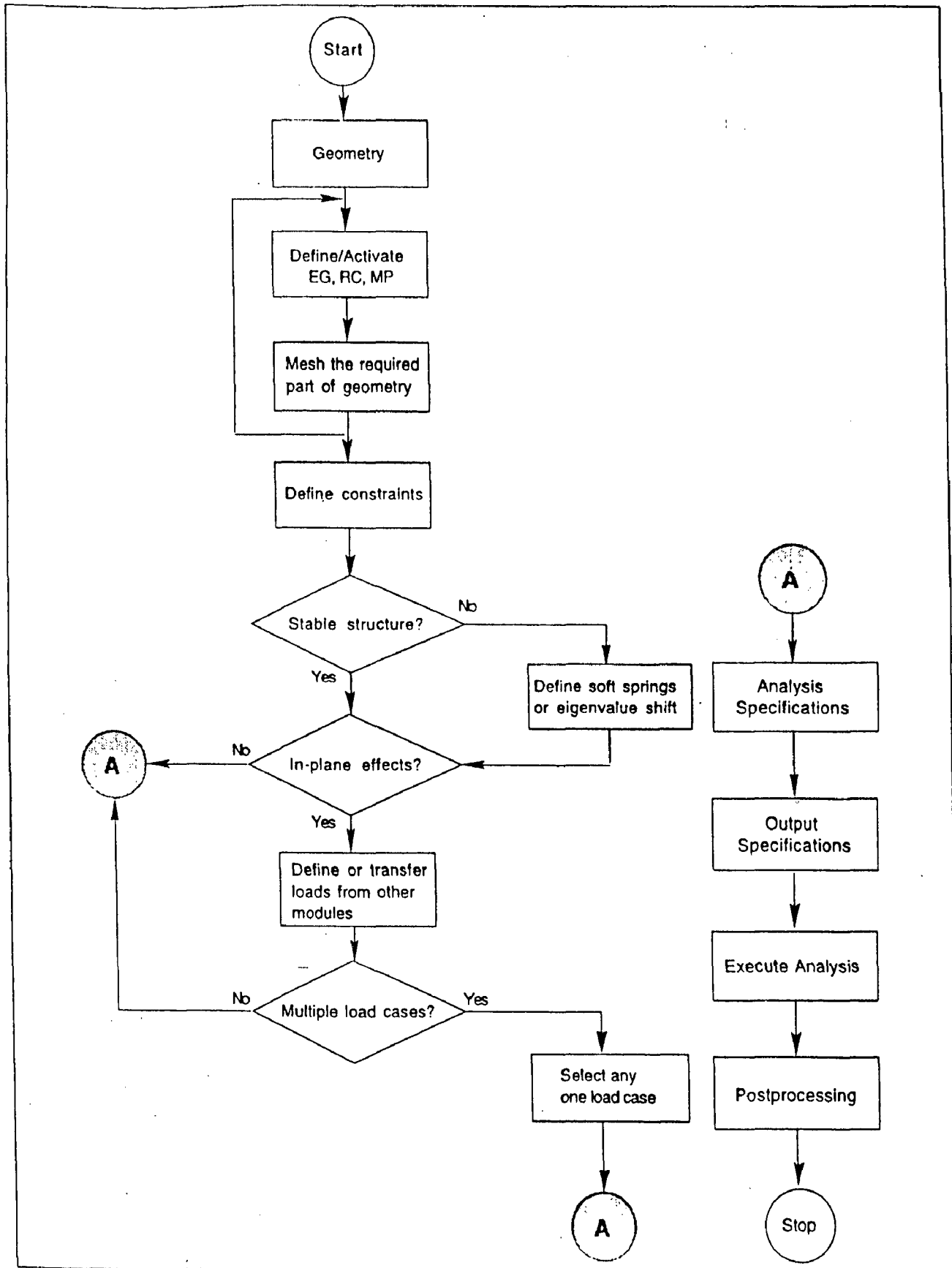
Fig. 2.6 Flow Chart for Modal Analysis in Basic System

2.3.8 Modal Analysis

The computation of mode shapes and frequencies is known as modal or normal modes analysis. The finite element system of equations for dynamic systems can be expressed as following :

$$[K]\{u\}+[C]\{\dot{u}\}+[M]\{\ddot{u}\}=\{F(t)\}$$

(2.1)

where,

$[M]=$ Mass Matrix,
$[K]=$ Stiffness Matrix,
$[C]=$ Damping Matrix.

For free vibrations, the above equation takes the form :

$$[K]\{u\}+[C]\{\dot{u}\}+[M]\{\ddot{u}\}=\{0\}$$

(2.2)

When undamped linear elastic structures are initially deformed into a certain shape, they will oscillate infinitely with the same mode shape but varying amplitudes. The oscillation shapes are called the mode shapes and corresponding frequencies are called natural frequencies. For undamped linear elastic structures, the above equation reduces to:

$$[K]\{u\}+[M]\{\ddot{u}\}=\{0\}$$

(2.3)

With no externally applied loads, the structure is assumed to vibrate freely in a harmonic form defined by:

$$u(t)=\phi\sin(\omega t+\phi)$$

(2.4)

which leads to eigen value problem:

$$[[K]-\omega^2[M]]\{\phi\}=\{0\}$$

(2.5)

15

where ω is natural frequency and ϕ is corresponding mode shape of the structure. (Ref. 1,8)

2.3.9   Eigenvalue Extraction Methods in Modal Analysis

There are four methods available in Basic system of COSMOS for computation of the eigenvalues. These are: (Ref. 1)

- Subspace Iteration
- Lanczos Method
- Jacobi Method
- Inverse Power Method

2.3.10   Treatment of Rigid Body Modes in Modal Analysis - Shifting

Shifting can be viewed as a displacement of the origin in a plot of the eigenvalues. In COSMOS, by appropriately selecting the shift points, the iteration process can be made to converge to any or all the modes (including rigid body modes) of the structural system. The speed of convergence can be accelerated by shifting close to the root being sought, and it is therefore a good practice to shift at intervals during an iteration process. The shift option is applicable to both subspace and inverse iteration methods. (Ref. 1)

2.3.11   Treatment of Rigid Body Modes in Modal Analysis - Soft Spring Option

In addition to or in lieu of frequency shifting, COSMOS allows to use the soft spring option for computing the natural frequencies and mode shapes of structures with rigid body modes. As in static stress analysis, the soft spring stiffnesses are added to the diagonal terms of stiffness matrix. However, the computed frequencies depend on the magnitude of the soft spring stiffness. In addition, the natural frequencies computed when using either the shift option or the soft spring addition, or a combination of both, may vary in each case, depending on the magnitudes of shift or spring stiffness specified. (Ref. 1)

2.3.12 In Plane Effects in Modal Analysis - Stress Stiffening and Softening

The effect of stress stiffening on structures in linear static analysis has been discussed in earlier section. In order to consider the in-plane effects on the natural frequencies of a structure, the structure must be first loaded and constrained for computing the geometric stiffness matrix. Therefore, a static stress analysis precedes the computation of natural frequencies with in-plane effects. In-plane loads have a stiffening or softening effect on the vibrational behaviour of structures. Tensile membrane forces increase the natural frequencies whereas compressive membrane forces decrease them. Similar to the static solution with in-plane effects, normal mode analysis in the presence of membrane forces is performed in two stages. In the first stage, the displacements $\{u_i\}$ for the loaded and constrained structure are computed using the conventional stiffness matrix $[K]$. In the second stage, the geometric stiffness matrix $[K_G(u_i)]$ is established based on the computed displacements $\{u_i\}$ and added to the conventional stiffness matrix $[K]$, and then along with the mass matrix, the natural frequencies (ω) and the corresponding virtual displacements which are eigenvectors, $\{\Psi_{i+1}\}$ are solved. With the inclusion of in-plane effects, the finite element system of equations for computing the natural frequencies and mode shapes can therefore be written as:

$$\left([K]+[K_G(u_i)]-\omega^2[M]\right)\{\psi_{i+1}\}=\{0\} \tag{2.6}$$

where $[K_G(u_i)]$ is the geometric stiffness matrix computed based on $\{u_i\}$, $[M]$ is the mass matrix, ω is the natural frequency, and $\{\psi_{i+1}\}$ represents the eigenvectors which describe the natural modes of the structure. (Ref. 1,4)

The inclusion of in-plane effects in natural frequency computation is specified using the A_FREQUENY command.

2.4 ADVANCED DYNAMIC ANALYSIS

In COSMOS, all the problems regarding the dynamic analysis are solved in module named ASTAR. This chapter throws a light on some of the salient features of the Advanced dynamic module ASTAR. The Advanced dynamic module ASTAR available in COSMOS gives a better hand over application of COSMOS in seismic

analysis. The Advanced Dynamic module, ASTAR, has three principal functions. The first is to perform linear dynamic analysis of systems subject to different categories of forcing functions; the second is to carry out stress calculations subsequent to a dynamic analysis; and finally to accommodate plot files required for graphic evaluations of the system response at specific nodes and/or solution steps.

The various dynamic capabilities of the program are based on the normal mode method (mode superposition method). It is therefore essential that in all instances the frequency and mode shape calculations are done prior to the application of this module for the solution of the desired dynamic response problem. (Ref. 1)

2.4.1 Analysis Capabilities

The Advanced dynamic module is used for the solution of dynamic response problems listed below :

- Modal Time History
- Response Spectra.
- Response Spectra Generation
- Random Vibration
- Steady State Harmonic Analysis

As stated earlier, these analysis options are based on the mode superposition method for which modes and frequencies must be determined in advance.

ASTAR may not be used if the A_FRQUENCY command was used to activate the consistent mass option. Only the lumped mass option is supported by ASTAR. Each of these analysis options can then be performed by considering any combination of the four excitation types noted below : (Ref. 1)

- Concentrated forces specified in any coordinate system.
- Pressure Loads specified in any coordinate system.
- Uniform Base Motion defined in Global Cartesian System.
- Multi-Base Motion defined in the Global Cartesian System.

2.4.2 Element Library

Various elements available in ASTAR are given in Table A.8. (Ref. 1)

2.5 THEORETICAL BACKGROUND

In this section, a discussion on the various linear dynamic response analysis options supported by the Post Dynamic module (ASTAR) is presented.

The problems with larger number of equations or degrees of freedom (DOF) often require less computation time if the dynamic behaviour of the linear structure can be approximated with sufficient accuracy by only the first few modes (nf) where nf<<DOF. The trade off between computational economy and accuracy revolves around the necessity of calculating the eigenvalues of the system of equations.

The process of approximating the solution of the equations of motion by considering only the first few modes of the system's natural frequency is called normal mode (or modal superposition) analysis and in the Advanced Dynamic module, all forced response vibration problems are based on this procedure. (Ref. 1)

2.5.1 Normal Mode Analysis

The equations of motion for a linear dynamic system (multi degree freedom system) are;

$$[M]\left\{\ddot{u}\right\} + [C]\left\{\dot{u}\right\} + [K]\left\{u\right\} = \left\{f(t)\right\} \tag{2.7}$$

where,

    [M] = mass matrix
    [C] = damping matrix
    [K] = stiffness matrix
    [f(t)] = time varying load$\left\{u\right\}$
    $\left\{u\right\}$ = displacement vector
    $\left\{\dot{u}\right\}$ = velocity vector
    $\left\{\ddot{u}\right\}$ = acceleration vector

For linear dynamic problems, the system of equations of motion (Eq. 2.7) can be decoupled into "nf" single degree of freedom equations in terms of the modal displacement vector { x }, where,

$$\{u\} = [\Phi]\{x\} \tag{2.8}$$

and [Φ] is the matrix of the lowest "nf" eigenvectors obtained from the solution of :

$$[K]\{u\} = \omega^2 [M]\{u\} \tag{2.9}$$

substituting for { u } from Eq. (2.8) in Eq. (2.7) and premultiplying it by $[\Phi]^T$, will yield :

$$[\Phi]^T [M][\Phi]\left\{\ddot{x}\right\} + [\Phi]^T [C][\Phi]\left\{\dot{x}\right\} + [\Phi]^T [K][\Phi]\{x\} = [\Phi]^T \{f(t)\} \tag{2.10}$$

With the mode shapes satisfying the orthohgonality conditions, Eq. (2.10) becomes :

$$[I]\left\{\ddot{x}\right\} + [\lambda]\left\{\dot{x}\right\} + [\lambda^2]\{x\} = [\Phi]^T \{f(t)\} \tag{2.11}$$

Equation. (2.11) represents "nf" uncoupled single degree of freedom (second order differential) equation as shown below :

$$\ddot{x}_i + 2\,\xi_i\,\omega_i\,\dot{x}_i + \omega_i^2\,x_i = \{\phi\}_i^T \{f(t)\} \tag{2.12}$$

These equations can be solved using step-by-step integration or other techniques, and the displacements { u } and other system responses can then be determined by performing the transformation shown in Eq. (2.8). (Ref. 1,11)

2.5.2 Damping Effects

The above analysis is not correct unless the damping matrix [C] satisfies the orthogonality conditions. It should be noted that in majority of cases, (a) the exact damping matrix is unknown, and (b) the effect of any non-orthogonality is usually small. In the Post Dynamic module, the following damping options are available : (Ref. 1)

2.5.2.1 Rayleigh Damping

Rayleigh damping is of the form :

$$[C] = \alpha[M] + \beta[K] \qquad (2.13)$$

This form of $[C]$ is orthogonal with respect to the system eigenvectors, and the modal damping C_i is :

$$C_i = 2\,\xi_i\,\omega_i = \alpha + \beta\,\omega_i^2 \qquad (2.14)$$

and in terms of the modal critical damping ratio :

$$\xi_i = \frac{\alpha}{2\omega_i} + \frac{\beta\omega_i}{2} \qquad (2.15)$$

where α and β are the Rayleigh damping coefficients. (Ref. 11)

2.5.2.2 Modal Damping

Modal damping is defined as a fraction of critical damping (Ref. 8)

$$\xi_i = \frac{C_i}{C_c} \qquad (2.16)$$

2.5.2.3 Concentrated Dampers

Concentrated dampers can be defined between any two nodes or any one node and the ground for only the modal time history analysis option. The damping coefficients are defined in terms of their components in the global X, Y and Z-directions as shown in Fig. 2.7. (Ref. 11)
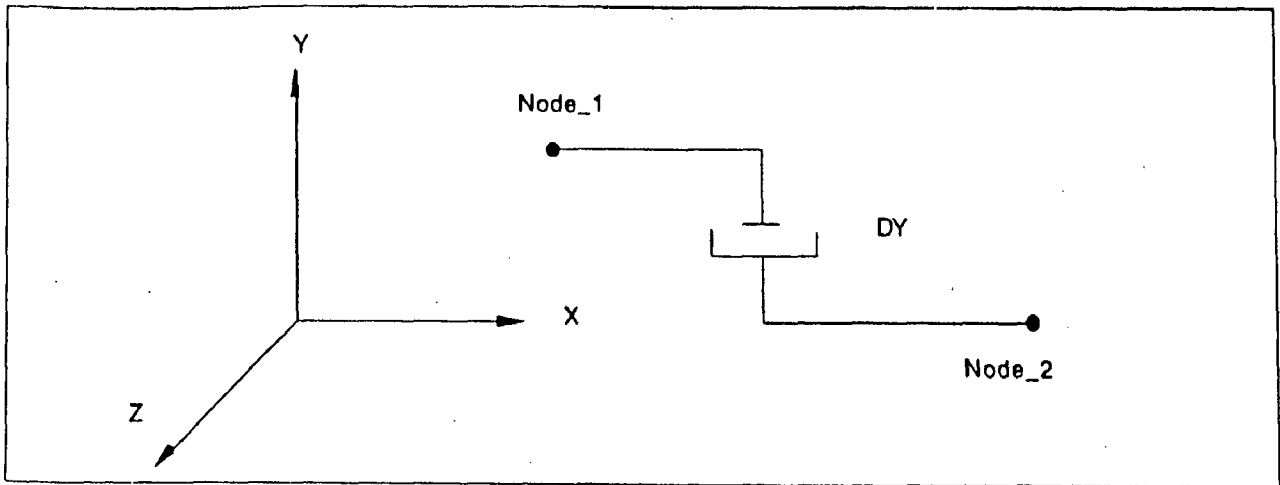
Fig.2.7 Concentrated Dampers

2.5.2.4 Composite Modal Damping

Composite material damping allows for the definition of the damping coefficient as a material property. Thus different element groups representing different materials can be assigned different damping coefficients during a post dynamic analysis. This option is defined below in the form of equivalent modal damping ratios : (Ref. 1)

$$\beta_j = \{\phi\}^T_j \left[\overline{M}\right]\{\phi\}_j \qquad (2.17)$$

β_j = equivalent modal damping ratio of the jth mode.

$\{\phi\}_j$ = jth normalized modal eigenvector.

$\left[\overline{M}\right]$ = Modified mass matrix constructed from element matrices formed by the product of the damping ratio for the element and its mass matrix.

2.5.3 Solution Accuracy Considering Mode Truncation

The solution accuracy of dynamic problems based on the normal mode method depends to a large extent on the number of modes considered. Below a few possible options as well as certain remedial steps available in COSMOS to improve the solution accuracy are discussed for the various analysis types and loading conditions. (Ref. 1)

2.5.4 Force Excitation Problems

In the case of systems under the influence of force excitations, it is essential that all modes which contribute to the static deformation shape of the structure are considered. The example in Fig. 2.8 shows that at least five modes should be considered for this case.

2.5.5 Base Excitation Problems

In dynamic problems under the under the influence of base excitations, the number of modes considered must contribute to a total mass participation factor of at least 80% of the system mass in the direction of the base motion.

For harmonic and random vibration problems, all modes up to those with natural frequencies including beyond the excitation frequency range, such that the 80% requirement is satisfied, must be satisfied.

2.5.6 Modal Acceleration Method (MAM) in Time History

The process of mode truncation, as was explained before, introduces some error in the response. The Modal Acceleration Method (MAM), in the time history analysis, approximates the effects of the truncated modes by their equivalent static effects. This approximation can be expressed for the displacement by :

$$U_c = [K]^{-1} R_c \qquad (2.18)$$

where, K is the structural stiffness matrix and R_c represents the static loading. It can be shown that this static load vector can be computed in terms of the included modes, according to,

$$R_c = [I - M \Phi \Phi^T] P(t) \qquad (2.19)$$

where, M and Φ are the mass matrix and modal matrix respectively and $P(t)$ is the applied dynamic load.

Thus by considering only a few number of modes, for even very complicated geometry, user is able to evaluate the response very accurately. (Ref. 11)
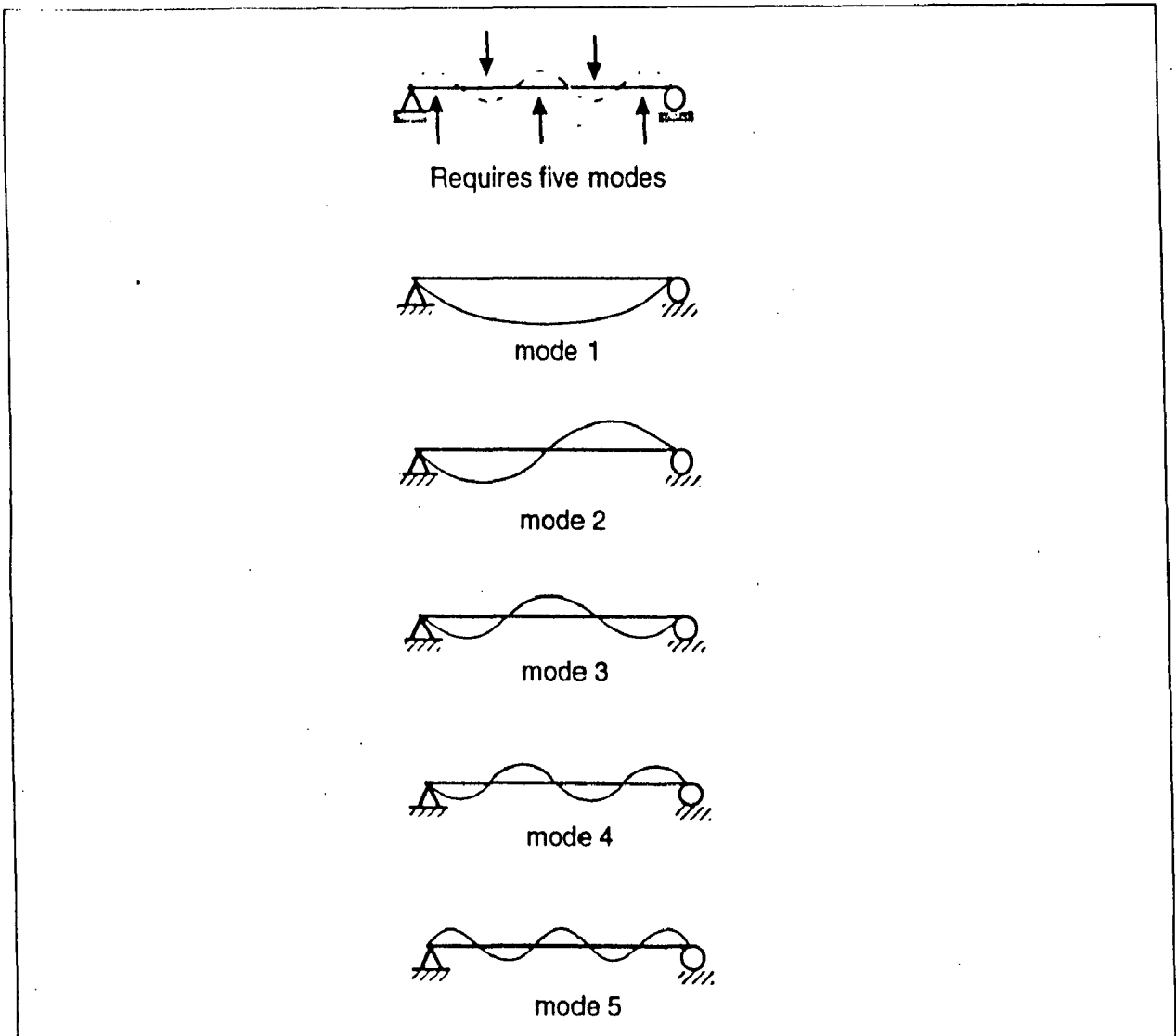
Fig. 2.8 Mode Shapes of a Simply Supported Beam

2.5.7 Missing Mass Correction Technique in Response spectrum

This is the biggest advantage of ASTAR module of COSMOS in dynamic analysis; Truncation of higher modes in the modal analysis always introduces some error in the results. This truncation means that some mass of the system is ignored. The distribution of this "missing mass" is such that the inertia forces associated with it will usually produce only small displacements and stresses. However, these ignored inertia forces will often produce significant displacements (stresses) for stiff systems or at the close proximity of the structural supports. The Missing Mass Correction Technique is incorporated to the ASTAR program for Response Spectrum Analysis in order to estimate the error introduced by the ignored higher modes and to improve the results. This correction is presented as a factor in the output file immediately after the printed accelerations. The user may apply this factor to improve the accuracy for the results obtained for accelerations or the stresses. (Ref. 1)

2.5.8 Excitation due to Base Motion

The various analysis modules available in ASTAR may be considered in conjunction with either uniform base motion, multi base motion or both. (Ref. 1)

2.5.9 Time History Analysis

In Time History Analysis problems the equations of motion for multi degree-of-freedom systems are solved subject to different dynamic loadings or base excitation functions. The normal mode method is first used to obtain the uncoupled equations of motion as derived earlier and shown as

$$\ddot{x}_i + 2\,\xi_i\,\omega_i\,\dot{x}_i + \omega_i^2\,x_i = \{\phi\}_i^T\,\{f(t)\} \tag{2.20}$$

Next one of two step-by-step integration methods available in COSMOS, that is either

(a) The Wilson-θ method, or

(b) The Newmark β Method

is used to evaluate response of each mode. These techniques use the results obtained in one previous step to solve for those in the next step. The integration is performed in the time domain starting from the time at the last step and ending with the time at the

current step (which equals to the time-step increment) . Thus by reducing the time increment between consecutive steps, accuracy of the solution can be improved. The system response is then determined at each time step using the following transformation : (Ref. 1)

$$\{u\}=[\phi]^T\{x\}$$ (2.21)

(A) Solution Accuracy

The solution accuracy in time-history analysis problems as in all cases depends on :

1. Number of modes considered
2. How accurately the modes are calculated (i.e., accuracy in modeling)
3. Integration increment or time step size, (smaller than 1/10 th of the last mode period is recommended). (Ref. 8)

(B) Loading Options Available

The following loading options are available in ASTAR : (Ref. 1)

1. Force or pressure loadings associated with time curves.
2. Uniform base motion, i.e., the entire constant portion of the model is subjected to the same motion specified by a time curve. (Using PD_BASE commands.)
3. Multi-Base motion application, i.e., different groups of constraint nodes are subjected to motions defined by different time curves. (Using PD_SUPPORT command.)
4. Initial conditions can be specified in the form of initial displacements, velocities or accelerations to a group of nodes.(Using INITIAL command.)

(C) Concentrated Damper and Gap Elements

Concentrated damper and gap elements (Fig. 2.7) can be modeled only in conjunction with the time history analysis option. Gap elements are introduced in modal analysis as truss elements which can resist either tension or compression, once a certain distance between two nodes is reached. Also concentrated dampers can be

defined between two nodes or between one node and the ground. Their effect is considered in the modal analysis by applying force at the proper nodes. The force due to gap elements are proportional to gaps' distances, while the forces resulting from dampers are in proportion with differential nodal velocities. (Ref. 1)

2.5.10 Response Spectrum Analysis

The capability to perform response spectrum analysis of linear elastic structures subject to base motion is included in the ASTAR module. (Ref. 1)

2.5.10.1 Structure Maximum Response

The maximum modal responses can not be simply added to obtain the structure maximum response because the occurrences of the maximum modal response in the time domain are not known.

However, several recommended approaches for mode combination are incorporated in COSMOS.

(A) Absolute Sum

This is a conservative approach in which it is assumed that all the modes have their maximum response in the same direction at the same time, i.e.,

$$\{u\}_{max} = \sum_{i=1}^{nf} \left| \{u\}^i_{max} \right| \tag{2.22}$$

(B) Square Root Sum Of Squares (SRSS)

This is a more rational approach where the modal responses are summed using the square root of sum of squares.

$$\{u\}_{max} = \sqrt{\sum_{i=1}^{nf} \left[\{u\}^i_{max} \right]^2} \tag{2.23}$$

(C) Complete Quadratic Combination (CQC)

The complete quadratic combination technique considers the effects of damping in combining the mode responses, i.e.,

$$\{u\}_{max} = \sqrt{\sum_{i=1}^{nf}\sum_{j=1}^{nf}\{u\}_{max}^{i}\{u\}_{max}^{j}\rho_{ij}}$$

(2.24)

where ρ_{ij} is the cross mode correlation coefficient given by,

$$\rho_{ij} = \frac{8\sqrt{\xi_i\,\xi_j}\,(\xi_i + r\,\xi_j)r^{3/2}}{(1-r^2)^2 + 4\,\xi_i\xi_j\,r(1+r^2) + 4(\xi_i^2 + \xi_j^2)r^2}$$

(2.25)

and

$$r = \frac{\omega_j}{\omega_i}$$

(2.26)

and ξ_i, ξ_j are modal damping coefficients for modes i and j

(D) Naval Research Laboratory (NRL)

The mode combination technique recommended by NRL takes the absolute value of the maximum response among all specified modes and adds it to SRSS response of the remaining modes for each degree of freedom as noted below :

$$\{u\}_{max} = \left|\{u_j\}_{max}\right| + \sqrt{\sum_{i=1}^{nf}\left[\{u\}_{max}^{i}\right]^2 - \{u_j\}_{max}^2}$$

(2.27)

where $\{u_j\}_{max}$ represents the maximum response among responses of all "nf" modes.

2.5.10.2 Multiple Response Spectra

The structure response to multiple response spectra is found by the square root of sum of the squares of the individual spectra response. The program output file contains R.M.S. values of relative displacements and velocities but absolute acceleration. The acceleration at fixed nodes are not listed. (Ref. 1)

2.5.11 Response Spectra Generation

This dynamic analysis option allows the generation of response spectrum curves at any point of the structure for any displacement degree of freedom.

The excitation input required for this analysis is a curve defining acceleration versus time at the desired point of the structure. However, since the excitation can not be input directly, the program uses the results obtained from a modal time history analysis to generate the spectrum curve at specified node. Thus, a response spectra generation is possible only after a modal time history analysis is performed.

The response spectra generated can then be used as base excitation input for a response spectra analysis. This is particularly useful for studying the effect of structure's response on a secondary system attached to a point in the structure.

2.5.12 Random Vibration Analysis

In COSMOS, the random vibration analysis is available for linear elastic systems when subjected to a random excitation. The excitation is assumed to be stationary, Gaussian, with a mean value of zero, and one-sided (defined for positive frequencies only).

The random excitation input required for this analysis consists of curves defining values of power spectral densities versus frequencies, which can be associated with base motion, nodal forces, or element pressure.

The curves' frequencies as well as the lower and upper frequency limits are input in radians per second or in cycles per second, and the units of PSD functions will be interpreted accordingly. Thus, the PSD units are either $(Force)^2 / Freq, (disp)^2 / Freq, (Vel)^2 / Freq$ or $(acc.)^2 / Freq$. Also, the exciting power spectral densities of nodal forces or base motions in different directions, can be specified either fully correlated or fully uncorrelated. In the case of element pressure, the power spectral density can only be defined as fully correlated.

Finally, this analysis outputs the root mean square (RMS) responses of displacements, velocities, accelerations and stresses. The output of modal PSD's at selected frequencies is optionally available in COSMOS. Also, curves of spectral density of response versus exciting frequencies at nodes can be requested.

2.5.13 Steady State Harmonic Analysis

The steady state harmonic analysis evaluates the maximum structural response due to harmonic excitations of varying magnitudes and varying frequencies. Maximum modal response is evaluated at different exciting frequencies in the range specified.

The excitation input required for this analysis consists of curves defining amplitudes versus frequencies of a harmonic forcing function, which can be associated with nodal forces, element pressures, or base motion. Also, a phase angle can be defined for each base motion curve or nodal force. The input curve's frequency as well as the lower and upper frequency limits can be specified either in radians per second or cycles per second.

Curves of maximum nodal response magnitude versus exciting frequencies may be requested for any node in the structure.

2.6 NONLINEAR ANALYSIS

The success of a finite element analysis depends largely on how accurately the geometry, the material behaviour, and the boundary condition of the actual problem are idealized. While elements with their geometric characteristics and boundary conditions are used to describe the geometric domain of the problem, material models are

introduced to capture the material behaviour. All real structures behave non-linearly in some way or other. Still, in some cases, due to particular nature of the problem a linear analysis may be adequate. However in many other cases non-linear analysis becomes a must. In following section some of nonlinearities which can be dealt with COSMOS are discussed.

2.6.1   Structural Nonlinearities

2.6.1.1   Geometric Nonlinearities

In nonlinear finite element analysis, a major source of nonlinearities is due to the effect of large displacements on overall geometric configuration of structures. Structures undergoing large displacements can have significant changes in their geometry due to load-induced deformations which can cause the structure to respond non linearly in a stiffening and/or a softening manner. For example, cable like structures (Fig. 2.9) generally display a stiffening behaviour on increasing the applied loads while arches may first experience softening followed by stiffening, a behaviour widely known as the snap-through buckling (Fig. 2.10).
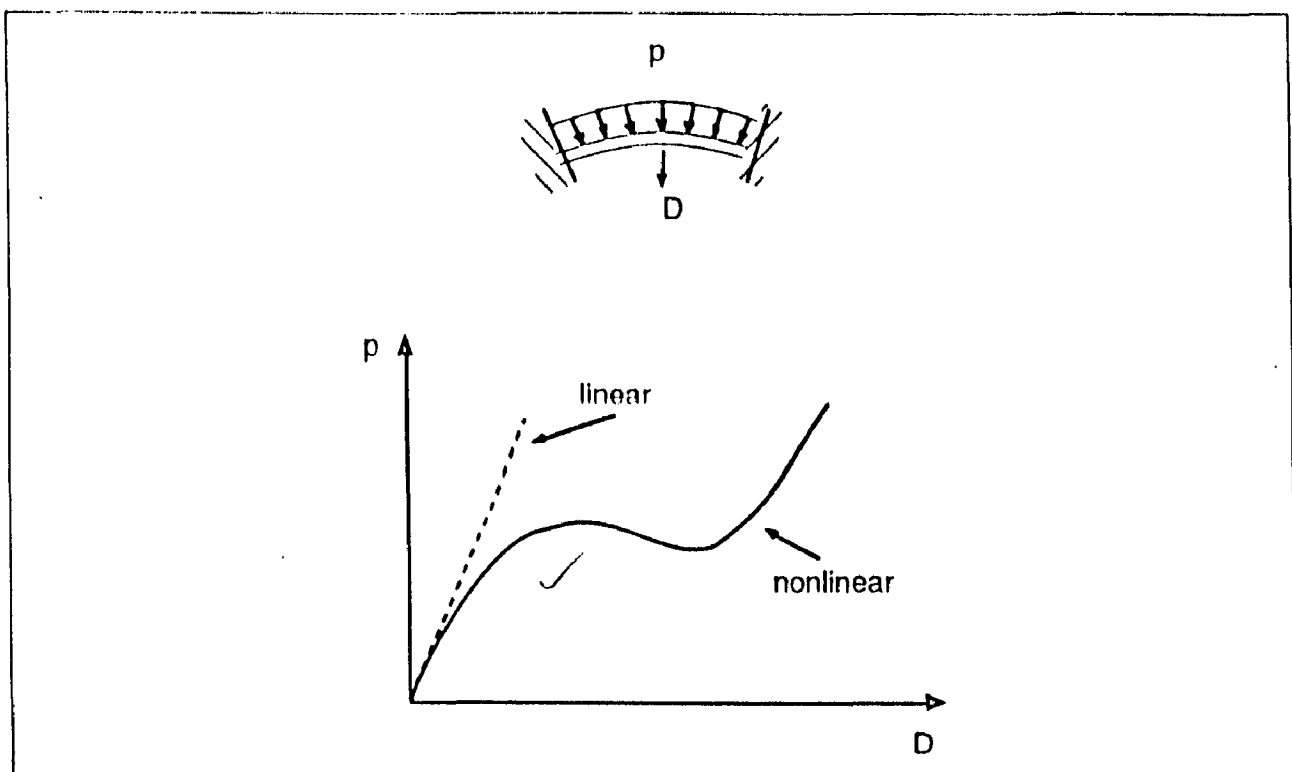
Fig. 2.10 Pressure (p) versus Centre deflection (D) for Shallow Spherical Cap

2.6.1.2 Material Nonlinearities

Another important source of nonlinearities stems from the nonlinear relationship between the stress and strain which has been recognized in several structural behaviours. Several factors can cause the material behaviour to the non linear. The dependency of the material stress-strain relation on the load history, load duration and temperature are some of these factors. This class of material nonlinearity can be idealized to simulate such effects which are pertinent to different applications through the use of constitutive relations. Yielding of beam-column connections during earthquakes (Fig. 2.11) is one of the applications in which material nonlinearities are plausible.

BRIDGE MODELING

Cable nodes

Anchorage   Cable bent

Y

X

Z

Suspension Bridge

Generalized Force

nonlinear

linear

Generalized Displacement

Qualitative Force-Displacement Curve for Suspension Bridge [10]

Fig. 2.9

Beam-Column Connection   Applied Loading   Stress-Strain Curve
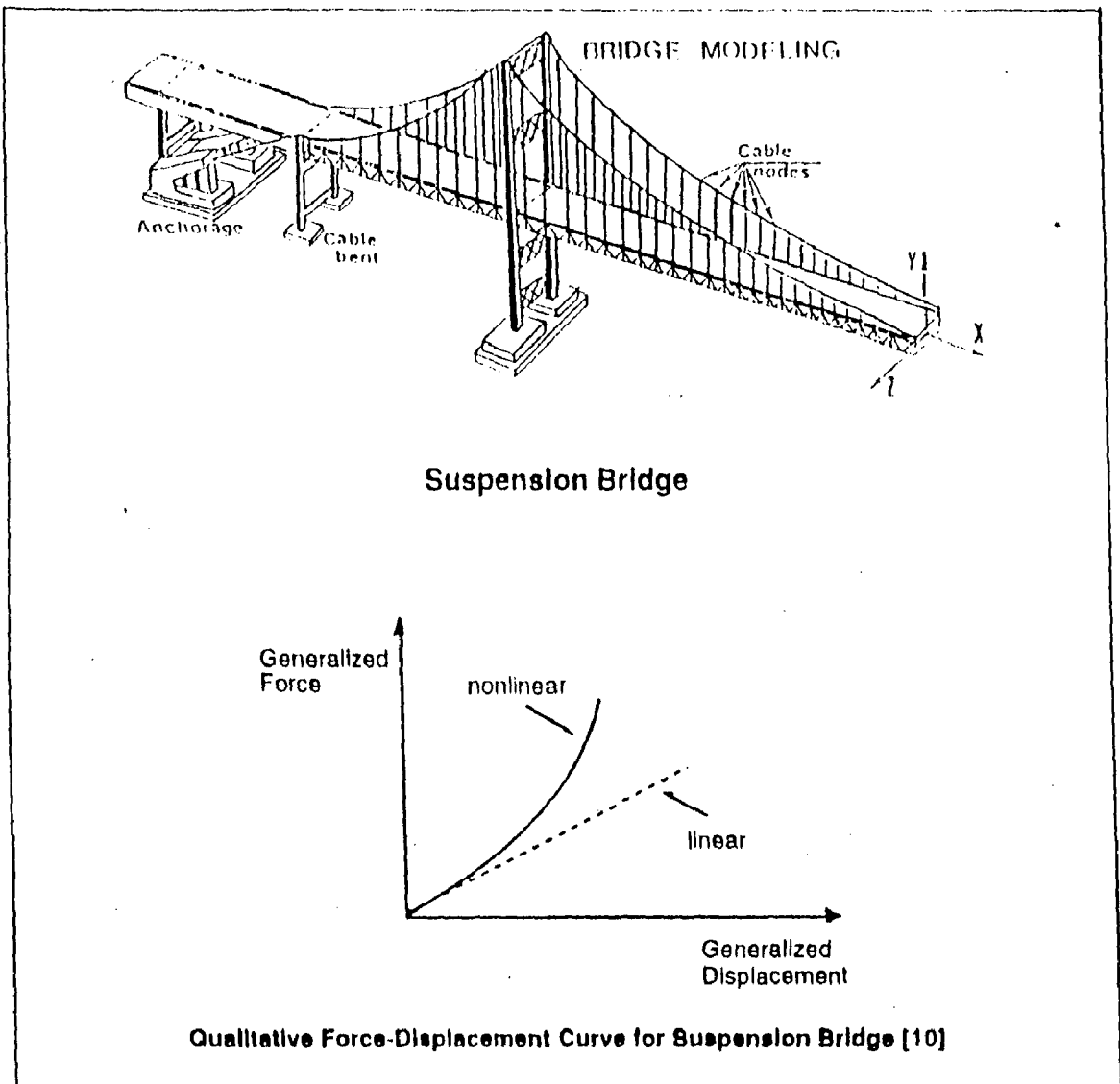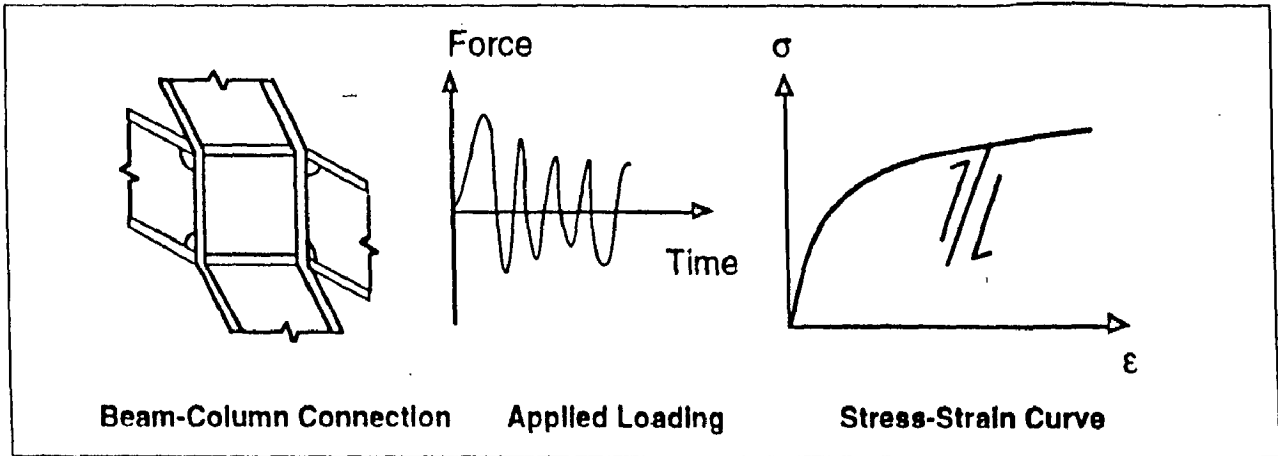
Fig. 2.11 Loading and Unloading of Beam Column Connection under Dynamic Loading

2.6.1.3 Contact (Boundary) Nonlinearities

A special class of nonlinear problems is concerned with the changing nature of the boundary conditions of the structures involved in analysis during motion. This situation is encountered in the analysis of contact problems. Fig. 2.12 shows pounding of structures due to seismic motion. In COSMOS the evaluation of contact boundaries (nodes, lines, or surfaces) can be achieved using gap (contact) elements between nodes on the adjacent boundaries.
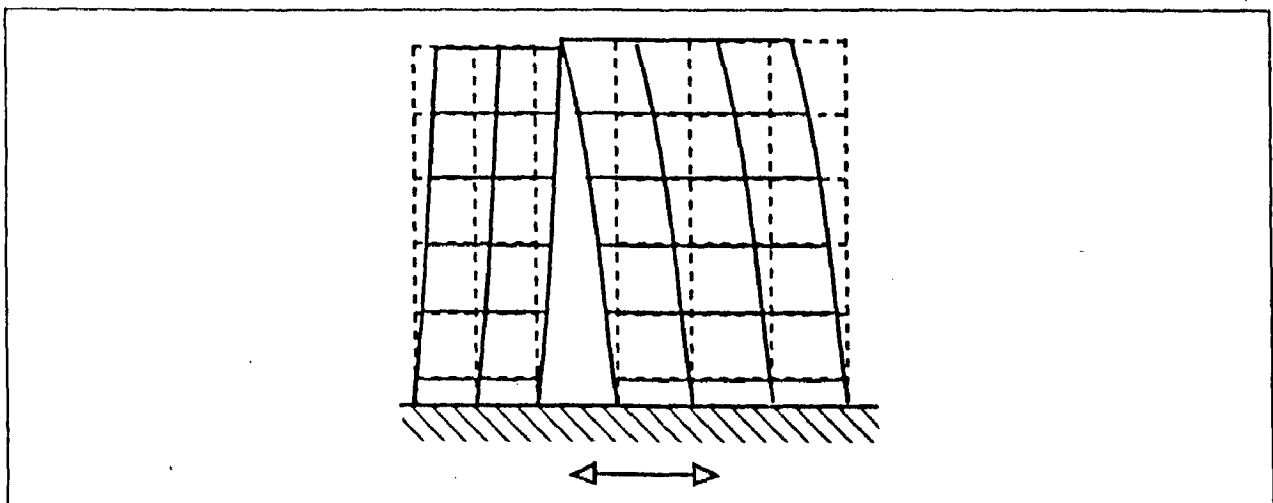
Fig. 2.12 Pounding of Structures Due to Seismic Motion

2.6.2 Concept of Time Curve

For nonlinear static analysis, the loads are applied in incremental steps through the use of `time' curves The "time" value represents a pseudo-variable which denotes the intensity of applied loads at a certain step. While, of nonlinear dynamic analysis with time-dependent material properties (eg. creep), "time" represents the real time associated with the loads' application. COSMOS is inbuilt with an adaptive automatic stepping algorithm to facilitate the nonlinear dynamic analysis.

2.6.3 Element Library

Element library for non-linear analysis is shown in Table A.9 .

ANALYSIS OF VARIOUS HYDRAULIC STRUCTURES

3.1 General

To explore the potential of the pre-processor of the COSMOS some of the problems have been modelled and then finite element discretisation of these problems has been carried out. Out of the several problems a few have been selected for different types of analysis. These are described hereunder.

3.2 PROBLEM- 1 : MODELLING OF WYE SECTION OF A PENSTOCK

3.2.1 GENERAL DESCRIPTION OF THE WYE SECTION

Figure 3.1 shows the Wye section of a penstock. Main penstock of diameter 5.25 m is bifurcated by two smaller penstocks. One of the smaller penstock runs in the same direction as the main penstock while the other penstock is bifurcating at an angle of 22.5^0. The transition of two penstocks had a conical shape with diameter decreasing from 5.25 m to 3.5 m. At the intersection of the two penstocks there is a C-clamp (sickle plate) inclined at an angle of 22.5^0. The C-clamp runs both inside and outside at the junction. This C-clamp has a thickness of 45 mm. At the intersection of the penstocks there is a ring girder all around the penstocks with thickness of web as 40 mm. The thickness of the flanges of ring girder and C-clamp is 45 mm.

Generation of the geometry: Modelling of the wye section of the penstock was a very tedious process as the bifurcating penstock is at an inclination to the main penstock. Also modelling of inclined C-clamp was another problem. Few steps used in the modelling are described very briefly here. The geometry has been developed with respect to the central line of the penstock and the plate and girders. Centre of the main penstock and four points on the circumference of the penstock at that section were located first. Then these points were used to generate a circle of diameter 5.25 m.

CRBRK feature in COSMOS was used to break this circle in twenty equal parts. These twenty equal parts were used to generate the twenty surfaces using "extrusion" feature with SFEXTR command. In the similar way twenty curves were generated at the smaller end of the main penstock. After identifying the twenty curves from the extruded surfaces using SELREF command, these curves were joined with twenty curves of the smaller end to make another twenty surfaces. SF2CR command was used to generate these surfaces. Similarly points, curves and surfaces were generated for the inclined penstock. Now CRINTSS feature of the COSMOS was explored to generate the curves of intersection of the two penstocks.

Using these curves and exploring "underlying surface" feature in COSMOS the actual shapes of the penstocks were drawn. Later points for the C-clamp were established first and after joining them with suitable curves, contours and separate regions were drawn for the C-clamp. Using "dragging" feature of the COSMOS (using SFDRAG command) web of the ring girder and the flanges of both i.e. the ring girder as well as the C-clamp were generated. To join the flanges of the lower ring girder , the upper ring girder and the C-clamp was a mind boggling process. CRONSF feature of the COSMOS was used to join these flanges. Lastly the extensions of the two penstocks were generated.

Finite Element Discretisation: Finite element discretisation of the above model was carried out using SHELL9T elements (thin shell elements). Quadrilateral element with two triangles is used for the meshing. "Auto meshing" feature of the COSMOS was used to generate the mesh. Meshing was carried out in several steps as the various portions of the assembly had varying thicknesses. Figure 3.2 shows the complete finite element model of the Wye section.

Concluding Remarks: A very difficult modelling problem of wye section of a penstock has been attempted. Using the curves, surfaces, contours and regions the geometry of wye section has been developed without much difficulty. The generation of C-clamp and the ring girders were quite difficult and several trials were made for the final generation. The most difficult part was the matching of the flanges at the tri-junction of the ring girders and the C-clamp. Special care was necessary to define the regions of different thicknesses for developing the geometry and meshing. Once

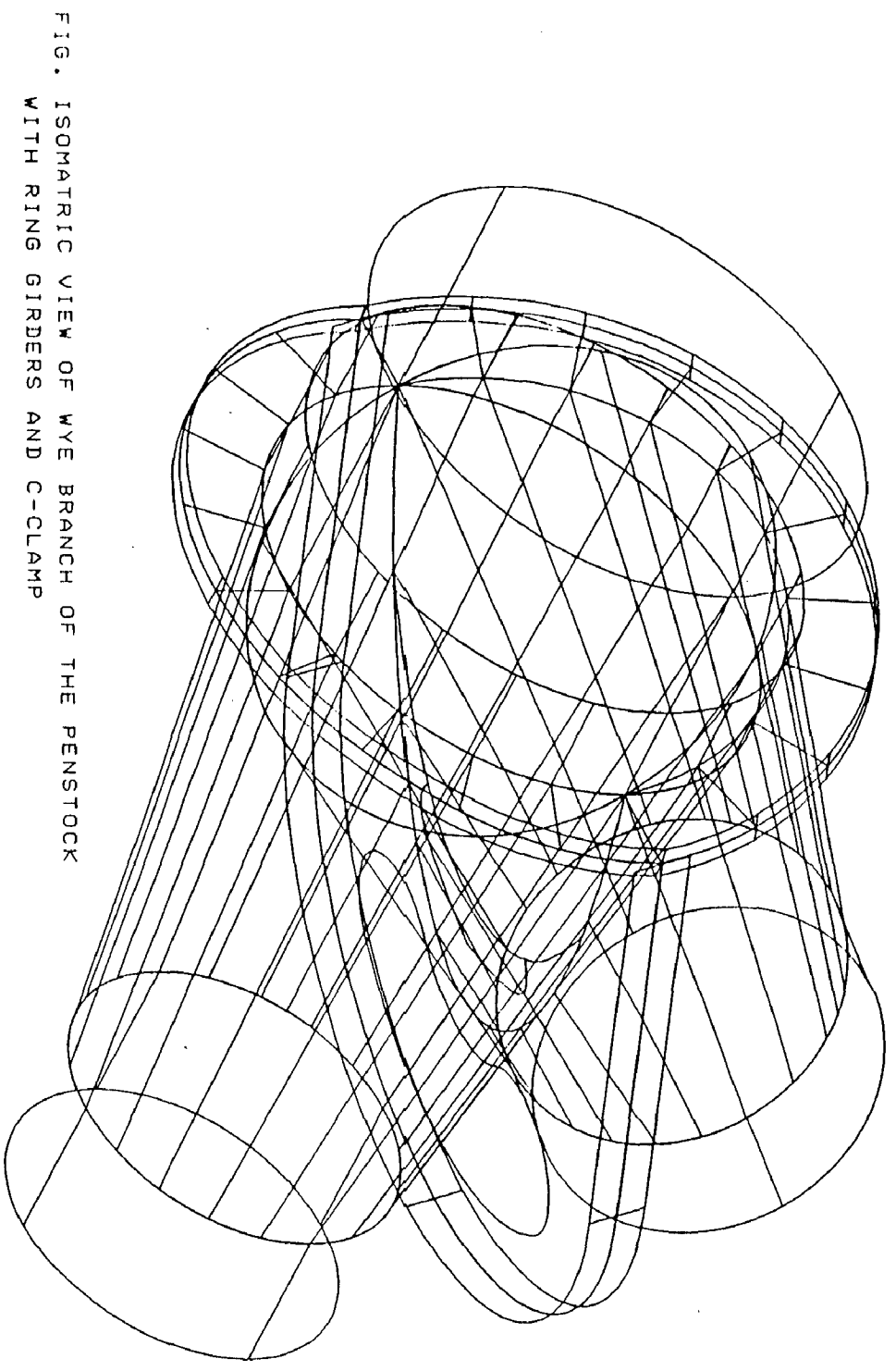geometry is created, finite element meshing is quite simple using the auto-meshing feature of the software.

FIG. ISOMATRIC VIEW OF WYE BRANCH OF THE PENSTOCK
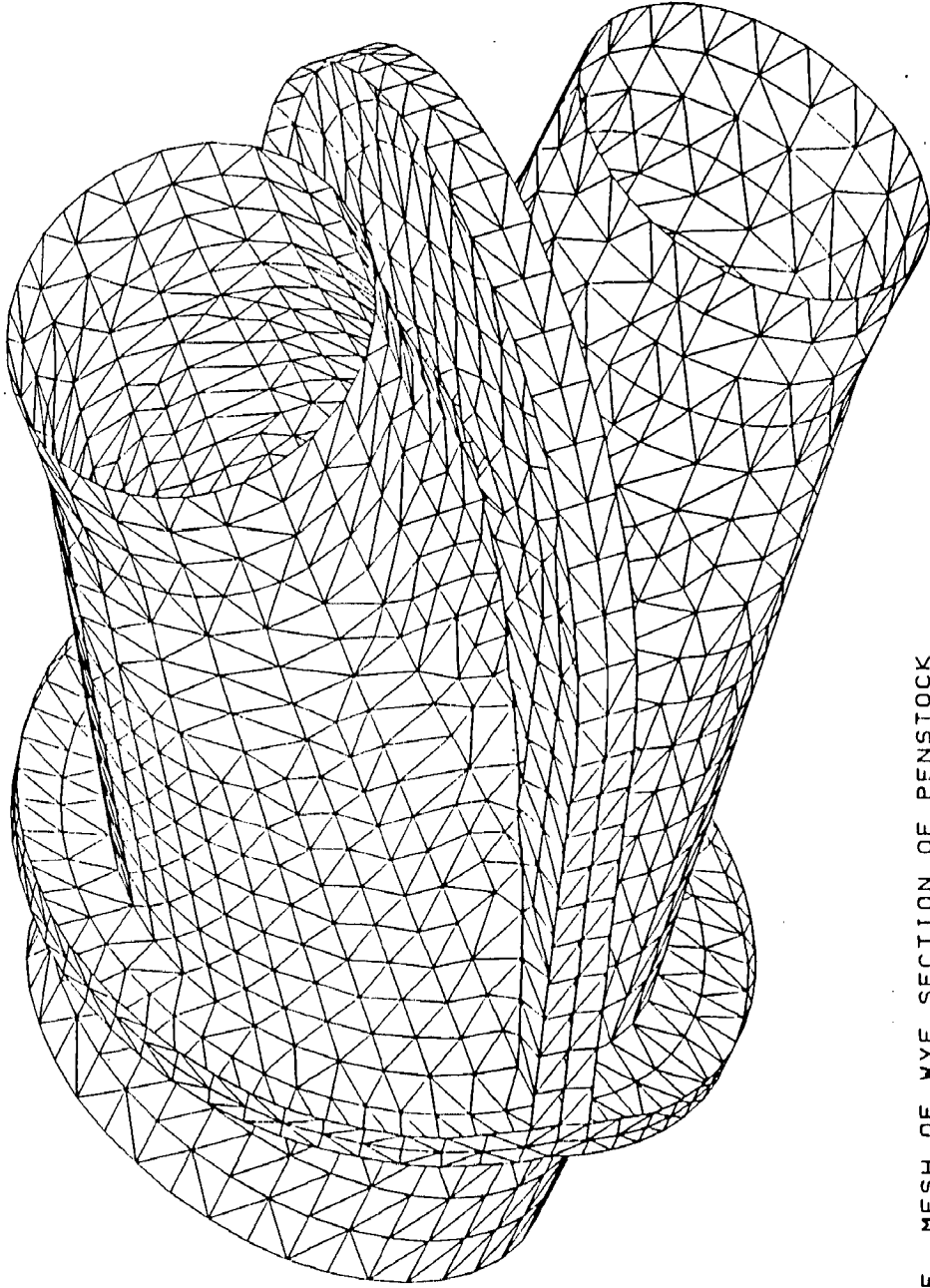WITH RING GIRDERS AND C-CLAMP

Figure 3.1

38

FIG. F.E. MESH OF WYE SECTION OF PENSTOCK

Figure 3.2

39

3.3 PROBLEM - 2 :   2D AND 3D MODELLING OF NONOVERFLOW AND OVERFLOW SECTION OF A DAM

3.3.1   GENERAL DESCRIPTION OF THE DAM

Figures 3.4 & 3.7 show the isometric views of the nonoverflow and overflow sections of the dam. Dam sections have been modelled for central sluice section with and without spillway. The modelling of the two sections is carried out in 2D as well as in 3D. Dam has a base width of 65.0 m and a height of 67.5 m. In both the sections viz. with and without spillway sections there is a sluice of 7.5m X 8.5 m. dimension. At the end of the sluice on the downstream side there is a bucket of 24.0 m radius. The thickness of the block is 16.0 m. The bottom of the sluice is defined by a parabolic curve. Section without spillway has three galleries of dimension 2.0m X 2.5 m and two galleries of 1.5 m X 2.5 m. There are two additional galleries in overflow section: one circular and one trapezoidal for the control of the gate. Following are some of the details of 2D and 3D modelling for the non overflow and overflow sections of the dam.

3.3.2   2D MODELLING OF THE NONOVERFLOW SECTION

Various steps used in the generation of the geometry of the model are briefly described hereunder.

, **Generation of the geometry :**   For 2D modelling of the dam points were first generated at the central pier section. These points were joined by suitable curves in several steps. CRARC command was used to generate the bucket portion while CRELLIPSE command was used to generate the top of the sluice opening. CRCONIC command was used to fit a parabolic curve at the base of the sluice opening. CRCONIC command requires the point of intersection of the two tangents at the ends of the curve to be fitted. Since the material around the five galleries is of 1.0 m. thick layer, extra points and thereby curves were generated to define these different material regions. These curves were now made to form different "contours" and later the "regions" for handling different materials in the dam section. In COSMOS word "contour" and "regions" are treated as different entities. Alongwith the nonoverflow section a part of the foundation with length equal to thrice the base width of

nonoverflow section and depth equal to height of the nonoverflow section is also modelled.

Finite Element Discretisation : These generated regions were now meshed with eight noded PLANE2D elements. The upper and lower portions of the nonoverflow section are meshed with elements of thickness 16.0 m. while elements in the middle sluice portion have a thickness of 8.5 m. Thickness of elements in the foundation is also taken equal to 16.0 m. Every time ACTSET command was used while generating the mesh for different material regions. The completed model is mapped with 2167 nodes and 615 elements. Base of the foundation is assumed fixed while at the sides of the foundation translation in longitudinal direction is restrained to apply the boundary conditions. Figure 3.3 shows the complete 2D finite element model of non-overflow section.

3.3.3 3D MODELLING OF THE NON-OVERFLOW SECTION

Generation of the geometry : To generate the 3D geometry of the nonoverflow section, regions were generated in similar fashion as were generated for 2D model. Since these regions were in a plane, so these regions were extruded to form the "polyhedra". "Polyhedra" is defined as a hollow entity in the COSMOS. The regions contributing to the geometry of the lower and upper portion of the dam were extruded by 16.0 m along the thickness of the section. To form the sluice portion of the dam, regions contributing to the geometry of this portion were copied first at a distance of 16.0 m. Now these regions were extruded to form the polyhedra corresponding to rectangular portion. Since the inner walls of the sluice portion are defined by an elliptical curve, ellipse were fitted first with the help of CRELLIPSE command. Now regions were dragged along these elliptical curves to form the inner walls of the sluice. This whole process generated the outer boundaries of the non-overflow section. Figure 3.4 shows the isometric view of the non-overflow section.

Finite Element Discretisation : Finite element discretisation of the 3D model of the non-overflow section was carried out exploiting the "solid meshing" feature of the COSMOS. Since the polyhedras formed so far were representing the hollow structure of the non-overflow section, a solid model was generated from these polyhedras using PART command. "PART" is another entity in COSMOS. Since the non-overflow section

41

have varying material properties at various sections, various polyhedras were converted to different PARTs in several steps. Now exploring the auto-meshing feature in COSMOS, MA_PART command was used to mesh the solid model with ten noded TETRA10 elements. The above command was used in several steps after ACTSET command to mesh the various portions with various material properties. After merging and compressing the nodes, the complete model is mapped with 905 nodes and 3450 elements. Finite element mesh of the completed 3D model of non-overflow section is depicted in Fig. 3.5.

3.3.4   2D MODELLING OF THE OVERFLOW SECTION

Generation of the geometry :   Generation of the 2D model of the overflow section was similar to non-overflow section except that the top of overflow section was provided with spillway. This spillway was generated by fitting the spline curve between the control points defining the spillway profile. Also there are two extra galleries for the operation of gate in overflow section. These two galleries were also defined as the two different regions.

Finite Element Discretisation :   Finite element discretisation of the 2D model of overflow section was also carried out in the similar way as of non-overflow section with PLANE2D elements. The completed model is mapped with 2293 nodes and 713 elements. Figure 3.6 shows the complete finite element 2D model of overflow section.

3.3.5   3D MODELLING OF THE OVERFLOW SECTION

Generation of the geometry :   3D modelling of the overflow section was also carried out as in the 3D non-overflow section. The pier portion at the top of the spillway was generated with thickness 1.5 m. at both the ends. Figure 3.7 shows the isometric view of the 3D model of the overflow section.

Finite Element Discretisation :   Again solid meshing feature of COSMOS was exploited. Element used are once again ten noded tetrahedral elements. Finite element

mesh of the completed 3D model of overflow section is depicted in Fig. 3.8. The completed model is mapped with 1062 nodes and 3570 elements.

Concluding Remarks: Generation of 2D models of both non-overflow and overflow sections was quite simple. "Spacing ratio" feature in COSMOS was used to generate the elements with increasing size in the foundation of 2D models. 3D modelling of both the sections was quite difficult due to shape of the sluice section. Since sluice opening is curved from all the sides, so curves were first required to generate the sluice opening. Also, generation of the spillway in the overflow section required special attention. Automeshing, specially solid meshing, is a very good feature in COSMOS but node compatibility has to be maintained at the curved portions.
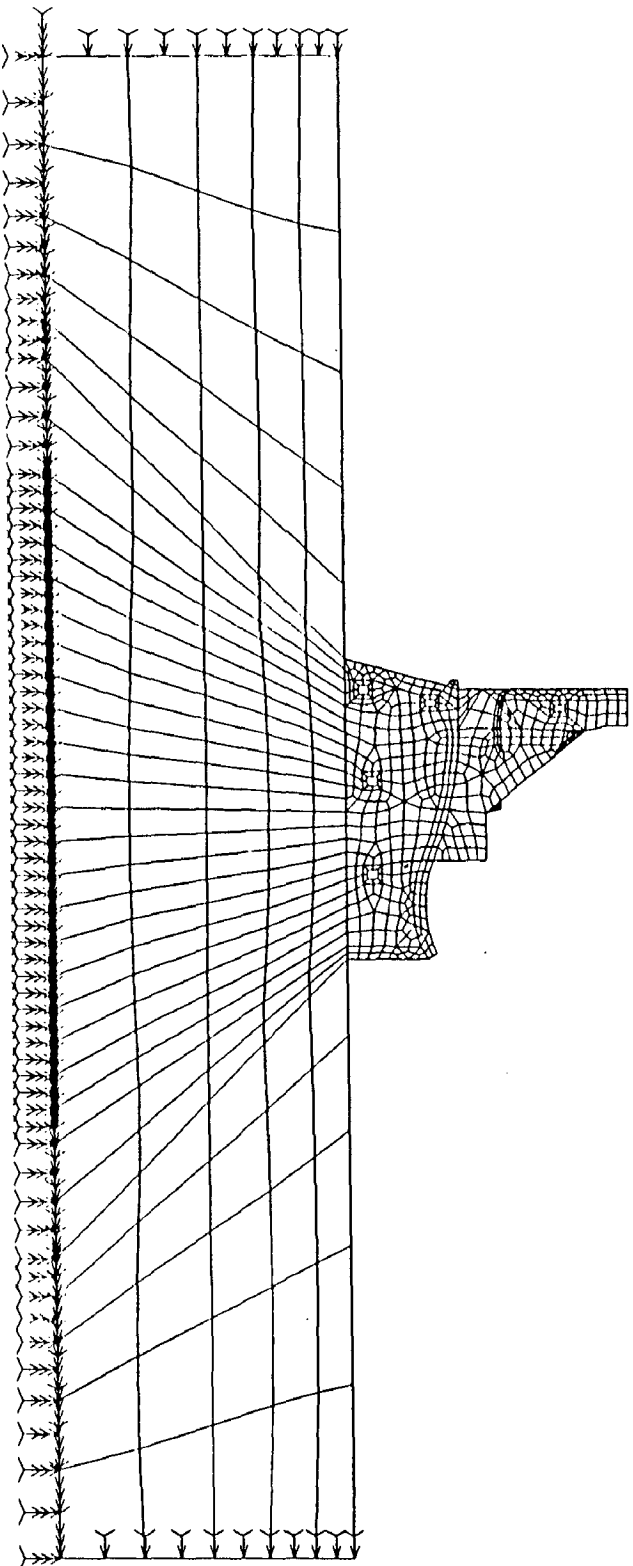
FIG. F.E. MESH AND BOUNDARY CONDITIONS OF MAXIMUM SLUICE SECTION WITHOUT
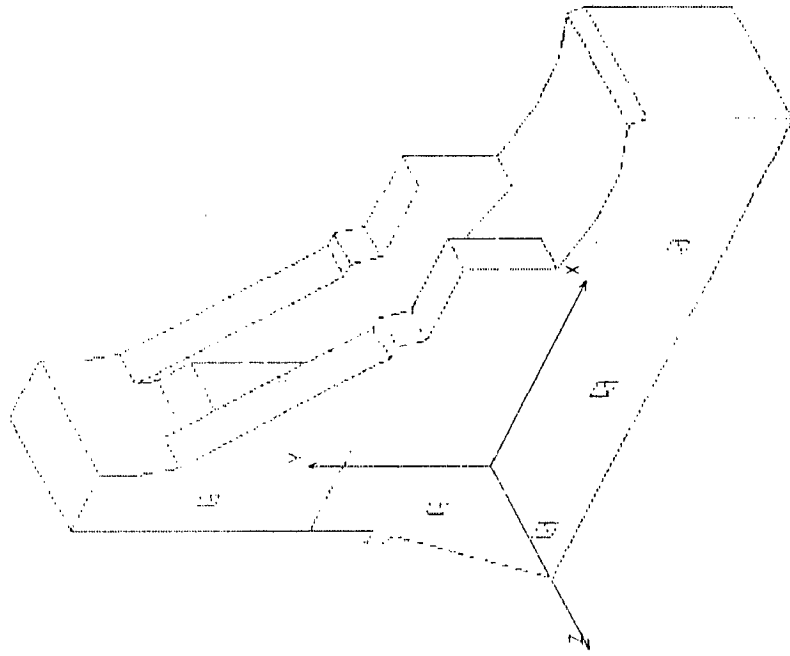CENTRAL SPILLWAY

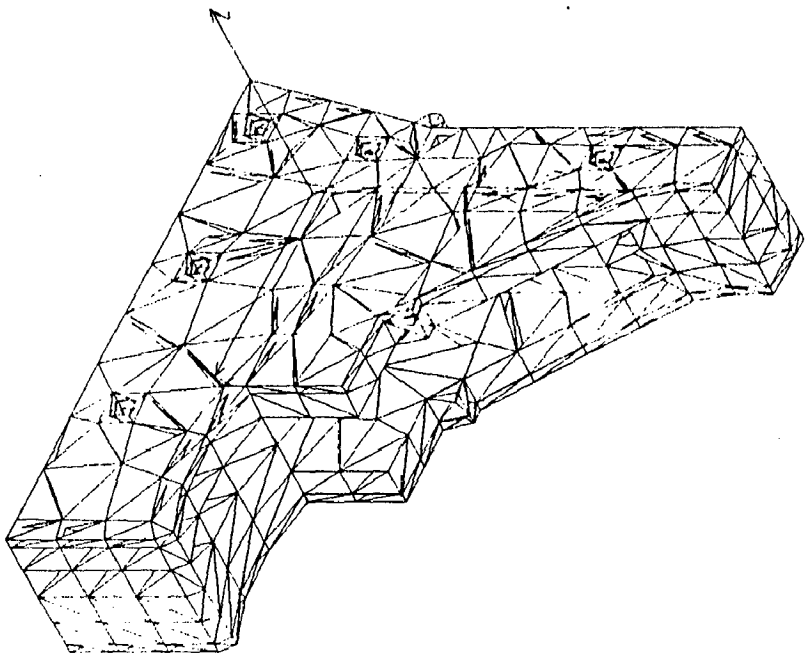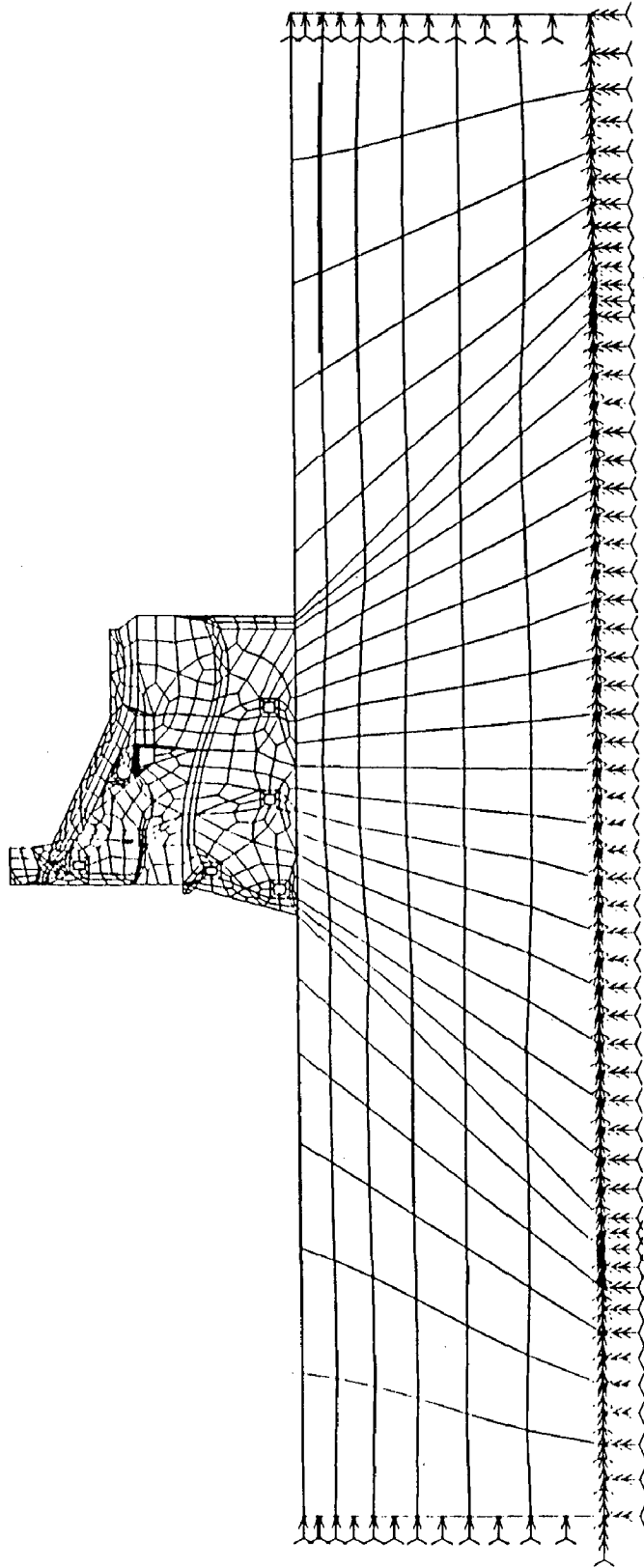Figure 3.3

44

Figure 3.4

45

Figure 3.5

46

FIG. F.E. MESH AND BOUNDARY CONDITIONS OF MAX. SLUICE, OVERFLOW AND CENTRAL SPILLWAY SECTIONS
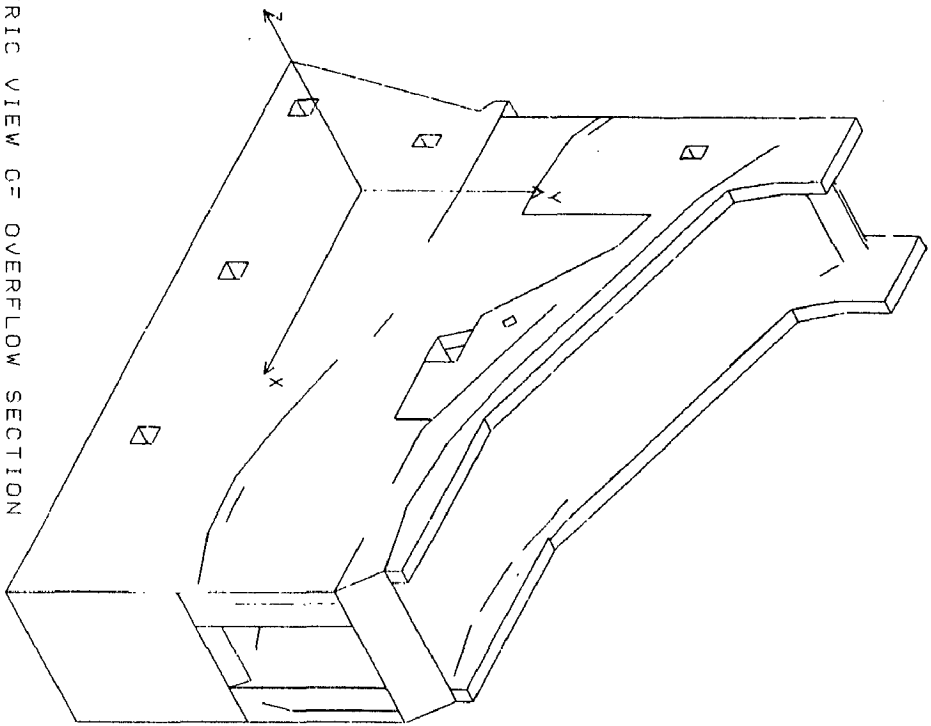
Figure 3.6
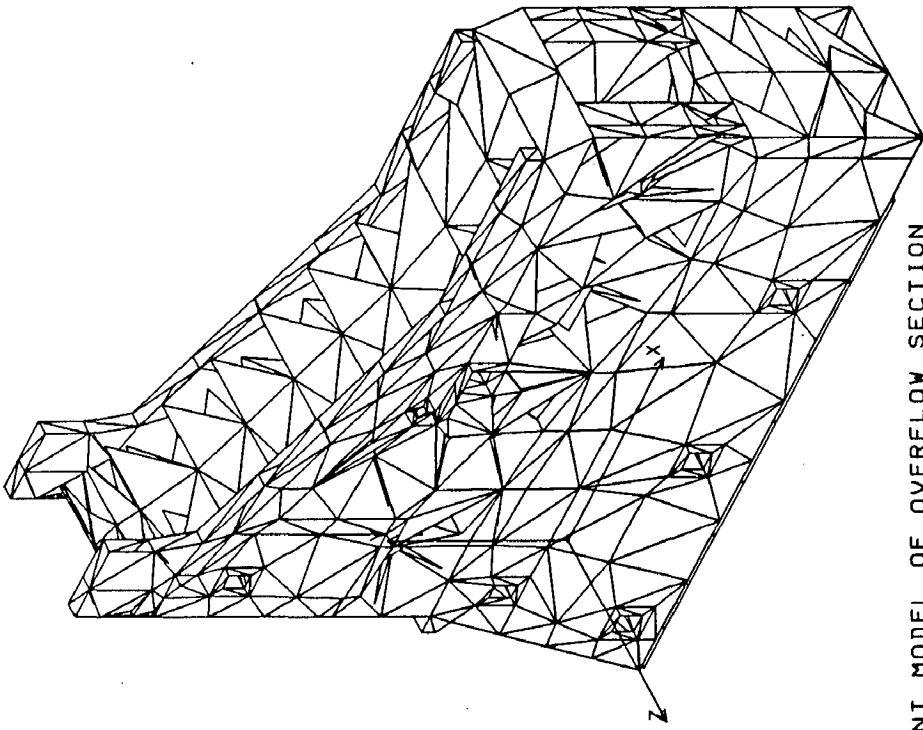
47

FIG. ISOMETRIC VIEW OF OVERFLOW SECTION

Fig. 3.7

48

FIG. 3D FINITE ELEMENT MODEL OF OVERFLOW SECTION

Fig. 3.8

49

3.4   PROBLEM- 3 :   A CONCRETE GRAVITY DAM (KOYNA DAM)

3.4.1   GENERAL DESCRIPTION OF THE DAM

Figure 3.9 shows the isometric view of the non-overflow section of the dam. The dam has a base width of 91.57 m and height of 103.022 m. The thickness of one block of the section of the dam is 15.24 m. The dam has a buttress portion starting at a height of 39.0144 m from the base and goes upto the top of the dam. The buttress portion tapers to downstream side from a thickness of 9.14m to 8.53m.

3.4.2   2D MODELLING OF THE DAM

The package requires to construct the geometry of the structure and then finite element discretisation is made. These steps are described here in brief :

Generation of the geometry: Generation of the geometry of the dam in 2D requires defining the plane in which geometry is to be built. After defining the X-Y plane, the control points at the face of the dam were generated and were joined by suitable curves. Using these curves, contours and then regions were defined. Care has been taken to define different regions for zones of different materials. In COSMOS word "region" defines an entity.

Finite Element Discretisation: The regions generated above were meshed with eight noded elements. The thickness of these elements for two dimensional plane stress analysis is taken as 15.24 m. For the tapering buttress portion of the dam the thickness of elements is taken as an average value of 8.885 m. For this study the dam has been considered fixed at the base. In order to apply these boundary conditions, curves at the base of the dam were identified and using the command DCR, boundary conditions were applied.

The structure is mapped with 1305 nodes and 402 elements. The elements used for two dimensional analysis are PLANE2D elements. Figure 3.10 shows the complete 2D finite element model with the boundary conditions.

247820

3.4.3 3D MODELLING OF THE DAM

Generation of the geometry: Regions at the face of the dam were generated in a similar way as were generated in 2D model but excluding the buttress portion of the dam. These regions were meshed with eight noded elements according to different material properties in different regions. These meshed regions were extruded in the lateral direction upto the thickness of the dam i.e. 15.24 m to form the twenty noded elements.

The buttress portion of the dam was generated in the form of two "volumes" for which points were first generated in three dimension space. During meshing of the buttress portion of the dam, NCRPUSH and ECHANGE features of COSMOS were exploited. While pushing the corner nodes care has to be taken that the mid side nodes are also pushed appropriately. ECHANGE command was used to change the eight noded elements to twenty noded elements as the volumes were first meshed with lower order elements.

The 3D model has 2733 nodes and 461 solid elements. Boundary conditions at the base of the dam are same as in 2D model. To apply the boundary conditions, surfaces and regions at the boundaries i.e. at the base and at the two sides were identified. At the two sides the movement in Z-direction (see Fig. 3.11) has been restrained in order to consider the restrained provided by the adjacent blocks.

3.4.4 MATERIAL PROPERTIES

Three different type of materials are used in the dam. The properties of the materials used in the dam are given in Table 3.1.

Table 3.1 Material Properties of the nonoverflow section of a concrete gravity dam: Prob3

S. No.	Type of the material	Young's Modulus (t/m^2)	Poission's Ratio	Density (t/m^3)
1.	Concrete 1	3.15e+06	0.15	2.48
2.	Concrete 2	4.00e+06	0.15	2.64
3.	Concrete 3	3.15e+06	0.15	2.59

3.4.5   FREE VIBRATION ANALYSIS OF THE DAM

Frequencies of natural vibration of the dam have been obtained by both the models i.e. the 2D and 3D models as described above. First ten natural frequencies and mode shapes are calculated. The method used to calculate the natural frequencies and mode shapes of the system was "Subspace iteration method". The convergence tolerance to be achieved was of the order of 1e-05. No virtual mass due to participation of the reservoir water has been considered.

3.4.6   RESULTS AND DISCUSSIONS

Table 3.2 gives the natural frequencies of the first ten modes of the dam for the two models :

Table 3.2 Natural Frequencies of nonoverflow section of a concrete gravity dam: Prob. 3

No. of mode	Frequency using two dimensional analysis (cycles/ sec)	Frequency using three dimensional analysis (cycles/ sec)
1.	4.48532	4.25073
2.	10.9747	10.7353
3.	12.0128	11.9368
4.	19.1841	14.7345
5.	26.2069	17.5443
6.	27.7415	18.1575
7.	31.4200	20.9582
8.	34.1099	21.0479
9.	37.1654	23.6161
10.	40.5113	25.0665

It is evident from the table 3.2 that frequencies upto fourth mode are nearly equal in both the cases, but beyond the fourth mode, the frequencies in 2D analysis increase sharply as compared to 3D analysis. Frequencies increase so sharply that

they reach beyond 33 Hz in eighth mode in 2D analysis while the frequencies reach only upto 25 Hz. even in tenth mode in case of 3D analysis. This is primarily due to inability of 2D model to represent all the frequencies.

In this variation the role played by the buttress portion of the dam is found to be very important. In 2D analysis, the thickness of the buttress portion is taken as an average of 8.885 m. instead of tapering from 9.14m. to 8.53 m. The taper was modelled exactly in the 3D analysis. The average thickness of the buttress did not influence first few frequencies and therefore modelling as such is quite acceptable.

Figures 3.12 to 3.17 show the mode shapes of the dam for 2D and 3D models. From the analysis of results it is found that in both the cases i.e. either using 2D or 3D analysis, first and second mode are transverse modes of vibration while the third mode is the vertical mode.

It is interesting to note that the fourth mode is predominantly the transverse vibration of the buttress of the dam. This was clearly visible in the animation of the mode. This is due to the restrained on the two sides of the dam in three dimensional analysis. Only the buttress portion was free to vibrate. The 2D modelling is, however, unable to predict this and therefore it is the limitation of the 2D model.

Concluding Remarks: For drawing and meshing the 2D model the pre-processor was used with ease. But for 3D model generation required a careful handling of the pre-processor. Solver of the software was very powerful to solve the problem within seconds. Also post-processor is capable of animating the various mode shapes as it would appear. Analysis of the dam was carried out for the natural frequencies with 2D and 3D modelling. From the above analysis conclusion is drawn that the first few frequencies and mode of vibration compare very well in the two cases. In 2D modelling of the buttress with an average thickness has yielded fairly good comparison of first few frequencies indicating that average thickness can be adopted without much loss of accuracy. The 2D modelling can therefore be used for analysis of a dam keeping in mind its limitations. The 3D analysis has predicted the transverse vibration of the buttress in the fourth mode while the 2D model was unable to predict this.

Figure 3.9

54
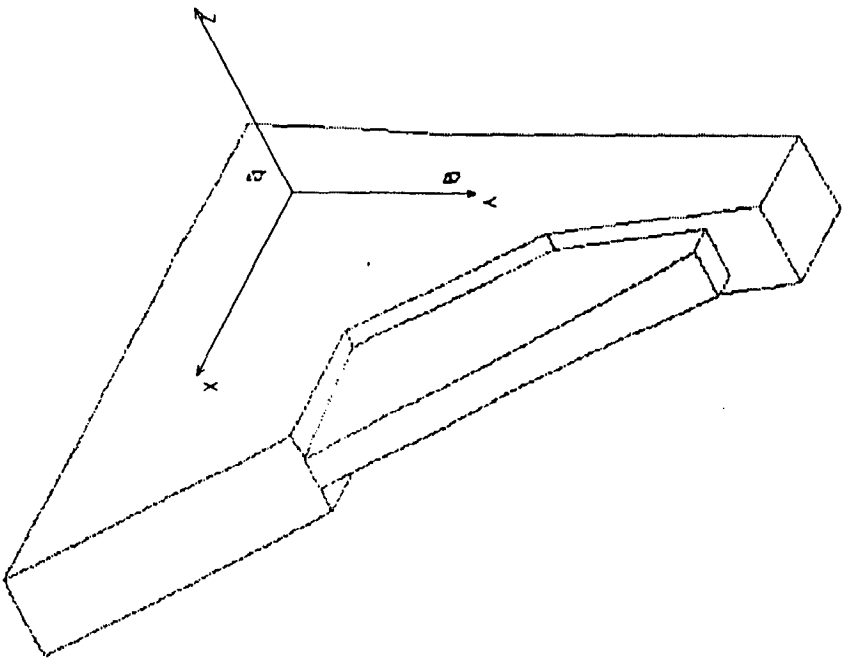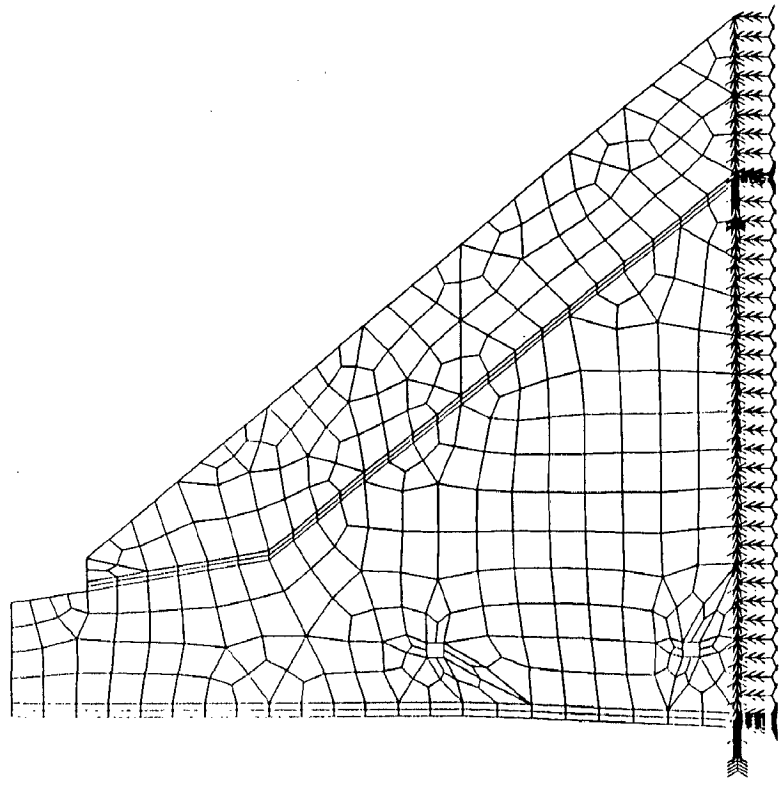
FIG. F.E. MESH WITH BOUNDARY CONDITIONS

Figure 3.10

55

FIG. F.E. MESH

Figure 3.11

F_Mode=1   4.5   Hz

FIG. FIRST MODE : TRANSVERSE MODE

Figure 3.12

57

F_Mode=2   11   Hz

FIG. SECOND MODE : TRANSVERSE MODE

Figure 3.13

58

F_Mode=3   12   Hz

FIG. THIRD MODE : VERTICAL MODE

Figure 3.14

59

F_Mode=1   4.3   Hz

Fig. 3.15

60

F_Mode=2   11   Hz

Fig. 3.16

61

Fig. 3.17

3.5 PROBLEM- 4: NON-OVERFLOW SECTION OF A DAM

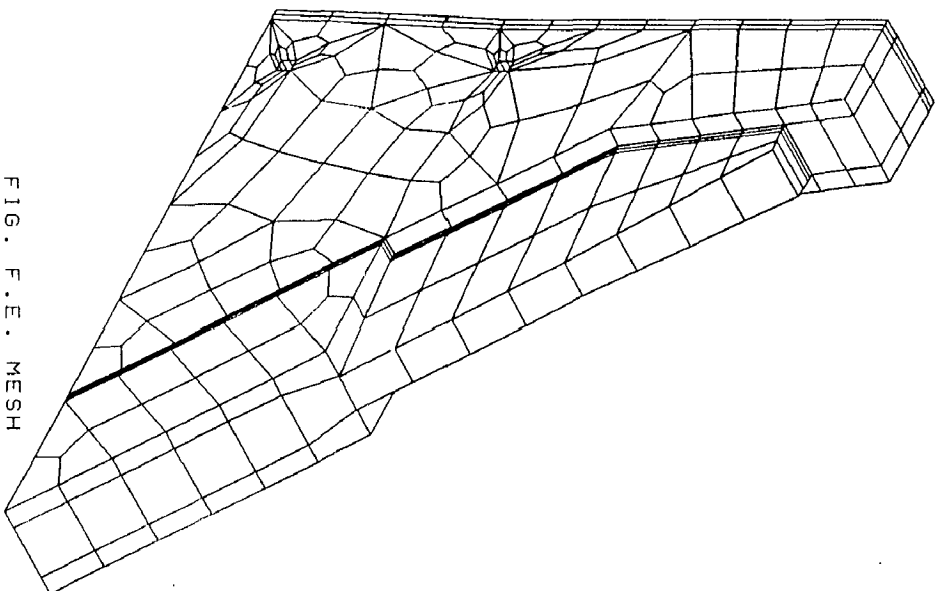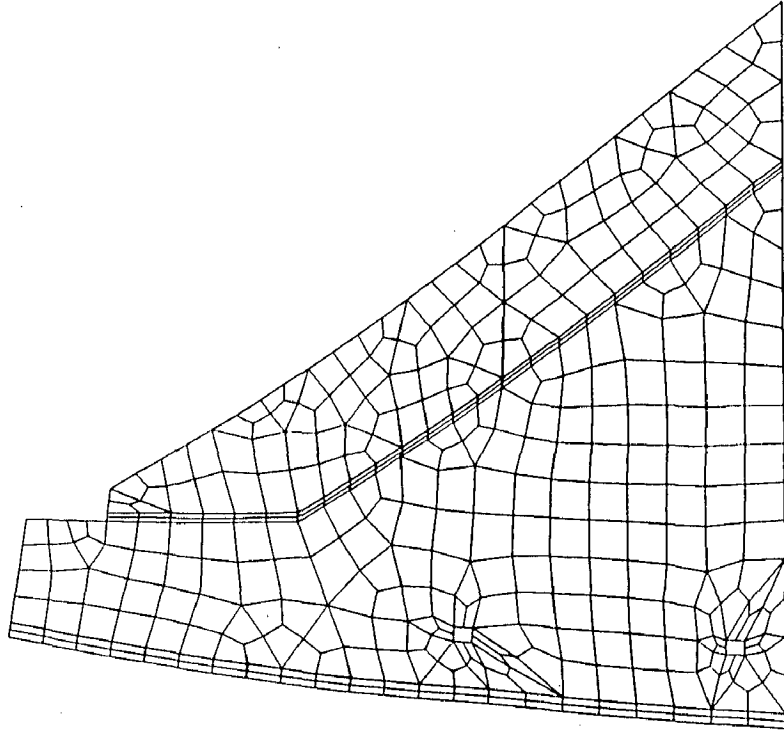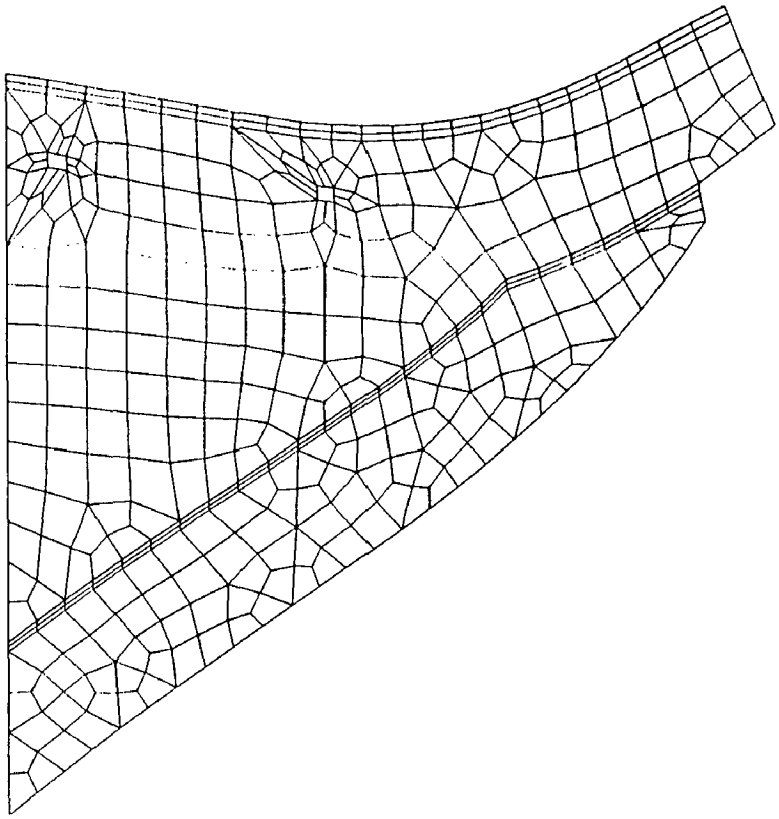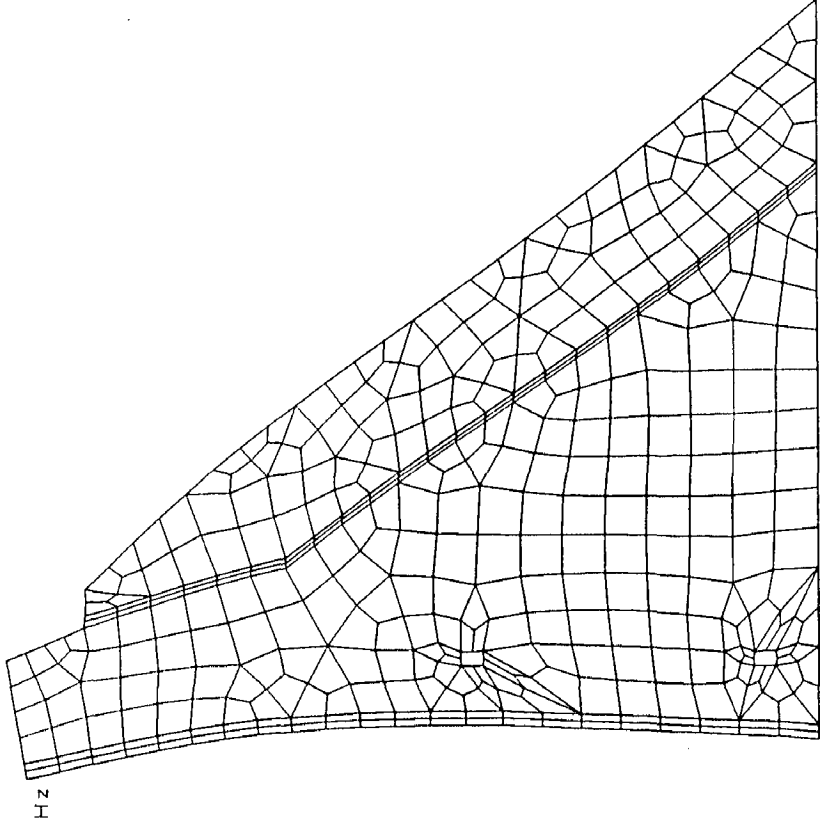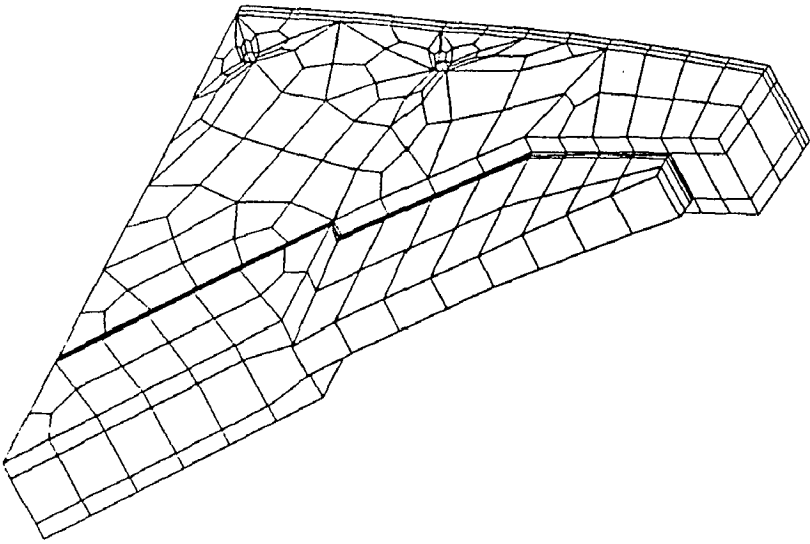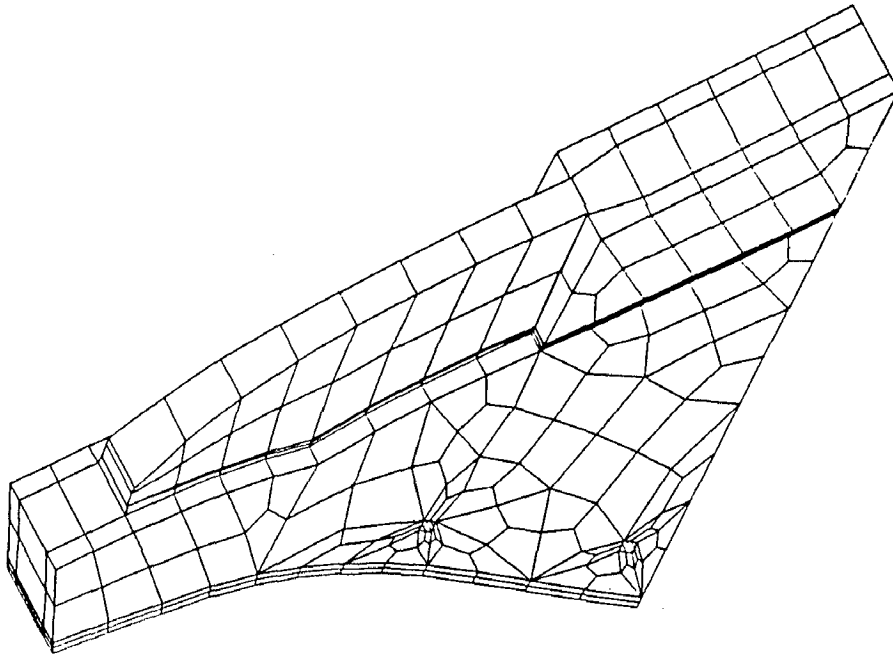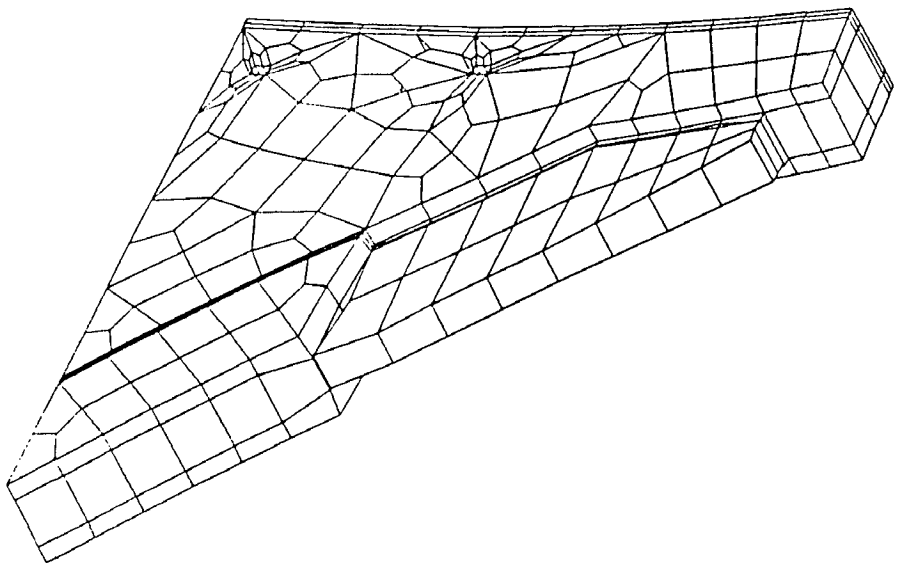In this problem analysis has been carried out for the non-overflow section of a dam with the use of 2D modelling. Foundation is also modelled alongwith the non-overflow section. Effect of inclusion of hydrodynamic mass on the natural frequencies of non overflow section of dam has been studied. Static analysis of non overflow section subjected to hydrostatic pressure, uplift and gravity loading has been carried out. Dynamic analysis of the non-overflow section subjected to earthquake in X-direction considering virtual mass of the reservoir water is also carried out.

3.5.1 GENERAL DESCRIPTION OF THE DAM

The non-overflow section of the dam has a height of 25.6 m and base width of 17.21 m. Non overflow section is analyzed using two dimensional model of the dam with unit thickness. In addition foundation portion with depth (25.4 m.) nearly equal to the height of the dam and length equal to thrice the base width of non overflow section is also considered in two dimensional model.

Generation of the model: As carried out in previous problem points were first located in X-Y plane and after joining them by suitable curves contours and regions were formed. While joining the points by curves CRFILLET feature of COSMOS was explored to form the throat section of the non overflow section. Before going for generation of the foundation, these regions were meshed with eight noded PLANE2D elements exploring "Auto Meshing" feature in COSMOS. Foundation section was generated after meshing the non overflow section to have the node compatibility. Meshing of the foundation was carried out with similar eight noded PLANE2D elements. But while meshing the foundation, "spacing ratio" feature in the COSMOS was explored. The elements in the foundation are of bigger size as compared to non-overflow section. After merging the nodes and elements the completed model has 1607 nodes and 486 elements.

Hydrodynamic pressure is cosidered as equivalent lumped mass. Virtual mass was calculated separately at the various wet nodes and the masses so obtained were lumped at the appropriate nodes. The thickness of all these two dimensional elements was taken equal to unity. Foundation of the model is assumed fixed at the base and is

63

restrained from translation in X-direction. Applying these boundary conditions led to the complete two dimensional model. Figure 3.18 shows the complete finite element model with the boundary conditions.

3.5.2 MATERIAL PROPERTIES

Materials used in the non-overflow section have the material properties as given in table 3.3:

Table 3.3 Material properties of nonoverflow section of a dam: Problem 4

Type of material	Section at which material was used	Young's modulus (t/m^2)	Poison's Ratio	Density (t/m^3)
material 1	non overflow section	4.0e+06	0.15	2.64
material 2	Foundation of non-overflow section	7.0e+06	0.15	2.9

3.5.3 LOADS APPLIED

For the non overflow section uplift and hydrostatic pressure are applied on the model. Hydrodynamic pressure is also taken into account in the form of virtual mass lumped at the appropriate nodes. Static analysis is carried out with these forces acting on the model and including the effect of gravity. Dynamic analysis is carried out with earthquake along the X direction.

3.5.4 FREE VIBRATION ANALYSIS

Free vibration analysis is carried out using subspace iteration method. Frequencies and mode shapes of first four modes are calculated.

3.5.5 RESULTS AND DISCUSSION

3.5.5.1 Frequency Analysis

Table 3.4 shows the results of the frequency analysis as obtained from the two cases viz. including the hydrodynamic mass and excluding the hydrodynamic mass.

Table 3.4 Natural Frequencies of nonoverflow section of a dam: Problem 4

Mode No.	Frequency without hydrodynamic mass (in cycles / sec)	Frequency with hydrodynamic mass (in cycles / sec)
1	13.0412	11.4167
2	32.1723	27.0076
3	33.4471	33.0914
4	43.5620	41.4990

From the analysis it is found that in both the cases fundamental mode and second mode are the transverse modes while third mode is vertical mode in both the cases.

It is self explanatory from the above table that inclusion of the hydrodynamic mass tends to decrease the natural frequency of the system.

3.5.5.2 Static Analysis

Table 3.5 shows the maximum stresses and maximum displacements calculated after static analysis as well as after dynamic analysis. Figure 3.19 shows the resultant displacement contour.

Displacements at the base of the non overflow section are between 0.15 mm. and 0.20 mm. At the top of the dam displacements are around 0.41 mm. In the lower

half of the dam, the displacements are between 0.15 mm. and 0.25 mm. while in the upper half displacements were in between 0.30 mm. and 0.41 mm.

Table 3.5 Results of the static and dynamic analysis of nonoverflow section: Problem 4

	Static Analysis	Dynamic Analysis
Maximum Displacement	0.41269 mm.	3.73000 mm.
Minimum Displacement	1 e -016 mm.	1 e -016 mm.
Maximum Major Principal Stress	34.483 t / m^2 (tension)	412.181 t / m^2 (tension)
Minimum Major Principal Stress	26.130 t / m^2 (compression)	No tension or Compression
Maximum Minor Principal Stress	88.448 t / m^2 (compression)	101.984 t / m^2 (tension)
Minimum Minor Principal Stress	5.322 t / m^2 (compression)	26.455 t / m^2 (compression)

The contours plot for major principal stresses show that the stresses at the bottom corner on the upstream of non overflow section are tensile and are between 26.9 t / m^2 and 34.5 t / m^2. This is due to the fact that hydrostatic pressure as well as uplift pressure have their maximum values at this point. Also weight acting on this point of non overflow section is maximum as compared to any other point of the non overflow section. Same figure also shows the compressive stresses in the zone just above the bottom corner and were spread upto the half of the non overflow section on upstream side with values ranging from 26.1 t / m^2 to 3.4 t / m^2 on moving from bottom to top.

In the plot of minor principal stresses almost whole of the non overflow section was under the effect of compressive stresses. The compressive stresses were maximum at the downstream bottom corner of the non overflow section with value 77.3 t / m^2 while at the bottom corner of the upstream these stresses were of the order of

10.4 t/ m^2. In the lower half the compressive stresses were increasing from 21.6 t/ m^2 to 55.0 t/ m^2 on moving towards the base of the non overflow section. In the upper half the compressive stresses were ranging from zero to 21.6 t/ m^2. In the topmost fibers there was very little tension of the order of 0.74 t/ m^2. As it is clear from the figure maximum compressive stress of 88.4 t/ m^2 was at the bottom of the foundation.

3.5.5.3 Dynamic Analysis

Dynamic analysis is carried out for earthquake in transverse direction using the response spectra method. First three modes are used for analysis and CQC method is used for combining the modes. Effect of foundation is also taken into account for dynamic analysis. A 5% damping is cosidered in all the modes in the analysis.

Table 3.5 gives the values of maximum displacements and maximum stresses calculated after dynamic analysis. Minimum displacement is found at the base of the non overflow section as approximately equal to zero and maximum at the top of the dam of the order of the 3.7 mm.

Figures. 3.20 - 3.21 show the contours for major principal stresses and minor principal stresses respectively for dynamic analysis. Maximum major principal stress is found at the bottom corner on the upstream side of the non overflow section and is of the order of 361 t/ m^2 tension. No tension zone at the top of the dam is found as the least major principal stress zone.

Maximum minor principal stress is found somewhat inner to the bottom corner on the upstream side of non overflow section. These stresses are of the order of 102 t/ m^2 tension. Minimum stress in the form of compression of the order of 26.5 t/ m^2 are there in the middle of the non overflow section. On the upstream side the minor principal stresses are tensile stresses with values in between 5.65 t/ m^2 and 21.7 t/ m^2.

Concluding Remarks: 2D modelling of the non-overflow section has been carried out easily. Frequency analyses with and without the inclusion of hydrodynamic pressure lead that hydrodynamic pressure tends to decrease the natural frequencies of

the system. Maximum principal stress, in static analysis, at the upstream bottom corner of the non overflow section are found to be maximum because hydrostatic pressure, uplift as well as weight of the dam are maximum at this point.
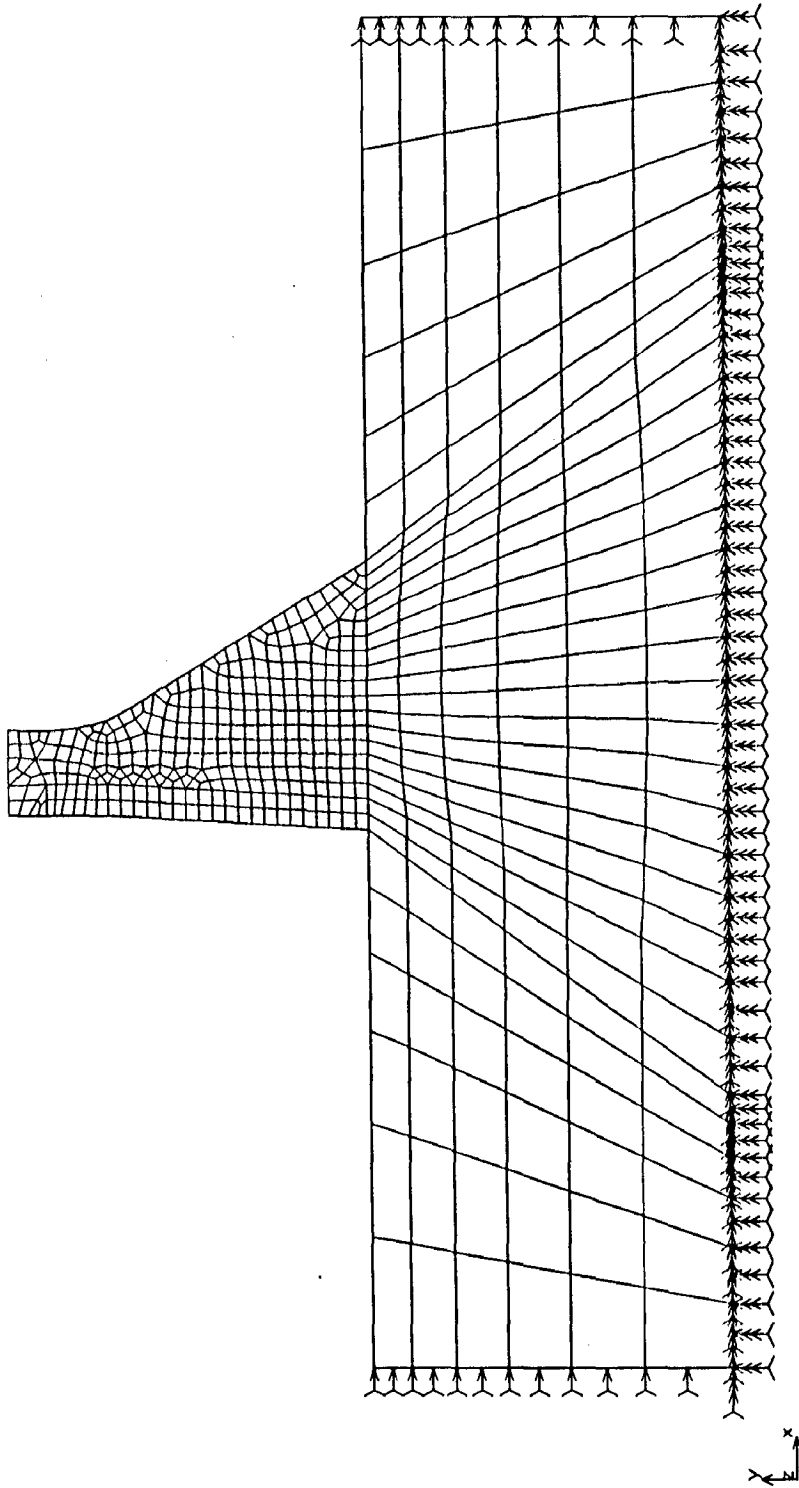
FIG. F.E.M. MESH WITH BOUNDARY CONDITIONS

Fig. 3.18

69
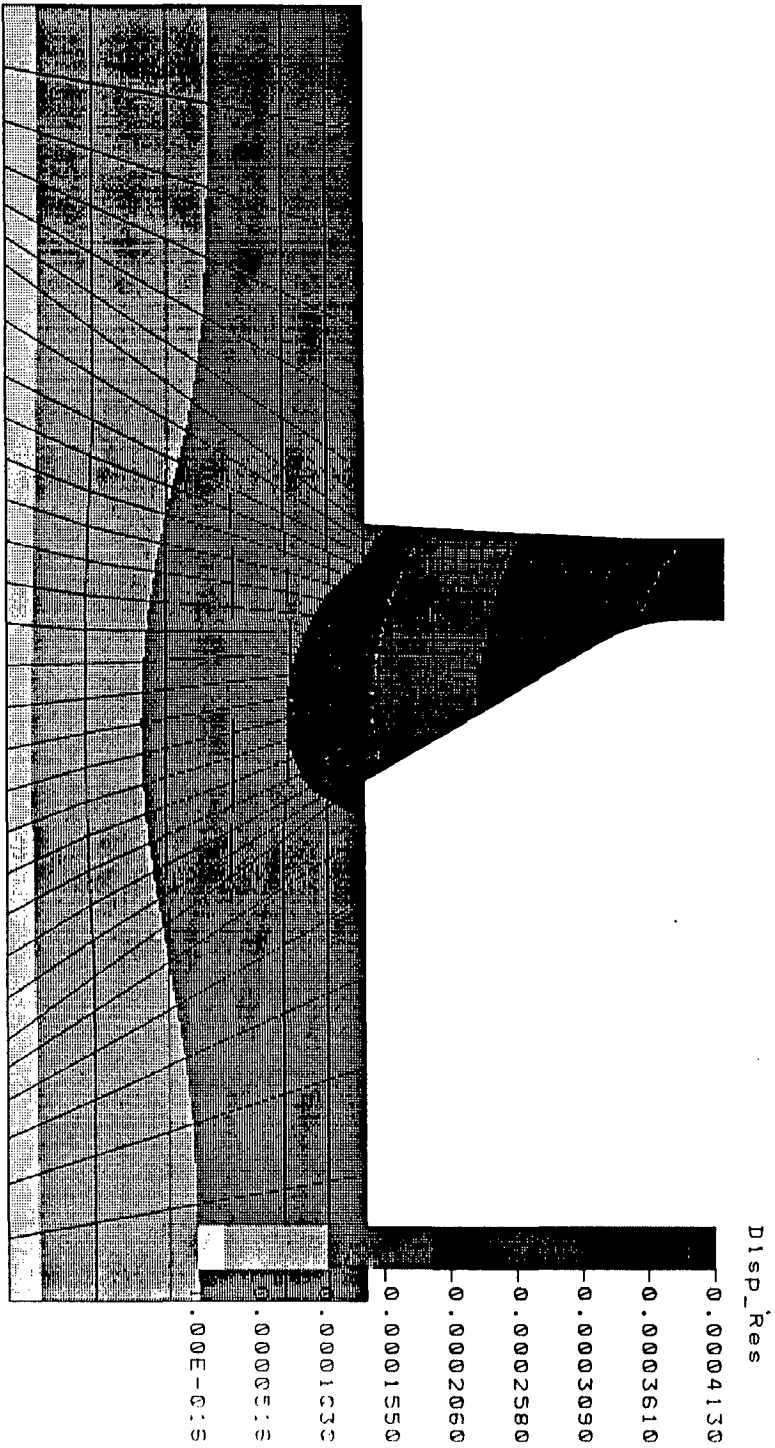
FIG. DISPLACEMENT CONTOUR FOR STATIC ANALYSIS

Fig. 3.19

Disp_Res

0.0004130
0.0003610
0.0003090
0.0002580
0.0002060
0.0001550
0.0001030
.00005
.00E-0

PDN Step:1   =0

Princ_1
412.00
361.00
309.00
258.00
206.00
155.00
103.00
51.500
0.0000

FIG. MAJOR PRINCIPAL STRESS CONTOUR : EARTHQUAKE IN X-DIR.

Fig. 3.20

71

FIG. MINOR PRINCIPAL STRESS CONTOUR : EARTHQUAKE IN Y-DIR.

Fig. 3.21

72

3.6 PROBLEM- 5: ANALYSIS OF PIER SECTION OF A DAM: PIER 1

A pier over an overflow section of a dam subjected to static loads (i.e. water pressure, uplift and gate reaction) and for earthquake forces has been solved and its behaviour studied.

3.6.1 GENERAL DESCRIPTION OF THE DAM

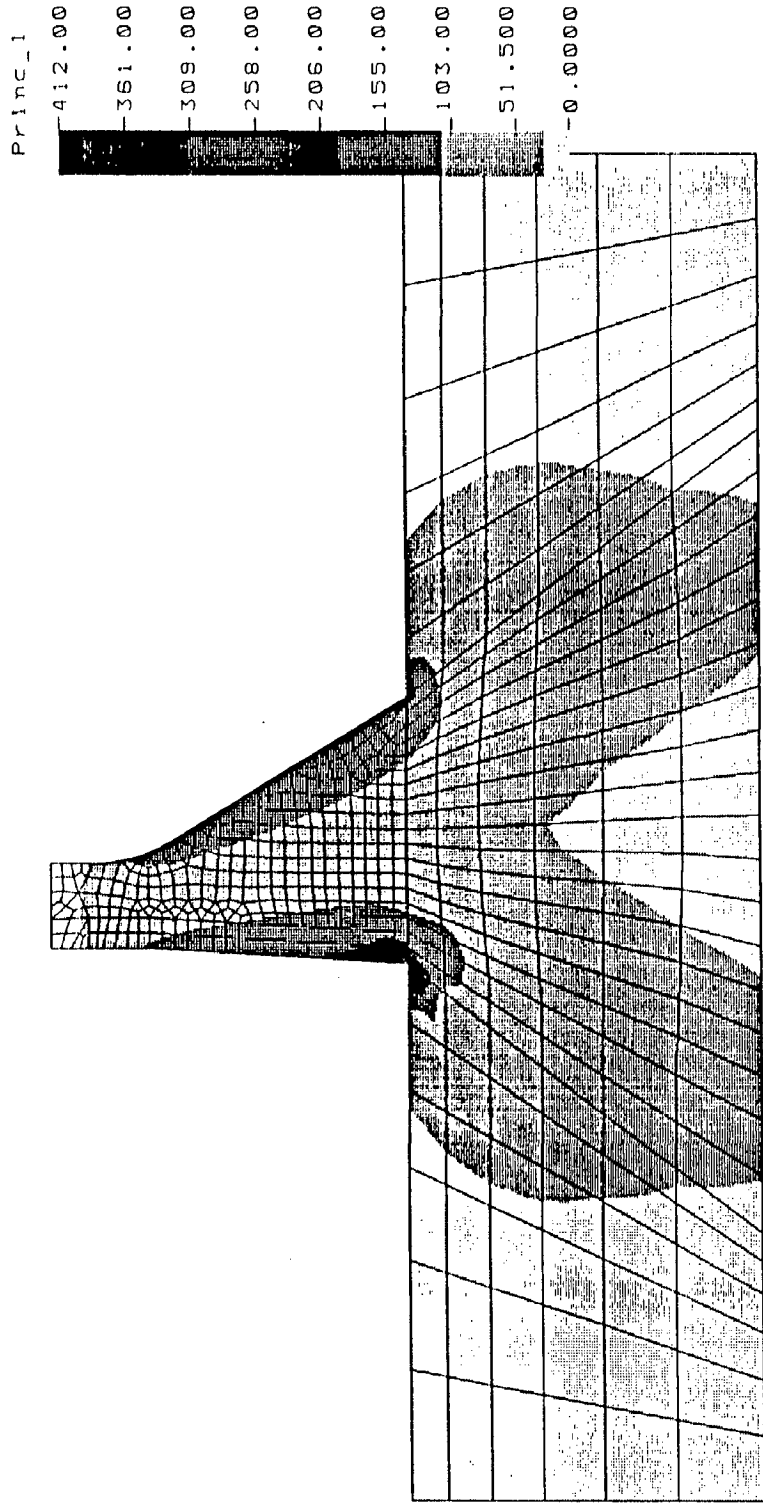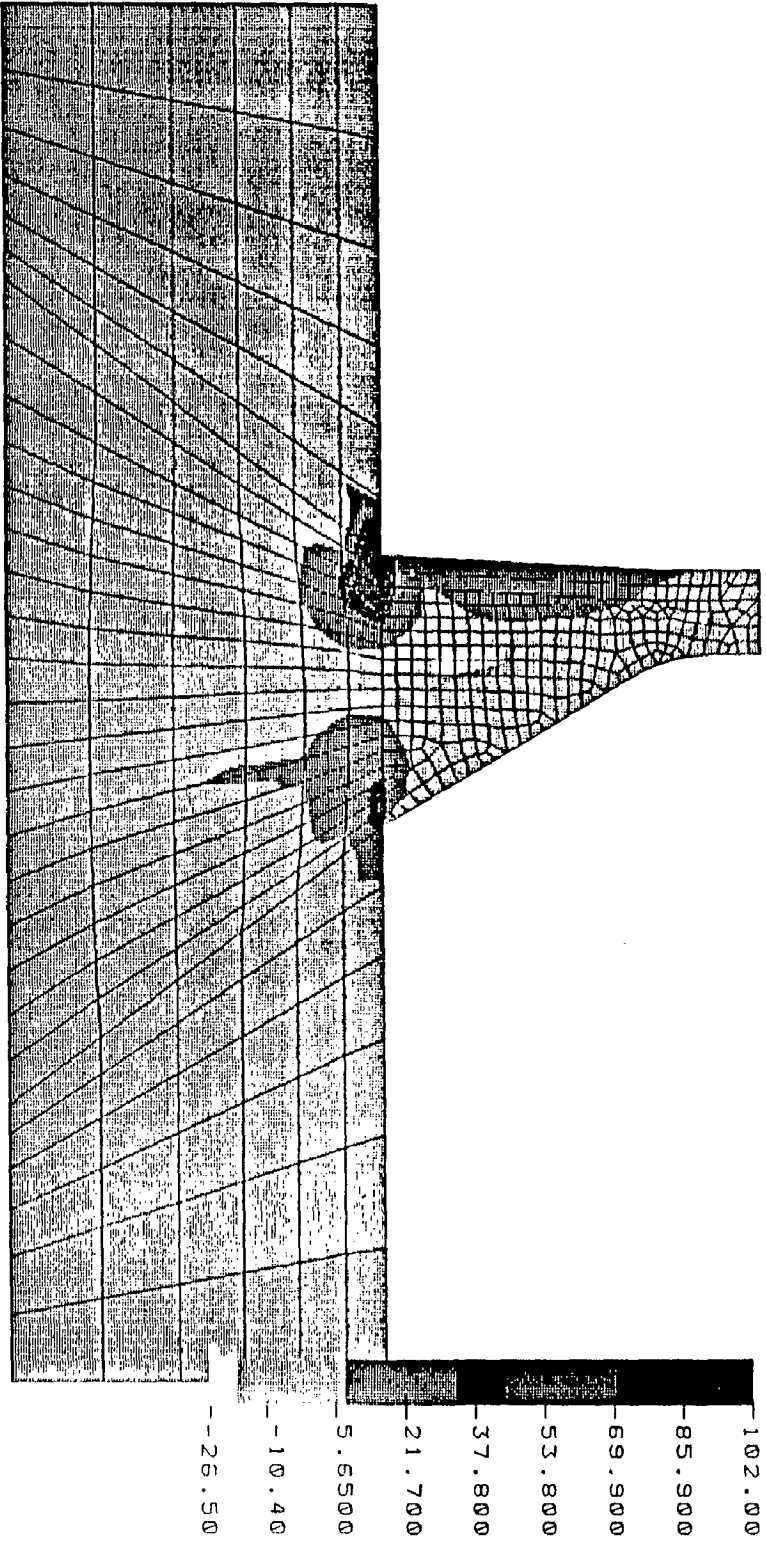Pier section of the dam is built up of uniform material i.e. M-15 concrete. Pier has a thickness of 3 m and has a curved portion of diameter 3 m on the upstream side. The height of the pier section is equal to 25.8 m. Lower portion of the pier is a curve joined by splines. Pier has gates on both the sides and is analyzed for gate opened on one side while on the other side of the pier the gate is closed. Figure 3.22 shows the isometric view of the pier.

Generation of the model: Generation of the pier section model was started from the central section of the pier. Points were located first and then were joined by suitable curves. Base of the pier section was generated after joining the points by splines. While generating any model in COSMOS, curves, surfaces or regions must be generated in the model where boundary conditions or loads are to be applied. So after generation of curves at the central section of the pier further new curves were formed to apply the hydrostatic pressure on the pier section as gate on one side of the pier is taken as closed. Meshing was started at the central section of the pier with eight noded elements but this time instead of going for "auto meshing", another feature of the software called "parametric meshing" was explored. These elements were changed to twenty noded solid elements using "extrusion" feature. But using this feature caused problem of node compatibility as the pier section has a groove of 1.15 m depth. To solve this problem extrusion was carried out in four steps. To generate the curved portion at the upstream of the pier "dragging" feature was used.

After merging of nodes and elements complete model had 1033 nodes and 674 solid elements. Effect of hydrodynamic pressure is also taken into account for the pier. Figure 3.23 shows the complete finite element model of the pier. Boundary conditions on the pier section of the model are applied as the fixed base.

3.6.2 MATERIAL PROPERTIES

Material used in the pier section has the material properties as given in table 3.6.

Table 3.6 Material Properties of Pier 1: Problem 5

Type of material	Young's modulus (t/m^2)	Poison's Ratio	Density (t/m^3)
M-15 concrete	2.2076e+06	0.15	2.40

3.6.3 LOADS APPLIED

Pier is subjected to hydrostatic forces and uplift. In addition, two components of the weight of the bridge at the top of the pier and hoist reaction at the downstream are also considered. Static analysis is carried out with these forces acting on the model and including the effect of gravity. Dynamic analysis is carried out with earthquake along the pier axis direction as well as pier thickness direction.

3.6.4 FREE VIBRATION ANALYSIS

Free vibration analysis is carried out using subspace iteration method. Frequencies and mode shapes of first four modes are calculated. The frequencies have been calculated upto 33 Hz.

3.6.5 RESULTS AND DISCUSSION

3.6.5.1 Frequency Analysis

Table 3.7 shows the natural frequencies computed in the first five modes of the system :

Table 3.7 Natural Frequencies of the Pier 1: Problem 5

Mode No.	Frequency (in cycles / sec)
1	7.065
2	16.980
3	22.512
4	34.172

It is observed that the first mode is along the pier thickness while third mode is along the pier axis. This is due to the fact that the stiffness along the pier thickness is lesser as compared to the stiffness along pier axis. Second mode is the twisting mode. Figures 3.24 - 3.26 show the mode shapes of the pier.

3.6.5.2 Static Analysis

Table 3.8 shows the various displacements and stresses after static analysis :

Table 3.8 Results of Static Analysis of Pier 1: Problem 5

	Results of Static Analysis
Maximum Displacement	0.40352 mm.
Minimum Displacement	1 e - 016 mm.
Maximum Major Principal Stress	419.963 t / m^2 (tension)
Minimum Major Principal Stress	17.153 t / m^2 (compression)
Maximum Intermediate Principal Stress	46.303 t / m^2 (tension)
Minimum Intermediate Principal Stress	37.0035 t / m^2 (compression)
Maximum Minor Principal Stress	194.16 t / m^2 (compression)
Minimum Minor Principal Stress	10.273 t / m^2 (compression)

Figure 3.27 shows the displacement contours for static analysis. Displacements are increasing from bottom to top with maximum displacements at the top corner on

upstream side of the pier with value 0.404 mm. Displacements at the node at which hoist reaction is acting as tension along pier axis is of the order of 0.35 mm.

Figures 3.28 - 3.30 show the contours of major principal stresses, intermediate principal stresses and minor principal stresses respectively for static analysis case.

Major principal stresses in most of the pier section are between zero and 37.5 t / m^2 tension. The major principal stresses in the zone where load of the bridge is acting are in the form of maximum compressive stress with value 17.2 t / m^2. Since hoist reaction is applied as tension, in response major principal stress is maximum tensile stress of the order of 365 t / m^2 in this region.

Intermediate principal stresses in most of the pier section are compressive stresses. But there is tensile stress of the order of 35.9 t / m^2 in the zone where hoist reaction is applied. Compressive stresses are of the order of 26.6 t / m^2 at the nodes where bridge load is acting.

Minor principal stresses in whole of the pier are of compressive nature with minimum value between zero and 10 t / m^2 at the base of the pier on upstream side while maximum in the hoist reaction zone with value 169 t / m^2.

3.6.5.3 Dynamic Analysis

Dynamic analysis is carried out using the response spectra method. First four modes are used for analysis and CQC method is used for mode combination. Dynamic analysis is carried out with earthquake along pier thickness direction as well as along pier axis direction. No hydrostatic pressure or uplift is taken into account while carrying out the dynamic analysis. Table 3.9 shows the results of the dynamic analysis in two perpendicular earthquake directions :

Earthquake along pier axis direction

Table 3.9 lists the maximum displacements as well as the maximum stresses using the earthquake in two perpendicular direction.

Table 3.9 Results of the Dynamic Analysis of Pier 1: Problem 5

	Earthquake along pier axis direction	Earthquake along pier thickness direction
Maximum displacement	0.427734 mm.	7.57107 mm.
Minimum Displacement	1 e - 016 mm.	1 e - 016 mm.
Maximum Major Principal Stress	123.175 t / m^2 (tension)	892.78 t / m^2 (tension)
Minimum Major Principal Stress	No tension or Compression	No tension or Compression
Maximum Intermediate Principal Stress	47.166 t / m^2 (tension)	172.755 t / m^2 (tension)
Minimum Intermediate Principal Stress	9.276 t / m^2 (compression)	6.740 t / m^2 (compression)
Maximum Minor Principal Stress	38.371 t / m^2 (compression)	89.183 t / m^2 (tension)
Minimum Minor Principal Stress	No tension or Compression	63.083 t / m^2 (compression)

Displacement contours are shown in the Fig. 3.31. Maximum displacements are there with a value around 0.40 mm at the top of the pier. Contours for major principal stress, intermediate principal stress and minor principal stress are shown in the Figs. 3.32 - 3.34 respectively for earthquake along pier axis direction.

In whole of the pier section major principal stresses are of tensile nature with value ranging from zero to 123 t / m^2. Maximum major principal stresses of the order of 123 t / m^2 tensile stress at the base of the dam are there on the upstream side of the pier.

Intermediate principal stresses are of compressive nature in whole of the pier section with value ranging from zero to 9.28 t/ m^2 except the regions in which major principal stresses are maximum (henceforth called zone A) and some portion on the downstream of the pier. In these two zones there are intermediate principal stresses of the order of 18.9 t/ m^2 tension.

Minor principal stresses are of compressive nature with value ranging from zero to 38.4 t/ m^2 in whole of the pier. The maximum minor principal stresses are of the order of 33 t/ m^2 in zone A. Except the middle portion of the pier in which minor principal stresses are between 6.39 t/ m^2 and 17.1 t/ m^2, these stresses are between zero and 6.39 t/ m^2 in rest of the pier.

Earthquake along pier thickness direction

On changing the direction of earthquake along pier thickness from pier axis direction, there is no change in the pattern of the displacements as it is depicted in Fig. 3.35, but values are increased tremendously. Again minimum displacements at the base of the pier are zero and maximum at the top of the pier but this time with values around 7.5 mm. Displacements increased so vigorously since the stiffness of the pier along the pier thickness was lesser as compare to pier axis direction.

Contours for major principal stress, intermediate principal stress and minor principal stress are shown in the Figs. 3.36 - 3.38 respectively for earthquake along pier thickness direction.

Again major principal stresses are maximum in zone A with values around 78 t/ m^2 and of tensile nature, of course. Whole of the pier is found under the influence of tension while evaluating major principal stresses. Least major principal stress is at the extreme top and extreme bottom of the pier.

Intermediate principal stresses in zone A are of tensile nature with values ranging from 105 t/ m^2 to 150 t/ m^2. Rest of the pier has intermediate principal stresses around 15.7 t/ m^2 tension.

Minor principal stresses are of the compressive nature in whole of the pier with values ranging from 5.98 t/ m² to 63.1 t/ m² with tension of 51.1 t/ m² in zone A only.

Concluding Remarks: Pre-processor of the software has been found to work efficiently in 2D modelling but 3D modelling of the pier was very difficult due to the groove on the upstream side. So preprocessor was not much efficient with auto meshing as node compatibility was being lost. Switching to parametric meshing reduced the level of trouble. Again solver was very fast and efficient in carrying out the various analyses. Frequency analysis shows that the first mode is along the pier thickness direction. This is due to the fact that stiffness of the pier in this direction is lesser as compared to pier axis direction. Displacements are maximum at the top of the pier. Displacements are very large when earthquake is applied along pier thickness. Here stiffness of the pier along the pier thickness plays a significant role. Effect of the weight of the bridge and hoist reaction on the stresses is more or less local. Dynamic analysis shows the high stresses in the lower portion of the pier on the upstream side.
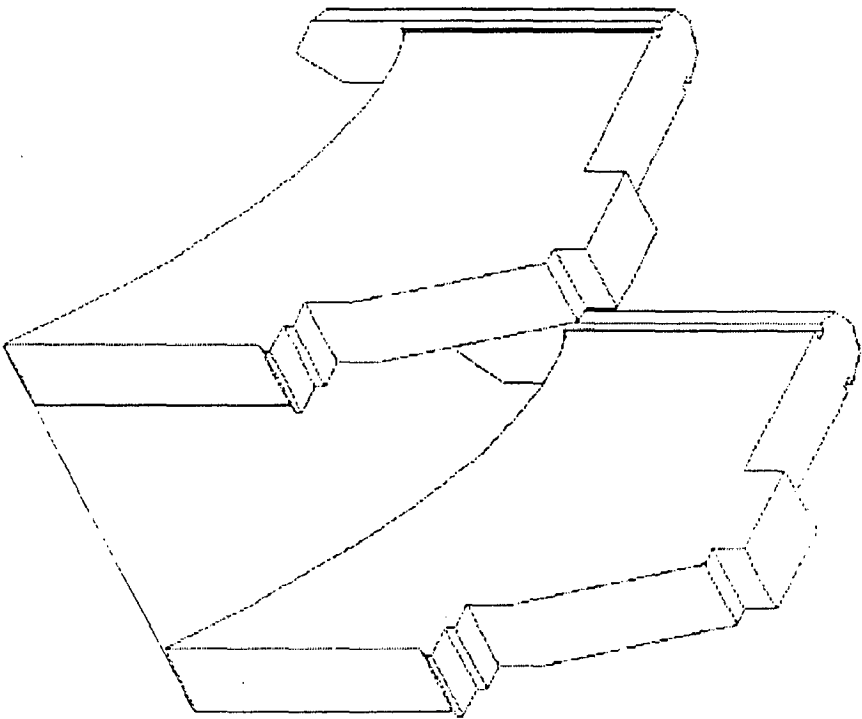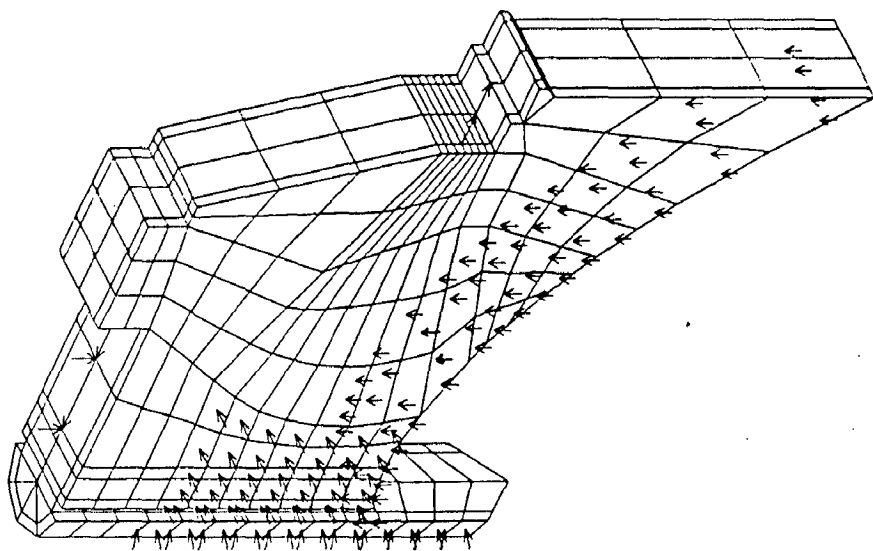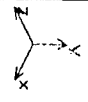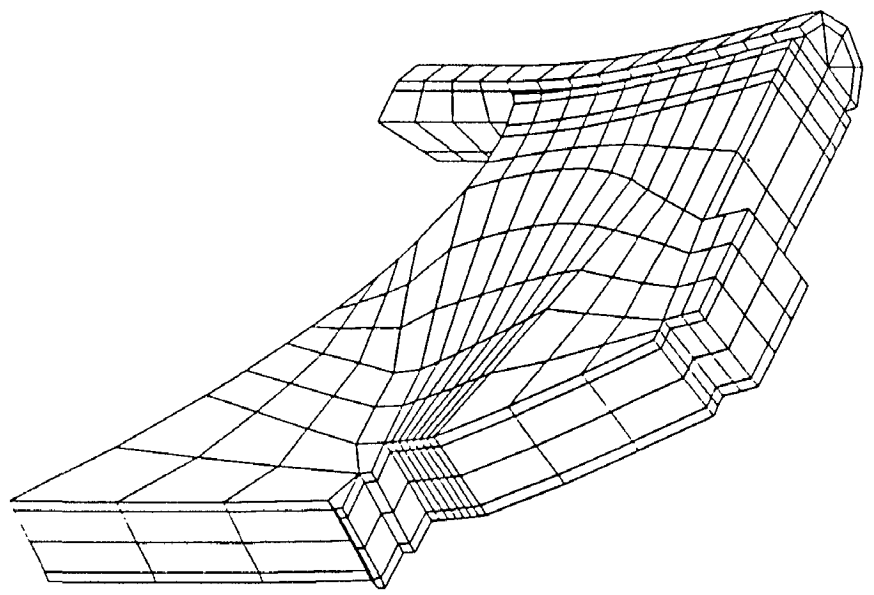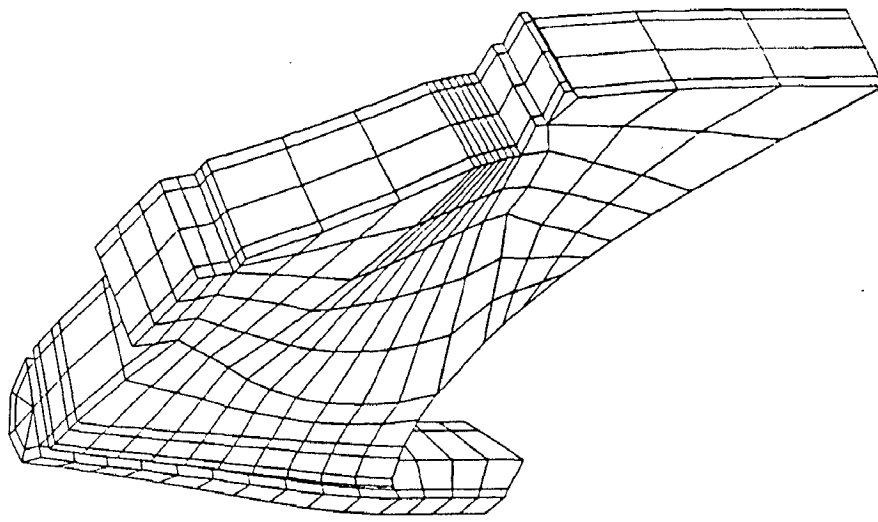
Fig. 3.22

80

Fig. 3.23

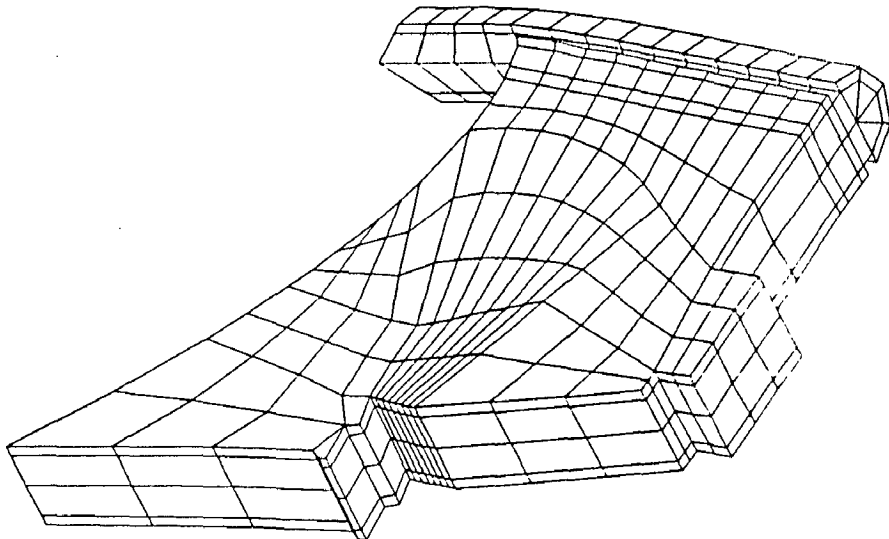F_Mode=1   7.1   Hz

Fig. 3.24

F_Mode=2 :7   Hz

Fig. 3.25

F_Mode=3   23   Hz
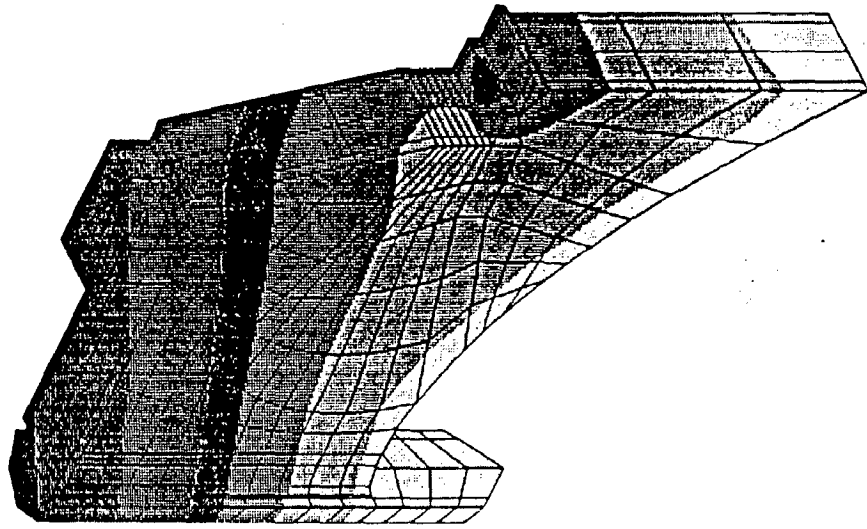

Fig. 3.26

- 84 -
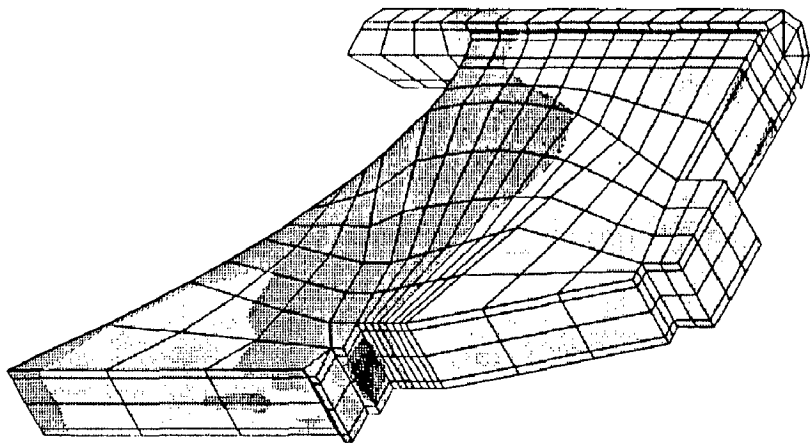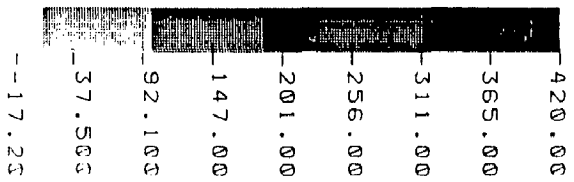
Fig. 3.27

FIG. MAJOR PRINCIPAL STRESS CONTOUR FOR STATIC ANALYSIS
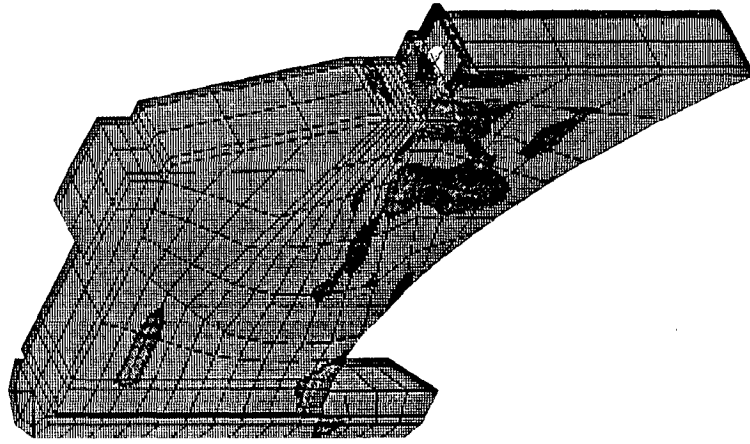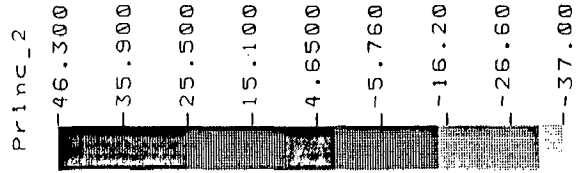
Fig. 3.28

FIG. INTERMEDIATE PRINCIPAL STRESS CONTOUR FOR STATIC ANALYSIS

Fig. 3.29

87

Lin STRESS Lc=1

FIG. MINOR PRINCIPAL STRESS CONTOUR FOR STATIC ANALYSIS

Princ_3

6.8400
-18.30
-43.40
-68.50
-93.70
-119.0
-142.0
-169.0
-194.0
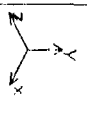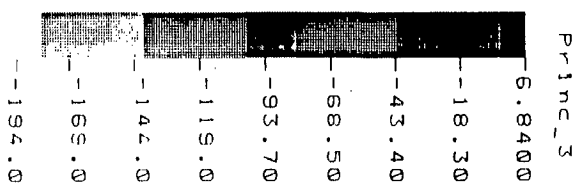
Fig. 3.30

PDN Step:1 = 0

Disp_Res

0.0004280
0.0003740
0.0003210
0.0002670
0.0002140
0.0001600
0.0001070
0.00005350
-1.00E-016
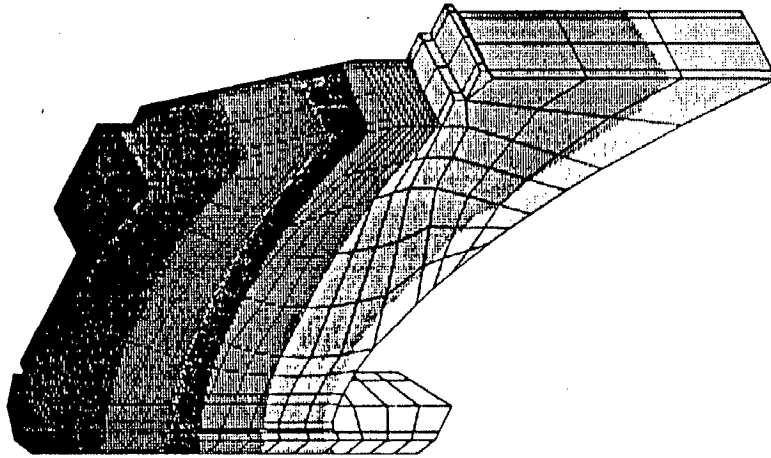
FIG. DISPLACCEMENT: EARTHQUAKE EXCITATION IN X-DIR.

Fig. 3.31

89

PDN Step:1   = 0

FIG. MAJOR PRINCIPAL STRESSES: EARTHQUAKE IN X-DIR.

Fig. 3.32

Princ_1

123.00
108.00
92.400
77.000
61.600
46.200
30.800
15.400
-0.0000

90
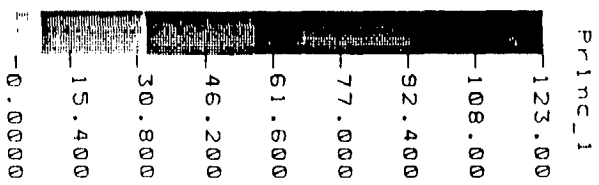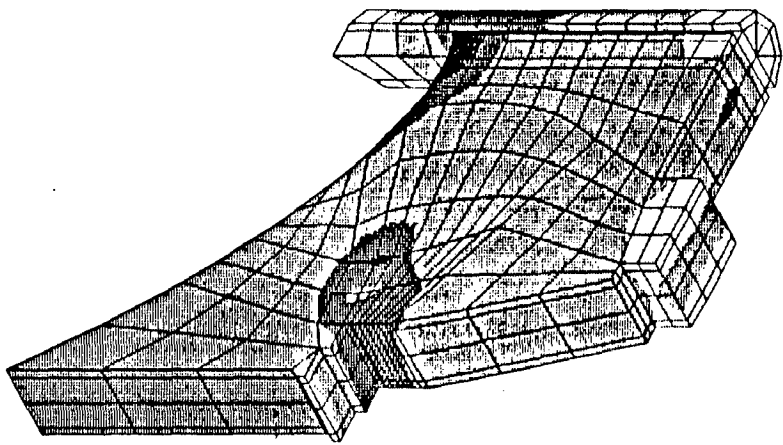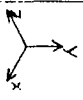
PDN Step:1   =0

Princ_2

47.200
40.100
33.100
26.000
18.900
11.900
4.8300
-2.220
-9.280
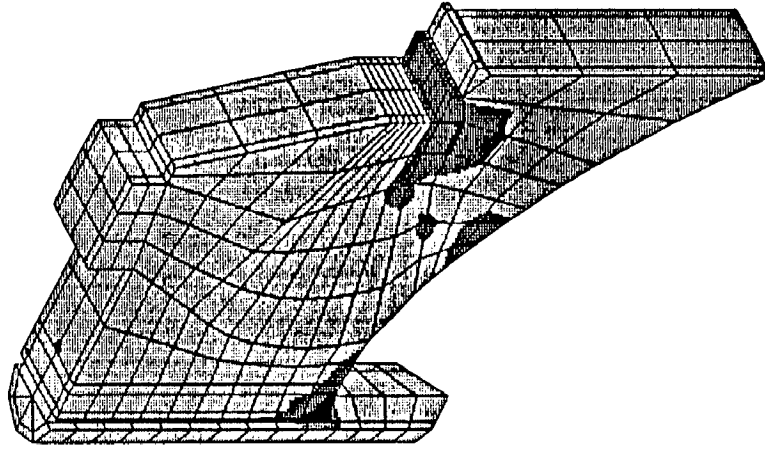
FIG. INTERMEDIATE PRINCIPAL STRESS : EARTHQUAKE IN X-DIR.

Fig. 3.33

91

PDN Step:1　=0

FIG. MINOR PRINCIPAL STRESSES: EARTHQUAKE IN X-DIR.

Fig. 3.34

Princ_3

4.2700
-1.050
-6.390
-11.70
-17.10
-22.40
-27.70
-33.00
-38.40
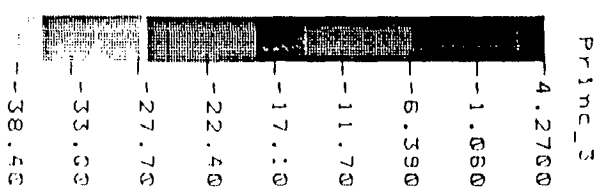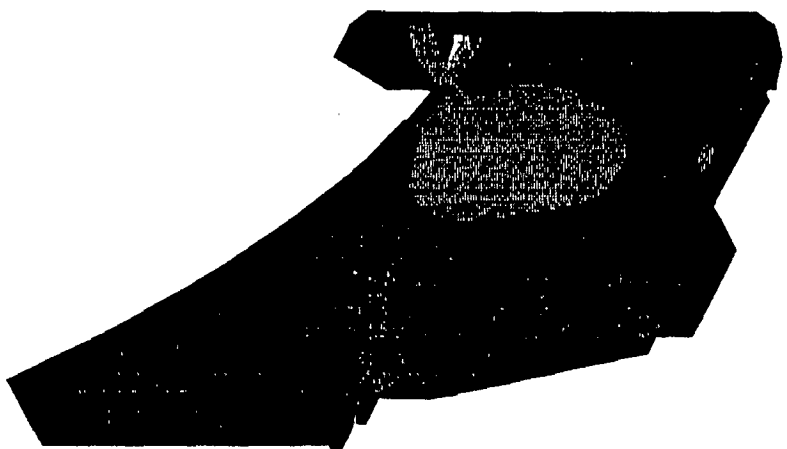
PDN Step:1   = 0

Disp_Res

0.007570
0.006620
0.005680
0.004730
0.003790
0.002840
0.001890
0.000946
1.0E-016
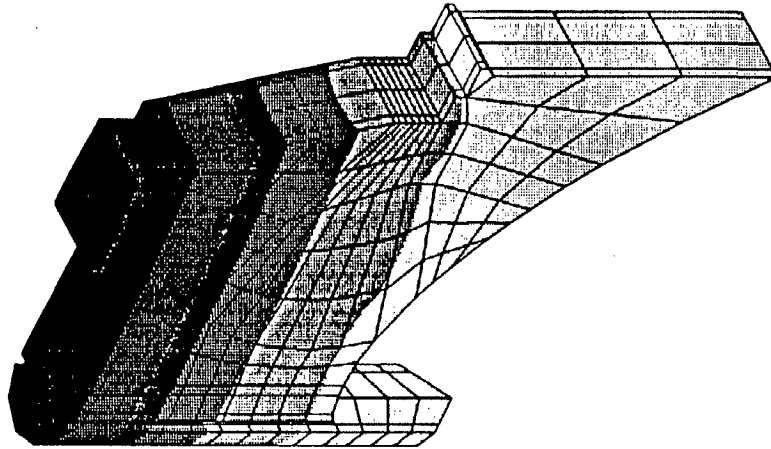
FIG. DISPLACEMENT CONTOUR : EARTHQUAKE IN Z-DIR.

Fig. 3.35

93

PDN Step:1   = 0

FIG. MAJOR PRINCIPAL STRESS : EARTHQUAKE IN Z-DIR.

Princ_1

893.00
781.00
670.00
558.00
446.00
335.00
223.00
112.00
-0.0000
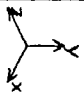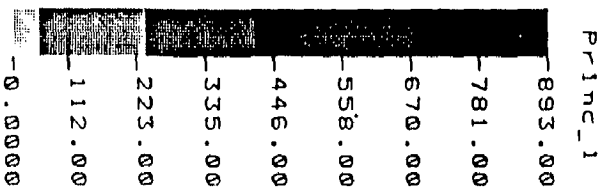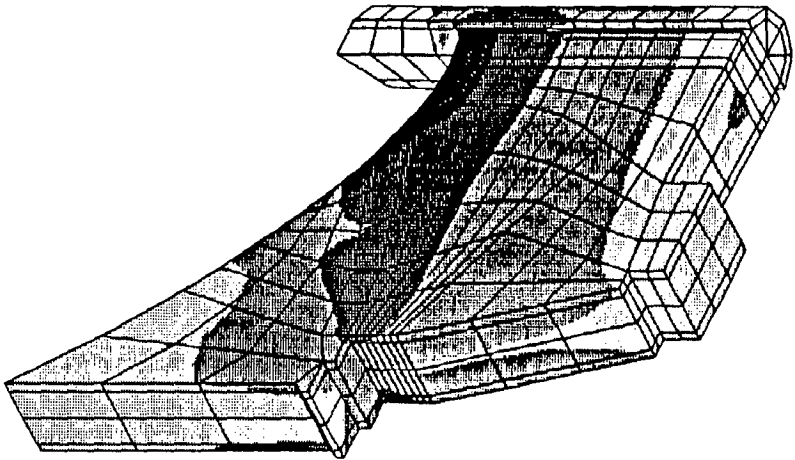
Fig. 3.36

PDN Step:1 = 0

Princ_2

173.00
150.00
128.00
105.00
83.000
60.600
38.100
15.700
-6.740
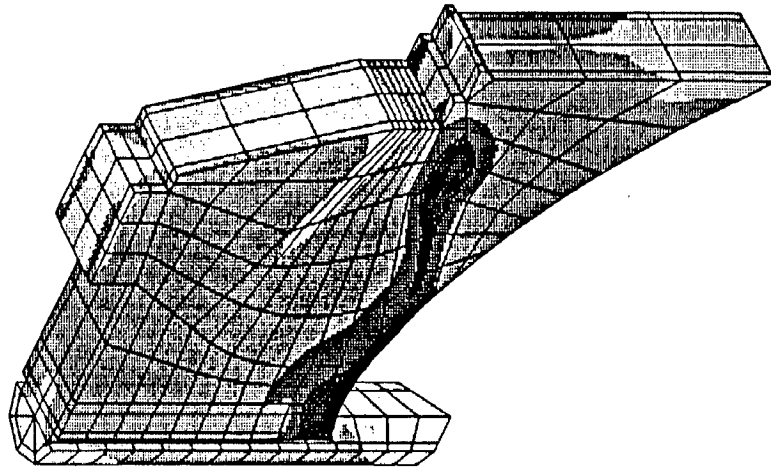
FIG. INTERMEDIATE PRINCIPAL STRESS : EARTHQUAKE IN Z-DIR.

Fig. 3.37

95

PDN Step:1   =0

FIG. MINOR PRINCIPAL STRESS : EARTHQUAKE IN Z-DIR.

Princ_3

89.200
70.200
51.100
32.100
13.100
-5.980
-25.00
-44.00
-63.10
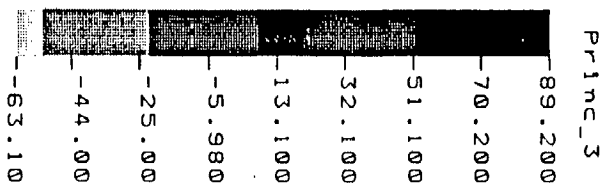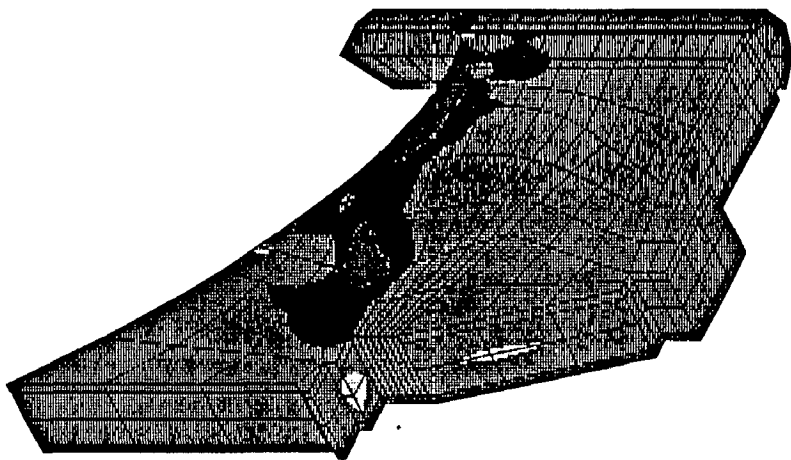
Fig. 3.38

3.7 PROBLEM- 6 :   3 D PIER ANALYSIS OF A DAM: PIER 2

This section briefly describes the 3D static analysis for gravity, pressure and gate reaction, frequency analysis and seismic analysis of the pier of a dam in transverse and longitudinal directions. The isometric view of the pier and breast wall over the overflow section of the dam is shown in Fig. 3.39.

Generation of the model: Generation of the model in COSMOS is a tedious process. Few steps used in model generation are described here. The points were first generated in X-Y plane at the central section of the pier excluding the curved portion. These points were joined by suitable curves first. The points at the base of the pier were joined by a parabolic curve. The fitting of a conic curve between two points in COSMOS requires the point of intersection of the tangents at the two points between which curve is to be fitted . After joining the points with suitable curves, contours and then regions were generated. Two different regions were generated for pier portion and breast wall. These two regions were copied in X-Y plane at a distance of 18.0 m to generate regions 3 & 4. Meshing requires that two different entities must have one common sub-entity. Using auto-meshing feature of software regions were meshed with eight noded elements. Meshed regions 1 & 2 were extruded in z-dir. for a distance 4.0 m to generate twenty noded elements. Region 2 was further extruded in z-dir. for a distance of 5.0 m. Similar operations were carried out with regions. 3 & 4 but in negative z-direction.

To form the curved portion of the pier, one surface in X-Z plane touching boundary with region 1 was generated. Using symmetry feature of COSMOS another surface touching boundary with region 3 was generated. The two surfaces were meshed with eight noded elements and then meshed surfaces were extruded in y-direction to generate twenty noded elements. Boundary conditions on the model are applied such that the model is fixed at the base. This completed the generation of the model. The completed model is mapped with 2597 nodes and 358 elements. Figure 3.40 shows the complete finite element model of the pier section.

3.7.1   MATERIAL PROPERTIES

The material properties taken for the pier analysis are listed in Table 3.10.

Table 3.10 Material Properties of the Pier 2: Problem 6

	E value (t/m^2)	V	unit weight (t/m^3)
concrete	0.22076×10^7	0.15	2.50

3.7.2 FREE VIBRATION CHARACTERISTICS OF THE DAM

After merging the nodes, the model was subjected to free vibration analysis. Using "shift option" of the COSMOS the frequencies upto 33 Hz. were found. Subspace iteration method was used to calculate the natural frequencies and mode shapes of the system.

Assuming the static material properties as mentioned above and for no reservoir water, the first few natural frequencies of vibration have been computed. First five frequencies of the pier are listed in table 3.11.

3.7.3 RESULTS AND DISCUSSION

3.7.3.1 Frequency Analysis

Table 3.11 gives the values of the first five natural frequencies of the system :

Table 3.11 Natural Frequencies of the Pier 2: Problem 6

Mode Number	Frequency (cycles/ sec)
1	4.763
2	6.913
3	8.430
4	10.536
5	12.869

From the analysis of the results it is found that first mode is the transverse vibration of the piers (Fig. 3.41), second and third modes are the torsional mode of the piers. The fourth mode is the longitudinal vibration of piers.

3.7.3.2 Static Analysis

Static analysis of the piers is carried out for gravity, water pressure and gate reaction when the gate is closed. The total gate reaction of 1020t acting on two piers has been used.

Static analysis has been carried out for (i) gravity stresses, (ii) water pressure and gate reaction and (iii) combined gravity, water pressure and gate reaction. On applying the gravity loads only, the maximum compressive stress is found to be 146.0 t/m^2. Under the influence of water pressure and gate reaction, for σ_y ,the maximum tension is found to be 246 t/m^2 and maximum compressive stresses is 156 t/m^2. Maximum horizontal stress occurs at the support of the gate i.e. 457 t/m^2.

On application of the combined gravity, water pressure and gate reaction, for σ_y , the maximum tension is found to be 129 t/m^2 and maximum compressive stresses is 155 t/m^2. Maximum horizontal stress occurs at the support of the gate i.e. 462 t/m^2.

3.7.4 DYNAMIC ANALYSIS

The motion at the top of spillway is taken as the input motion for this analysis. For earthquake loading only horizontal earthquake is considered to act only in one direction at a time. 5% damping was considered in each mode.

In the seismic analysis, response spectrum method has been used to obtain the response in longitudinal and transverse directions.

Figure 3.42 shows the contours of displacement when the earthquake motion is taken in the transverse direction. The maximum displacement at the top is found to be 8.2 mm. From the investigation of σ_x and σ_y stresses, the maximum tensile horizontal stress is 109 t/m^2 and maximum tensile vertical stress is 454.00 t/m^2.

When the earthquake motion is taken in the longitudinal direction, the maximum displacement at the top is found to be only 1.44 mm. From the investigation of σ_x and σ_y stresses, the maximum tensile horizontal stress is 34 t/m^2 and maximum tensile vertical stress is 154.00 t/m^2.

Concluding Remarks: The static analysis for gravity load, water pressure and gate reaction has been made. First couple modes of free vibration have been worked out; First mode is the transverse vibration of piers, second and third modes are torsional vibration of the piers and fourth mode is longitudinal vibration of piers. Seismic response of the piers are worked out using response spectrum analysis in transverse and vertical directions.
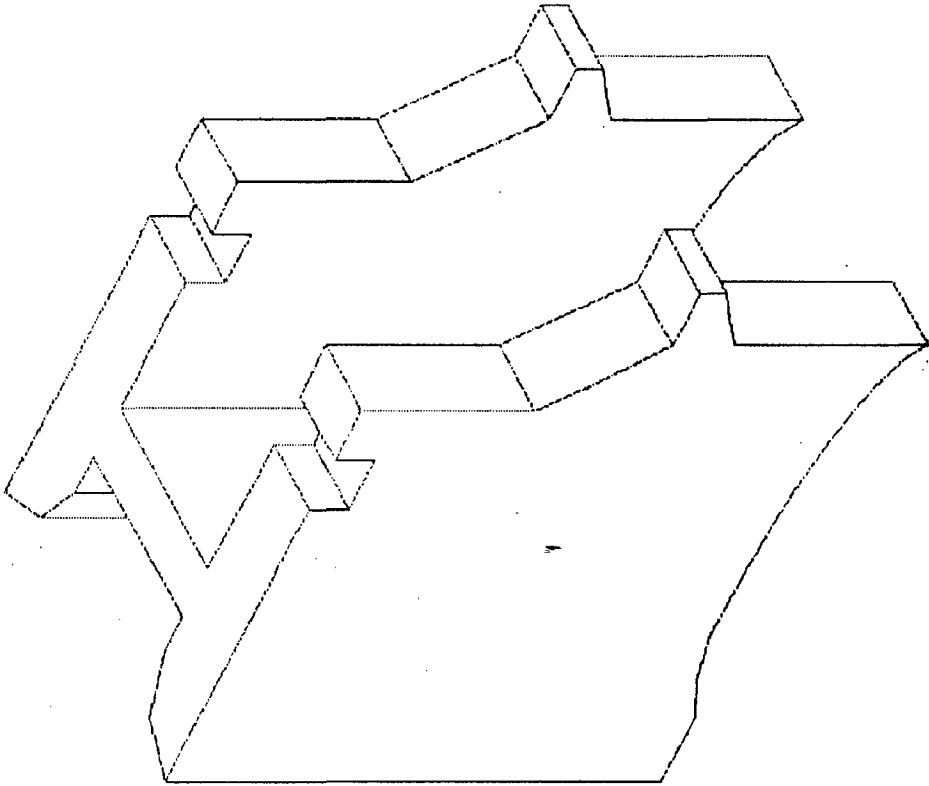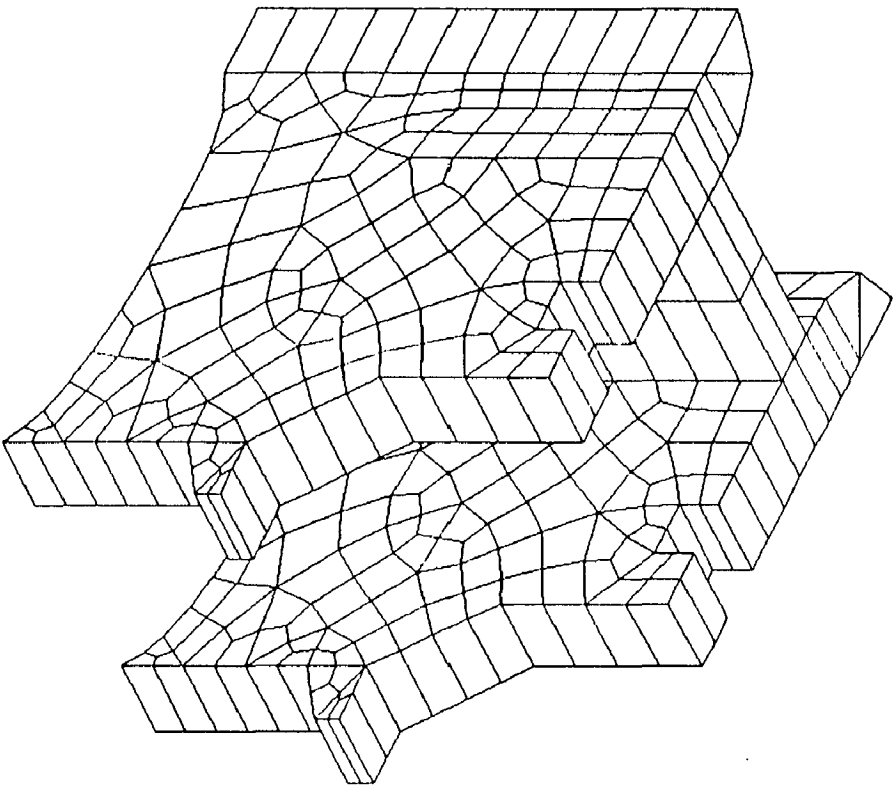
Fig. 3.39

101

Fig. 3.40

102

F_Mode=1   1.8   Hz

Fig. 3.41

103
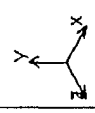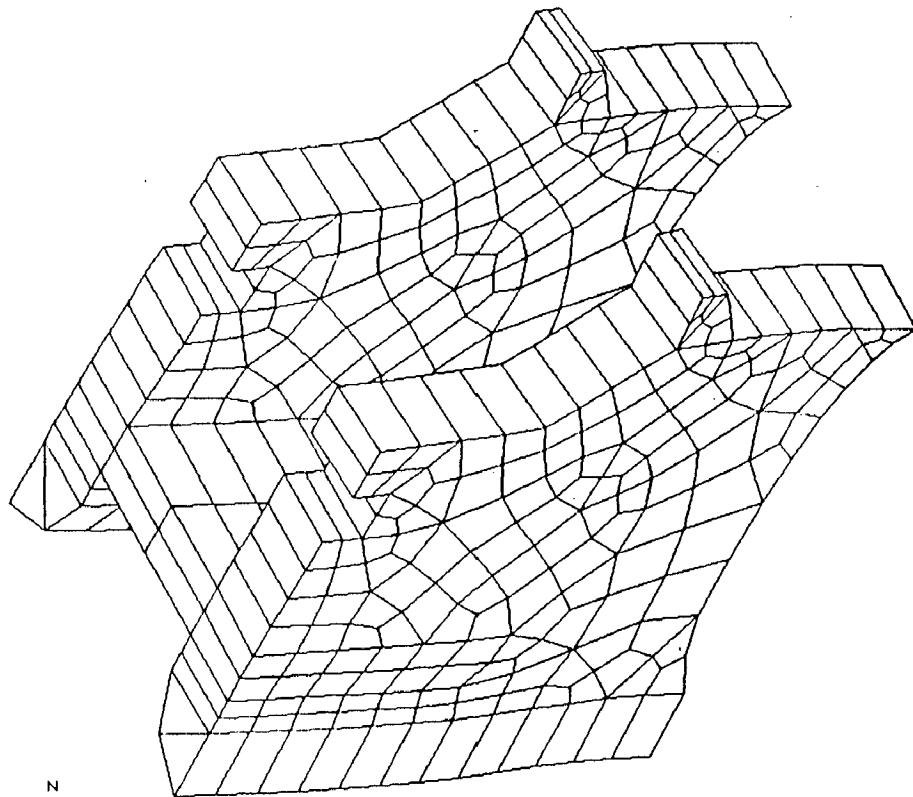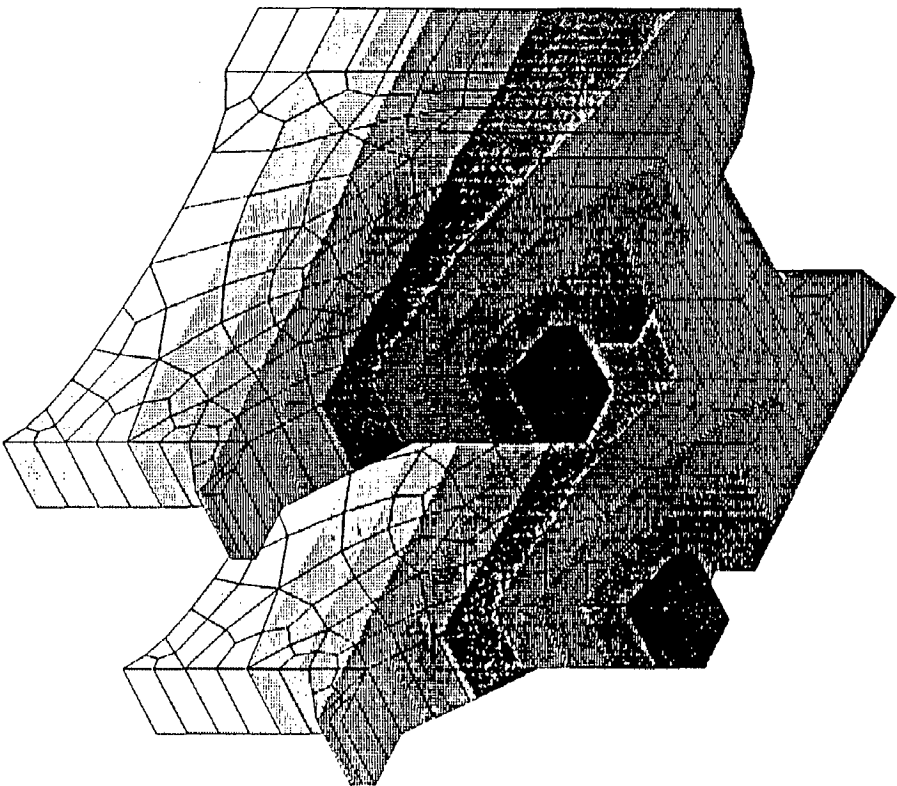
Fig. 3.42

Disp_Res
0.008170
0.007350
0.006540
0.005720
0.004900
0.004090
0.003270
0.002450
0.001630
0.000817
1.0E-016

CONCLUSIONS

In this investigation some of the major hydraulic structures have been modelled and analysed using 2D/3D finite elements for static and earthquake forces. Here a finite element package COSMOS has been used to model and analyze the problems Effort has been mainly directed to study and understand this powerful package and exploit it in the solution of some of the hydraulic structures thereby projecting its capabilities and inadequacies in handling such problems. A variety of hydraulic structures ranging from various shapes and sizes of nonoverflow and overflow sections of concrete gravity dams, piers and wye section of a penstock have been solved. The conclusions are limited to the extent of the experiences gained with the use of the few modules (Basic System modules and Advanced Dynamic module) of the package. The total package however contains many more modules which have not been used in this study.

4.1   Capabilities of the Preprocessor

Preprocessor of the COSMOS is very efficient while generating the 2D models of the nonoverflow and overflow sections of the dams. 2D modelling has been used in Problems 2, 3 & 4. It is found that generating the curves, contours or regions in a plane is quite simple. Also meshing of the sections in 2D models is quite easier. But 3D modelling of non-overflow and overflow sections of the dams require special attention. Extrusion, Dragging etc. are some of the good features of the pre-processor of the COSMOS. But as in Problem 2, sluice portion generation was a tedious process as all the sides of the sluice opening are defined by curves. Fitting of a conic curve in pre-processor requires point of intersection of tangents at the ends of the curve to be fitted. The 3D modelling of piers is used in Problems 4 & 5. Wye section modelling in Problem 1 was very difficult process as one of the penstock was inclined. The efficient modelling with the help of pre-processor of the COSMOS requires preplanning the curves, surfaces or regions for the description of the loads and boundary conditions. So model generation with the help of pre-processor requires thorough knowledge of various

commands and features of COSMOS. Meshing in pre-processor with auto-meshing is quite easier but not always useful.

4.2 Capabilities of the Solver

Solver of the COSMOS was used mainly for three types of analyses: Linear Static Analysis, Frequency Analysis and Linear Dynamic Analysis. Frequency analysis was carried out in Problems 3, 4 ,5 & 6. Subspace iteration method was used in all the problems. Defining "convergence tolerance" prior to the analysis is very good feature of the COSMOS. Solver is found to produce accurate results within seconds on PC-486 as in some of the problems frequencies were found out using the 2D as well as 3D models which were almost similar in first few modes of vibration. Static and Dynamic analysis was carried out in Problems 4, 5 & 6.

4.3 Capabilities of the Postprocessor

In most of the problems results of displacements, mode shapes, stresses were immediately processed with the help of powerful postprocessor. Only few commands are supplied to get the desired result in either deformed shape or in the form of contours. Contours can be plotted with combination of different colours which can be increased or decreased. Animation of the mode shapes and the other deformed shapes at different time intervals reveals lot of important information about the type of vibration of different parts of the structure. Whatever plots/ graphs are generated, can be taken the form of hardcopy with insertion of titles at appropriate locations. As such the capabilities of postprocessor are very powerful and simple to use.

4.4 3D response of the dam and pier sections

The 3D modelling of the two piers taken as examples is quite involved and difficulty arises to map the curves, transitions and the grooves for the gates. After the generation of the solid, the discretisation also creates problems specially at corners. A method of trial was adopted to get the acceptable finite element discretisation. The 3D responses of the piers are found for linear static and dynamic analyses. The natural frequencies are also calculated for the piers. With the help of the postprocessor results has been plotted and studied.

4.5 Comparison of 2D and 3D Analysis

The 2D and 3D analyses of the Koyna dam revealed that the first few natural frequencies and mode of vibration compare very well. The approximation of the buttress by average thickness is therefore an adequate representation. The 2D modelling of dam of varying thickness can therefore be used for the frequency analysis of the dam. 3D analysis has predicted the transverse vibration of the buttress in the fourth mode while the 2D model was unable to predict this.

4.6 Limitations of the Software

Preprocessor of the software is not always very powerful. To have the node compatibility at the curved portions model has to be planned earlier such that two entities touching each other have one common sub-entity. Solid meshing of the model is possible with ten noded tetrahedral elements only. Moreover model with these elements can be used only for static analysis. Another problem in using the COSMOS is non availability of the "undo" command. As a whole the package is quite robust and capable of handling the hydraulic structures. However, the package is limited to handle the hydrodynamic pressure and therefore it has to be calculated separately as virtual mass and mass are to be lumped at the virtual nodes.

REFERENCES

1. Lashkari M. and Eshraghi H. (1994), *Advanced Modules User Guide Part-1, Vol.4*, Structural Research And Analysis Corporation, Santa Monica, California.

2. William Weaver,Jr. and Paul, R. Johnson (1984), *Finite Elements For Structural Analysis*, 2nd ed., Prentice-Hall, INC., Engelwood Cliffs.

3. Basic FEA System User Guide (1994), part 1, vol.3, Structural Research And Analysis Corporation, Santa Monica, California.

4. William Weaver,Jr. and Paul, R. Johnson (1984), *Structural Dynamics by Finite Elements*, 2nd ed., Prentice-Hall, INC., Engelwood Cliffs.

5. The COSMOS Manual, User Guide (1994), Structural Research And Analysis Corporation, Santa Monica, California.

6. Annales de L'INst. Du Bat. Trav. Pub. (France) (Jan.1985), COSMOS software for design of three dimensional structures : New Developments, vol.38, no.431, pp. 66-83.

7. Bathe, K.J., and Wilson, E.L.,(1978), *Numerical methods in Finite Element Analysis*, Prentice-Hall of India Pvt. Ltd., N.Delhi

8. Clough, R.W., and Penzien, J., *Dynamics of Structures*, McGraw-Hill Bokk Company, New York, 1975.

9. Niazy, A.S., Kahyai, S., and Chang, S.,(1994), *Advanced Modules (NSTAR) User Guide*, Part 1, Vol.4, Structural Research And Analysis Corporation, Santa Monica, California.

10. Mathies, H., and Strang, G., *The Solution of Nonlinear Finite Element Equations*, Int.J. Numer. Meth. Eng., 15:529-551,1979.

11. Mario, P., (1987), *Structural Dynamics*, 2nd edition, CBS Publishers and Distributers, N.Delhi.

12. Singh, A.V., (1996), *Nonlinear Static and Dynamic Analysis of a Rockfill Dam*, M.E. Thesis, University of Roorkee, Roorkee.

13. Dixit, M.K., (1971), *Stress Analysis of Concrete Gravity Dams*, M.E. Thesis, University of Roorkee, Roorkee.

14. Chandrashekharan, R., (1987), *Vibration Analysis of Dams*, M.E. Thesis, University of Roorkee, Roorkee.

APPENDIX

Quantity	Size Limit	Quantity	Size Limit
Preprocessing		**Miscellaneous**	
Nodes	32,000*	Consecutive zooms	10
Elements	32,000*	Selection sets per entity	10
Keypoints	8000	Number of saved views	10
Curves	8000	Text messages	100
Surfaces	4000	Function keys (GEOFUN file)	50
Volumes	2000	Number of windows	4
Contours	1000	Colors	256
Regions	1000	Length of file (including path)	40
Polyhedra	100	Length of a parameter name (single variable, array, function)	10
Parts	100	Number of parametric arrays	20
Coordinate systems	500	Number of user-defined parametric functions:	200
		-length of a function argument name	10
		-number of arguments for a function	20
		-length of a function parametric expr.	200
Curves for contour	250	Length of a macro name	10
Contours for a region	20	Number of arguments for a macro	10
Surfaces/Region for a polyhedron	1000	Number of local user defined parametric variables in a macro	50
Polyhedra for a part	60	Number of local user defined functions in a macro	50
Bond target surfaces	20	Number of local arrays in a macro	10
Bond sets	100	Number of command lines starting with # in the entire session file or macro	500
Material property sets	90		
Real constant sets	5000	–	
Element groups	20		
Postprocessing			
Isoplanes	12		
Section planes	12		
Number of XY curves per plot	6		

Table A.1Modelling size limits in GEOSTAR

Quantity	Size Limit
Degrees of freedom	100,000
Primary load cases	50
Secondary load cases	50
Coupled degrees of freedom	1500
Constraint equations	1500
Gap elements	300
Temperature curves -Points for a temperature curve	100 5000

Superelements
    -Super nodes for a superelements
    -Degrees of freedom associated with a superelement
	99
	180
	2000

Reaction forces	3000
Prescribed non-zero displacements	3000
Concentrated forces for beam loading	5
Distributed loads for beam loading	3

Number of eigenpairs
    -Lanczos method
    -Subspace method
	
	150
	100

Table A.2　Analysis limits in Basic System Modules

Function	COSMOS/M Menu	Command
Property definition	PROPSETS	EGROUP, MPROP, RCONST, PICK_MAT, USER_MAT, PICK_SEC, BMSECDEF, EPROPSET, EPROPCHANGE

Loads	LOADS-BC
	  STRUCTURAL
	    DISPLMNTS
	    FORCES
	    PRESSURE
	    REACTION
	    GRAVITY
	  THERMAL
	    TEMPERATURE
		
		D__ commands for displacements
		F__ commands for forces
		P__ commands for pressure
		RF__ commands for reaction forces
		Gravity load commands
		
		NT__ commands for temperatures

Boundary conditions	LOADS-BC
	  STRUCTURAL
	    DISPLMNTS
	    COUPLING
	    BONDING
		
		D__ commands for displacements
		CP__ commands for coupling
		BOND__ commands for bonding

Model verification	MESHING ELEMENTS ANALYSIS	 ECHECK DATA_CHECK, R_CHECK
Specifying analysis options	ANALYSIS STATIC	LCSET, ADAPTIVE, P_ORDERLABS, A_STATIC, A_STRESS, STRESS
Specifying output options	ANALYSIS OUTPUT_OPS	PRINT_OPS
Executing linear static analysis	ANALYSIS STATIC	R_STATIC, R_STRESS
Postprocessing	RESULTS	Refer to COSMOS/M User Guide (V.1) for more details.

Table A.3 Important Commands for Linear Static Analysis

Function	COSMOS/M Menu	Command
Property definition	PROPSETS	EGROUP, MPROP, RCONST, PICK_MAT, USER_MAT, PICK_SEC, BMSECDEF, EPROPSET, EPROPCHANGE

Loads	LOADS-BC
	  STRUCTURAL
	    DISPLMNTS
	    FORCES
	    PRESSURE
	    GRAVITY
	  THERMAL
	    TEMPERATURE
		
		D__ commands for displacements
		F__ commands for forces
		P__ commands for pressure
		Gravity load commands
		
		NT__ commands for temperatures

Boundary conditions	LOADS-BC
	  STRUCTURAL
	    DISPLMNTS
		
		D__ commands for displacements

Model verification	MESHING
	  ELEMENTS
	  ANALYSIS
		
		ECHECK
		DATA_CHECK, R_CHECK

Specifying analysis options	ANALYSIS FREQ/BUCK	 A_BUCKLING
Specifying output options	ANALYSIS OUTPUT_OPS	 PRINT_OPS
Executing linear static analysis	ANALYSIS FREQ/BUCK	 R_BUCKLING
Postprocessing	RESULTS	Refer to COSMOS/M User Guide (V.1) for more details.

Table A.4 Important Commands for Buckling Analysis

Function	COSMOS/M Menu	Command
Property definition	PROPSETS	EGROUP, MPROP, RCONST, PICK_MAT, USER_MAT, PICK_SEC, BMSECDEF, EPROPSET, EPROPCHANGE

Loads (only if in-plane effects are considered)	LOADS-BC
	   STRUCTURAL
	      DISPLMNTS
	      FORCES
	      PRESSURE
		
		D__ commands for displacements
		F__ commands for forces
		P__ commands for pressure

Boundary conditions	LOADS-BC
	   STRUCTURAL
	      DISPLMNTS
		
		D__ commands for displacements

Model verification	MESHING
	   ELEMENTS
	   ANALYSIS
		
		ECHECK
		DATA_CHECK, R_CHECK

Specifying analysis options	ANALYSIS FREQ/BUCK	 A_FREQUENCY
Specifying output options	ANALYSIS OUTPUT_OPS	 PRINT_OPS
Executing linear static analysis	ANALYSIS FREQ/BUCK	 R_FREQUENCY
Postprocessing	RESULTS	refer to COSMOS/M User Guide (V.1) for more details.

Table A.5 Important Commands for Modal Analysis

Element Name	Description	Basic FEA System
BEAM2D	Two dimensional elastic beam element	o
BEAM3D	Three dimensional elastic beam element	o
BOUND	Boundary element	o
BUOY	1-node spherical buoyant element (usually used with IMPIPE element)	N/A
CLINK	Convection link	N/A
ELBOW	Elastic curved pipe (elbow) element	o
ELINK	Electrical link	N/A
FLOW2D	Two dimensional fluid flow element	N/A
FLOW3D	Three dimensional fluid flow element	N/A
GAP	Gap element	o
GENSTIF	General stiffness element	o
HLINK	Hydraulic link	o
IMPIPE	2-node immersed pipe or cable element	N/A
MAG2D	2-D magnetic element	N/A
MAG3D	3-D magnetic element	N/A
MASS	General mass element	o
PIPE	Elastic Straight pipe element	o
PLANE2D	4 to 8-node plane and axisymmetric element	o
RBAR	Rigid bar element	o
RLINK	Radiation link	N/A
SHELL3	3-node thin shell element	o
SHELL3L	Multi-layer 3-node shell/plate element	o
SHELL3T	3-node thick shell element	o
SHELL4	4-node thin shell element	o
SHELL6	6-node thin shell element	o
SHELL4L	Multi-layer 4-node shell/plate element	o
SHELL4T	4-node thick shell element	o
SHELL9	9/8-node shell element	o
SHELL9L	Composite 9/8-node shell element	o
SHELLAX	Axisymmetric shell element	o
SOLID	8- to 20-node 3-D solid element	o
SOLIDL	Composite 8-node solid element	o
SOLIDPZ	8- to 20-node 3-D solid piezoelectric element	o
SPRING	Spring element	o
TETRA10	10-node tetrahedral solid element	o
TETRA4	4-node tetrahedral solid element	o
TETRA4R	4-node tetrahedral solid element with translational and rotational dof	o
TRIANG	3- to 9-node triangular plane and axisymmetric element	o
TRUSS2D	Two dimensional truss/spar element	o
TRUSS3D	Three dimensional truss/spar element	o

Table A.6 Element Library in Basic System Modules

COSMOS/M Element Name	Material Properties					Section Constants	Mass		Element Loads		
	Iso	Orth	Anis	Th	Pz		Lu	Dis	Me	Th	Gr
TRUSS2D	●			●		2	●	●		●	●
TRUSS3D	●			●		2	●	●		●	●
BEAM2D	●			●		8	●	●	●	●	●
BEAM3D	●			●		14 to 27	●	●	●	●	●
RBAR	N/A	N/A	N/A	N/A	N/A	1	●	●	N/A	N/A	N/A
SPRING	N/A	N/A	N/A	N/A	N/A	2	●	●	N/A	N/A	N/A
PIPE	●			●		3	●	●	●	●	●
ELBOW	●			●		4	●	●	●	●	●
GAP	N/A	N/A	N/A	N/A	N/A	2	N/A	N/A			
MASS	N/A	N/A	N/A	N/A	N/A	7	●		N/A	N/A	N/A
BOUND	N/A	N/A	N/A	N/A	N/A	2	N/A	N/A			
PLANE2D 4-NODE	●	●		●		2	●	●	●	●	●
PLANE2D 8-NODE	●	●		●		2	●	●	●	●	●
PLANE2D 4-NODE (Axi.)	●	●		●		1	●	●	●	●	●
PLANE2D 8-NODE (Axi.)	●	●		●		1	●	●	●	●	●
TRIANG 3-NODE	●	●		●		2	●	●	●	●	●
TRIANG 6-NODE	●	●		●		2	●	●	●	●	●
TRIANG 3-NODE (Axi.)	●	●		●		1	●	●	●	●	●
TRIANG 6-NODE (Axi.)	●	●		●		1	●	●	●	●	●
SHELL3	●			●		2	●	●	●	●	●
SHELL4	●			●		2	●	●	●	●	●
SHELL 6	●	●		●		2	●	●	●	●	●
SHELL3T	●			●		2	●	●	●	●	●
SHELL4T	●			●		2	●	●	●	●	●
SHELL3L	●	●		●		2+3NL*	●	●	●	●	●
SHELL4L	●	●		●		2+3NL*	●	●	●	●	●
SHELL9	●			●		1	●	●	●	●	●
SHELL9L	●	●		●		2+3NL*	●	●	●	●	●
SHELLAX	●			●		1	●	●	●		●
TETRA4	●			●		N/A	●	●	●	●	●
TETRA4R	●			●		N/A	●	●	●	●	●
TETRA10	●			●		N/A	●	●	●	●	●
SOLID	●	●		●		9**	●	●	●	●	●
SOLIDL	●	●		●		2+6NL*	●	●	●	●	●
SOLIDPZ	●	●	●	N/A	●	N/A	●	●			
GENSTIF	●	●	●	N/A	●	N/A	●	●	N/A	N/A	N/A

* depends on the number of layers (NL)

** for defining orthotropic material axis orientation only

Table A.7 _ Summary of properties for elements in Basic System Modules

Element Type	Element Name
2D Spar/Truss	TRUSS2D
2D Elastic Beam	BEAM2D
3D Elastic Beam	BEAM3D
3D Spar/Truss	TRUSS3D
2D 4- to 8-node Plane Stress, Strain, Body of Revolution	PLANE2D
3D 3- to 6-node Plane Stress, Strain, Body of Revolution	TRIANG
Triangular Thin Shell	SHELL3
6-Node Triangular Thin Shell	SHELL6
Quadrilateral Thin Shell	SHELL4
Triangular Thick Shell	SHELL3T
Quadrilateral Thick Shell	SHELL4T
Triangular Composite Shell	SHELL3L
Quadrilateral Composite Shell	SH3LL4L
8 or 9-node Isoparametric Shell Element	SHELL9
8 or 9-node Isoparametric Composite Shell	SHELL9L
Axisymmetric Shell	SHELLAX
3D 8- to 20-node Continuum Brick	SOLID
8-node Composite Solid	SOLIDL
3D 8- to 20-node Isoparametric Piezoelectric Solid *	SOLIDPZ
3D 4-node Tetrahedron Solid	TETRA4
3D 4-node Tetrahedron Solid with Rotation	TETRA4R
3D 10-node Tetrahedron Solid	TETRA10
2-node Gap/ with Friction **	GAP
Spring Element	SPRING
General Stiffness	GENSTIF
2-node Rigid Bar	RBAR
Elastic Straight Pipe	PIPE
Boundary Element	BOUND
General Mass Element	MASS
Elastic Curved Pipe	ELBOW

* DSTAR only

** STAR and ASTAR only

Table A.8   Element library for linear Structural Analysis

COSMOS/M ELEMENT NAME	DESCRIPTION	NUMBER OF DOF/ NODE	ELEMENT DIMENSIONAL BEHAVIOR
TRUSS2D	Plane Truss	2	1-D/ 2-D (XY-Plane)
TRUSS3D	Space Truss	3	1-D/ 2-D/ 3-D
BEAM2D	Plane Beam	3	1-D/ 2-D (XY-Plane)
BEAM3D	Space Beam	6	1-D/ 2-D/ 3-D
IMPIPE	Immersed Pipe	6	2-D/ 3-D
SPRING	Axial and/or Torsional Spring	3 to 6	1-D/ 2-D/ 3-D
PLANE2D	4 to 8-node (Plane Stress, Strain, Axisymmetric)	2	2-D (XY-Plane)
TRIANG	3 to 6-node (Plane Stress, Strain, Axisymmetric)	2	2-D (XY-Plane)
SHELL3	3-node Triangular Thin Shell	6	2-D/ 3-D
SHELL4	4-node Quadrilateral Thin Shell	6	2-D/ 3-D
SHELL3T	3-node Triangular Thick Shell	6	2-D/ 3-D
SHELL4T	4-node Quadrilateral Thick Shell	6	2-D/ 3-D
SHELL3L	3-node Triangular Composite Shell	6	2-D/ 3-D
SH3LL4L	4-node Quadrilateral Composite Shell	6	2-D/ 3-D
SOLID	8 to 20-node Continuum Brick	3	3-D
TETRA4	4-node Continuum Tetrahedron	3	3-D
TETRA10	10-node Continuum Tetrahedron	3	3-D
GAP	Gap/Contact with Friction	1/2/3*	1-D/ 2-D/ 3-D
MASS	Concentrated Mass	6	1-D/ 2-D/ 3-D
BUOY	Immersed Spherical Mass	6	1-D/ 2-D/ 3-D

* According to the contact nodes

Table A.9   Element Library for Non-Linear analysis